ALMA MATER STUDIORUM

UNIVERSITA' DI BOLOGNA

SCUOLA DI INGEGNERIA E ARCHITETTURA

- Sede di Forlì -

CORSO DI LAUREA

IN INGEGNERIA AEROSPAZIALE

Classe: LM-20

TESI DI LAUREA

In *Strutture e Materiali Aerospaziali LM*

Laser Shock Peening Treatment to Control and Moderate Fatigue Crack Growth in Aircraft Structure Based on Residual Stress Engineering Approach

CANDIDATO   RELATORE

Jessica D'Ermilio   Prof. Ing. Enrico Troiani

                                                          CORRELATORE

                                               Dott. Ing. Domenico Furfari

Anno Accademico 2012-2013

Sessione III

"Strive For Perfection In Everything You Do.

Take The Best That Exists And Make It Better.

When It Does Not Exist, Design It"

(Henry Royce)

Index

Table Of Figures

Table of Tables

Acknowledgments

It is with immense gratitude that I acknowledge the support and help of my Professor Eng. Enrico Troiani who supported me enormously with his constant feedback during the draft of my thesis. I am especially grateful for trusting me and providing me the chance to have a truly rewarding experience in Airbus GmbH. I would like to acknowledge him for his assistance and valuable suggestions during all stages of this work.

I cannot find words to express my gratefulness to Dr. Domenico Furfari who first helped me clarify my ideas and formulate my own concepts. He constantly supported me during my internship in Airbus GmbH both professionally and humanly. I would like to thank him for sharing his knowledge and friendship with me and I consider it an honor to have had the possibility to work with him. I would also thank him for his continued support and encouragement during all of the ups and downs of my work.

A special thanks to Eng. Sara Taddia who gave me precious and useful suggestions. I extend my thankfulness to Fabio Laudicina, the one and only who was always there for cheering me up during my university studies and I owe my gratitude to all my colleagues in Airbus who made me feel like I was home.

Last but not least, I am indebted with my amazing family. They gave me the courage to overcome all difficulties during this work and the strength to aim high for my life's goal. I would like to express all my gratitude to them for the love and support they dedicated to me without complaining. This thesis would have remained a dream if it wasn't for you.

Abstract

Laser Shock Peening (LSP) is a surface enhancement treatment which induces a significant layer of beneficial compressive residual stresses of up to several mm underneath the surface of metal components in order to improve the detrimental effects of the crack growth behavior rate in it.

The aim of this thesis is to predict the crack growth behavior in metallic specimens with one or more stripes which define the compressive residual stress area induced by the Laser Shock Peening treatment. The process was applied as crack retardation stripes perpendicular to the crack propagation direction with the object of slowing down the crack when approaching the peened stripes.

The finite element method has been applied to simulate the redistribution of stresses in a cracked model when it is subjected to a tension load and to a compressive residual stress field, and to evaluate the Stress Intensity Factor (SIF) in this condition.

Finally, the Afgrow software is used to predict the crack growth behavior of the component following the Laser Shock Peening treatment and to detect the improvement in the fatigue life comparing it to the baseline specimen.

An educational internship at the "Research & Technologies Germany – Hamburg" department of AIRBUS helped to achieve knowledge and experience to write this thesis. The main tasks of the thesis are the following:

- To up to date Literature Survey related to "Laser Shock Peening in Metallic Structures"
- To validate the FE model developed against experimental measurements at coupon level
- To develop design of crack growth slowdown in Centered Cracked Tension specimens based on residual stress engineering approach using laser peened strip transversal to the crack path

- To evaluate the Stress Intensity Factor values for Centered Cracked Tension specimens after the Laser Shock Peening treatment via Finite Element Analysis
- To predict the crack growth behavior in Centered Cracked Tension specimens using as input the SIF values evaluated with the FE simulations
- To validate the results by means of experimental tests

I. The Fatigue Phenomenon

1.1 Introduction

The current metallic aircraft manufacturing technology is in a highly saturated level and it is rather challenging to obtain significant weight and manufacturing cost savings without introduction of radical changes on the current design and fabrication routes and materials. Such a development was experienced in the recent years by application of Laser Shock Peening technology for metallic and aeronautics materials.

New design and manufacturing methodologies which can give rise to significant improvements in the damage tolerance of metallic airframe components may bring two fold advantages. In fact, introducing new concepts which offer higher damage tolerance not only enables producers to use thinner sheets for manufacturing, but also it may become possible to take the advantage of the Laser Shock Peening technology on the more severely loaded sections of the fuselage.

For an improvement in damage tolerance of structures, two basic methodologies exist. Firstly, the damage tolerance properties of the material can be improved, and secondarily, the design of the structures can be modified to provide crack retardation, turning or arrest. In this thesis, it is studied the latter case, in particular, the improvement on the crack growth behavior gained after the Laser Shock Peening process.

1.2   The Fatigue Life of Components

Many mechanical components are often subject to cyclic stresses, or rather stresses which change their amplitude in time and a history load in which there are an alternate sequence of minimum and maximum values. These cyclic loads can lead some components to damage failure even though the applied loads are lower than the ultimate strength: this is the failure caused by the fatigue phenomenon.

The fatigue life of a structural element depends only on the highest and lowest values of loads to which the material is exposed and it does not depend on the shape of the temporal history of the load function.

Building materials are often irregular and anisotropic, to the contrary of what it is presumed by the static analysis, and this leads to an unequal aggregation of crystal grains in the component. One of the consequences is that, even though the nominal load does not exceed the yield strength, it can be seen locally a plastic deformation of the element due to an unequal distribution of the stresses loads. Generally, the fracture caused by the fatigue phenomenon occurs after thousands cyclic loads and it has been noticed that the most disadvantaged areas are those with the highest tensile stress and they are usually located on the surface of the specimen.

The rate of the crack growth inside a material depends on its ductility or brittleness proprieties. In brittle materials it can be noticed that there is no plastic deformation before fracture. In fact, the fracture can occur by cleavage as the result of a tensile stress acting normal to crystallographic planes with low bonding. On the other hand, in amorphous solids, the lack of a crystalline structure results in a shell-shape fracture, with cracks that proceed normal to the applied tension. In ductile fracture, it can be observed an extensive plastic deformation before fracture. Rather than cracking, the material splits and generally leaves a rough surface. In this case, there is a slow propagation and absorption of large amount energy before fracture. Many ductile metals, especially materials with high purity, can sustain very large deformation before fracture under favorable loading conditions and environmental conditions, the strain at which the fracture happens is controlled by the purity

of the materials. In this case, some of the energy from stress concentrations at the crack tip is dissipated by plastic deformation before the crack actually starts to propagate.

The fatigue phenomenon can be developed into four phases:

1. Crack nucleation

2. Stage I crack-growth, prevalent in malleable materials

3. Stage II crack-growth, prevalent in brittle materials

4. Ultimate failure

The first step of the fatigue phenomenon is identified by a microscopic flaw, which is difficult to notice; as the fracture goes forward, the velocity of the crack growth increase more and more, to the contrary, the tough section decreases in amplitude as long as the stress load reaches the breakdown level.

The fatigue failure is characterized by different fracture areas: the first one is where the flaw were born and spread and it is entirely smooth; the second area is where the crack propagates and it is characterized by concentric bench marks; the last area is where the catastrophic rupture happens and it can be distinguished by its rough surface.
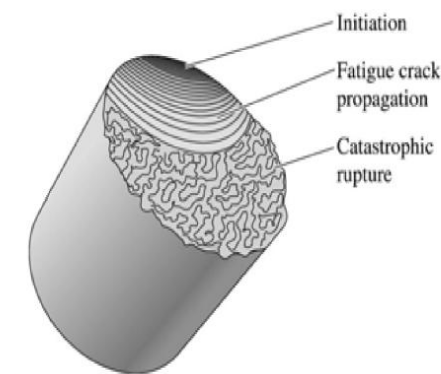
Fig. I-IFatigue Failure Phases

An element which is exposed to static loads experiences high deformation which can be detected and they permit a prompt maintenance service to

avoid the fracture. To the contrary, the fatigue rapture is an unexpected event that affects the whole element and it is the reason why it is more dangerous.

Listed below are some of the main parameters that affect the fatigue life of an element:

- Cyclic stress state
  - Stress amplitude
  - Mean stress
  - In-phase or out-of-phase shear stress
  - Load sequence
- Geometry
  - Notches
  - Variation in cross section
  - Surface quality
  - Shape and dimensions
- Environment
  - Temperature
  - Residual stresses
  - Air or vacuum
  - Corrosion

1.3   Design of Aeronautical Structures

The very first catastrophic failure due to the fatigue phenomenon goes back to the 1954, when two civil Comet aircrafts were destroyed during their flight causing the death of all of their passengers. These structural failures were attribute to cracks which were originated and propagated on the skin of the pressurized fuselage. Nowadays in the aeronautical industry there are two principal approaches to fatigue life assurance of structural elements: safe-life design and the damage tolerant design.

Although the major focus of structural design in the early development of aircraft was on strength, now structural designers also deal with fail-safety, fatigue, corrosion, maintenance and possibility of inspection, and reproducibility of the aircraft.

Manufacturers of modern aircraft are demanding more lightweight and more durable structures. Structural integrity is a major consideration of today's aircraft fleet. For an aircraft to economically achieves its design specification and satisfy airworthiness regulations, a number of structural challenges must be overcome.

Fatigue failure life of a structural member is usually defined as the time to initiate a crack which would tend to reduce the ultimate strength of the member. Fatigue design life implies the average life to be expected under average aircraft utilization and loads environment.

Criteria for fatigue design have evolved through the years from infinite life to damage tolerance, each of the successively developed criteria still has its place, depending on the application; these criteria are:

- Infinite-Life Design
- Safe-Life Design
- Fail-Safe Design
- Damage-Tolerant Design

1.3.1   Infinite-Life Design

In this design approach it is used the oldest criterion which is the unlimited safety. It requires local stresses or strains to be essentially elastic and safely below the fatigue limit. This criterion may still be used for parts subjected to many millions of cycles, like engine valve springs, but may not be economical (i.e. global competitiveness) or practical (i.e. excessive weight of aircraft) in many design situations.

1.3.2   Safe-life Design

The safe-life design predicts and assigns a design life to each structural element presuming the timing at which fatigue failure is going to happen. It is clearly needed a wide amount of tests in order to determine the average life of each component exposed to cyclic loads. The drawback of this design methodology is that it results very expensive and it predicts to replace many elements at the end of their design life in order to maintain the design safety, even though they may still have a considerable life ahead of them. Furthermore, it has to be noticed that this philosophy has brought to severe structural failure in the armed forces, as it was for F-111. One of the main problems is that in safe-life design it is not taken into consideration that the material may have original defects due to its manufacturing method or caused by maintenance operations. It is then supposed that elements, as machined, have a perfect structure, without any kind of damages and this is actually unworkable. Nevertheless, the safe-life technique is successfully employed in critical systems which are either very difficult to repair or may cause severe damage to life and property. For instance, it is used for the landing gear of airplanes which are designed to work for years without requirement of any repairs.

It is used in many industries (e.g. automotive industry) in pressure vessel design and in jet design; the calculations may be based on stress-life, strain-life or crack growth relations.

The safe life must include a margin for the scatter of fatigue results and for other unknown factors. The margin for safety in safe-life design may be taken in terms of life, in terms of load or by specifying that both margins must be satisfied.

In this case "the structural component needs to be designed so as to be able to sustain the real life loads, for the whole operational life, without showing any dangerous crack". Once the predicted life of the structural element is reached, it needs to be replaced, even if it doesn't show ay relevant failure.

This criterion is used for some structural elements which cannot be redundant or for those which is not possible to identify flaws due to the cracks through inspections, and which are replaced before the crack reaches the critical dimension.

1.3.3   Fail-Safe Design

Fail-Safe design requires that if one part fails, the system does not fail. This design methodology recognizes that fatigue crack may occur and structures are arranged so that crack will not lead to failure of the structure before they are detected and repaired.

Multiple load paths, load transfer between members, crack stoppers built at intervals into the structure, and inspection are some of the means used to achieve fail-safe design.

Fail-Safe design is achieved through material selection, proper stress levels, and multiple load path structural arrangements which maintain high strength in the presence of a crack of damage.

1.3.4   Damage Tolerance Design

The philosophy of damage tolerance design is based on the assumption that flaws can exist in any structure from the begging of their life and such flaws propagate with usage. Therefore, the damage tolerance design considers the growth of a defect in the structure and the need to carry out recurring inspections to check whether the crack growth has reached or not its critical value. In the first place, the design evaluates an initial slow growth of flaws so that as they start to propagate into the material they have a stabile growth that will not lead to a sudden and unstable failure. In the second place, the design predicts a recurring maintenance program which main purpose is to intervene before cracks reach a critical value and to avoid an unexpected failure of the structure. Essentially, a structure is considered to be damage tolerant if a maintenance program has been implemented that will result in the detection and repair of accidental damage, corrosion and fatigue cracking before such damage reduces the residual strength of the structure below an acceptable limit.

This philosophy is a refinements of the fail-safe philosophy. It assumes that cracks will exist, caused either by processing or by fatigue, and uses fracture mechanics analyses and tests to check whether such cracks will grow large enough to produce failures before they are detected by periodic inspection.

This philosophy looks for materials with slow crack growth and high fracture toughness. Three key items are needed for successful damage-tolerant design:

- ✓ Residual strength:
  It is the strength at any instant in the presence of a crack. With no crack, this could be the ultimate tensile strength or yield strength, as a crack forms and grows under cyclic loading, the residual strength decrease.
- ✓ Fatigue crack growth behavior
- ✓ Crack detection involving nondestructive inspection:

Different nondestructive inspection techniques have been developed. All inspection periods must be laid out such that as the crack grows, the applied stresses remain below the residual strength.

1.4   Residual Stresses

Some structural elements can show, during their life cycle, a premature failure or an improvement of their characteristic depending on the interaction between the material and stress to which it is exposed. In fact, it takes a lot of importance to know not only stresses to which the material is exposed during its life, but also stresses that are present inside the material and that can be introduced during its productive process: these are the so called residual stresses.

Most of the times residual stresses are unwanted since they reduce the yielding stress and they can cause deformations in materials during following manufacturing processes. However, residual stresses can also lead to beneficial effects, it depends on whether they are tensile or compressive residual stresses.

As a matter of fact, tensile residual stresses on the surface of a component reduce mechanical performance and resistance to corrosion, as well as they facilitate the fatigue phenomenon which leads to the collapse of a structure.

On the other hand, compressive residual stresses may have a good effect on structural components as they stunt flaws origin and propagation, leading to an increase of the fatigue life of components.

The component which is exposed to residual stresses has to be in equilibrium, reason why every compressive residual stress field is always associated to tensile residual stress field. In general, in elastic field, residual stresses are simply added to the applied load, justifying the reason why compressive residual stresses reduce the tension level where more elevated loads are applied.

II. Fracture Mechanics

The fracture mechanics studies the nucleation and propagation of flaws in material when it is subjected to external loads. This discipline was born between the 1920 and 1950 with a view to explain the brittle failure of some structural components, and it would have been extend also to explain the concept of the instable failure, which can be brittle or ductile.

After the 1950 it was born the concept of a flaw propagation due to the fatigue phenomenon which was studied to prevent the failure in aeronautical structure. One year after the other, this discipline has begun more and more important and it had been tried to find out new theories more reliable and exact in order to understand the reason why such structural elements were brought to failure even though the load applied was under the ultimate load of the material.

2.1   Linear Elastic Fracture Mechanics

Advanced crack growth predictions are essential to the damage-tolerance philosophy which is undisputed a major component to any aircraft design. The theory of Linear Elastic Fracture Mechanics (LEFM) enables all engineers who are involved in the assessment and improvement of structures' performance to study the propagation of crack in metallic structures and the structure's resistance to fracture. The prediction of crack growth and residual strength is the key for the damage-tolerance design philosophy, and is applied when

small flaws, defect or crack, are already assumed to be in a structure. In the aerospace industry, fracture analysis by analytical and testing approach is applied to justify safe operation of aircraft. Moreover, it used to define inspection thresholds and inspection intervals to ensure continued airworthiness of aircraft's damage-tolerant structures.
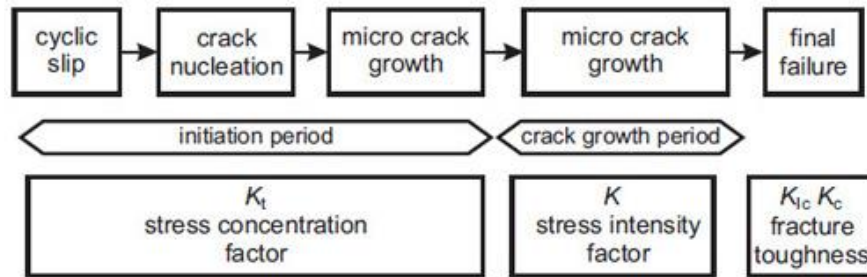
Fig. II-I Crack Life Periods

The crack life of a structure is typically divided into three periods:

- ➢ Crack initiation
- ➢ Crack growth
- ➢ Final failure

For every period, different concepts and factors are used in the analysis because every stage has its own susceptibility to different parameters and effects.

For instance, the initiation period is characterized by local microscopic processes which are mainly influenced by material surface condition and heterogeneous stress distribution which is described by the stress concentration factor K_t.

On the other hand, the crack growth period is studied by means of the Linear Elastic Fracture Mechanics. The Stress Intensity Factor (SIF) K is the most important parameter which is used for the crack growth behavior prediction.

Finally, the final failure stage is described by the fracture toughness factors K_{Ic} and K_C.

The crack growth behavior also depends on the material properties of the type of structure which is loaded. There are three different ways of applying a force to enable a crack to propagate:
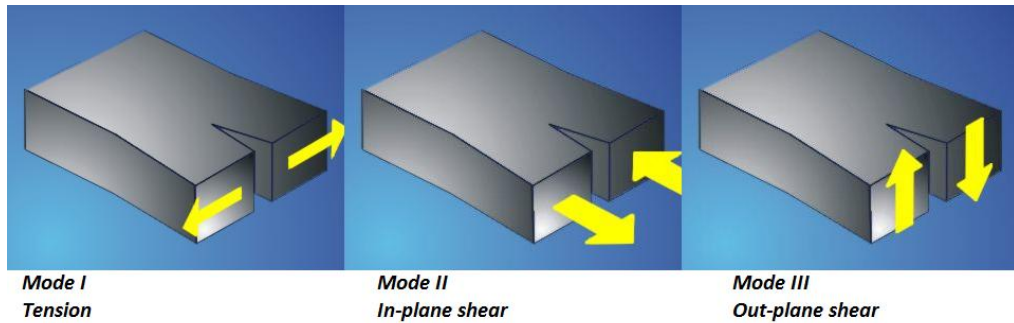
Fig. II-II Crack Opening Modes

It should be mentioned that stress intensity factor for crack opening mode I can be written as K_I, but since crack mode I is the appropriate crack mode for most engineering cases, and it is the one which is studied in this thesis, K usually refers to the stress intensity factor in crack mode I. Therefore, further explanations refer to mode I only. This main crack opening mode let the crack propagate perpendicular to the tensile stress direction, leading the tensile loading to open the crack at every cycle [1][2][3].

Summarizing the assumptions of linear elastic fracture mechanics are:

➢ Crack has been initiated
➢ Material in linearly elastic
➢ Material is isotropic
➢ Crack has started to propagate
➢ Plastic zone near crack is small
➢ Points of analysis are near (r < 0.1·crack length) the crack tip

2.2   Stress Intensity Factor

For the crack growth period, the stress intensity factor K is a meaningful parameter to describe the severity of the stress distribution around the crack tip. It is considered an infinite sheet containing a central hole through-the-thickness and a crack length of 2a under a tension load (crack opening mode I).
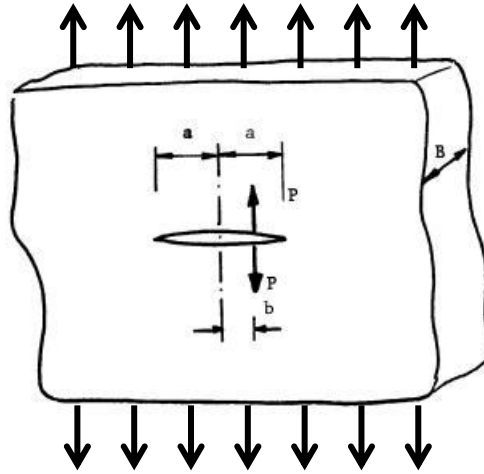
Fig. II-III Ideal Infinite Sheet Under Tension Load
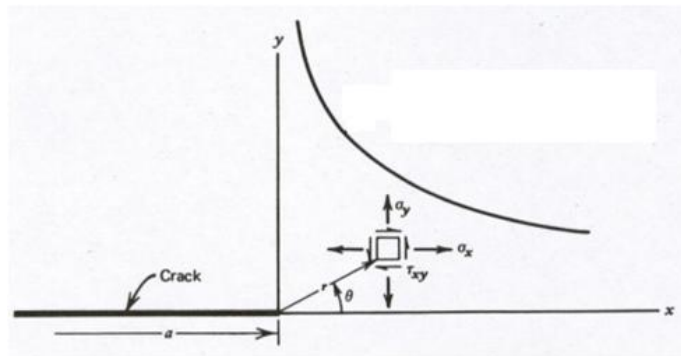
Fig. II-IV Stress Distribution Near Crack Tip

For this case, the elastic stress field near the crack tip (r<<a) in a polar coordinate system is define by following equations:

$$\sigma_x = \frac{S\sqrt{\pi a}}{\sqrt{2\pi r}} \cdot \cos\frac{\vartheta}{2}\left(1 - \sin\frac{\vartheta}{2}\sin\frac{3\vartheta}{2}\right) - S$$

$$\sigma_y = \frac{S\sqrt{\pi a}}{\sqrt{2\pi r}} \cdot \cos\frac{\vartheta}{2}\left(1 + \sin\frac{\vartheta}{2}\sin\frac{3\vartheta}{2}\right)$$

$$\tau_{xy} = \frac{S\sqrt{\pi a}}{\sqrt{2\pi r}} \cdot \cos\frac{\vartheta}{2}\sin\frac{\vartheta}{2}\cos\frac{3\vartheta}{2}$$

Where σ is the remote loading and a is the half crack length.

The three above mentioned equations are often summarized as:

$$\sigma_{i,j} = \frac{K}{\sqrt{2\pi r}} f_{i,j}(\vartheta)$$

The stress intensity factor K describes the stress field in the elastic region around the crack tip and it can be expressed as:

$$K = \beta S \sqrt{\pi a}$$

The parameter β is the so-called beta correction factor. It accounts for various influences of geometrical and loading conditions in the comparison of the infinite sheet (β=1) under a far field tension load and any real engineering structure under more complex loading. The β parameter is a geometrical factor which depends upon the geometry of the cracked body and the position of the crack.

The stress intensity factor for cyclic loading is formulated by the following equation:

$$\Delta K = \beta \cdot \Delta S \sqrt{\pi a}$$

Where ΔS is the load stress range:
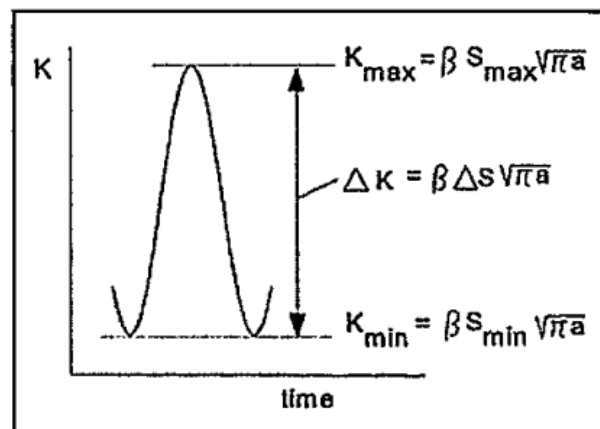
Fig. II-V Load Range Cycle

By applying the cyclic loading with a stress range of $\Delta S = S_{max} - S_{min}$, the stress intensity factor range ΔK can be written as $\Delta K = K_{max} - K_{min}$ [1][2][3]. The stress intensity factor range is the major parameter in any crack growth prediction model.

The Stress Intensity Factor plays a fundamental role in the fracture mechanics as:

- ✓ It is the crack-tip characterizing parameter
- ✓ It measures the magnitude of the stress field near the crack tip
- ✓ It can be used to compare different problems: any crack in a body that has the same K_I as another crack in another body is effectively in the same condition
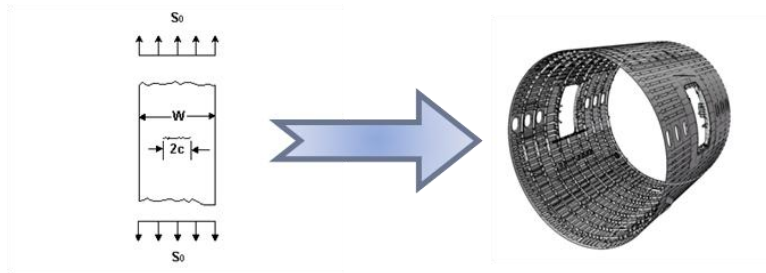
Fig. II-VI Stress Intensity Factor Similitude

2.3   Beta Correction Factor

The dimensionless factor β is called beta correction factor (also geometry correction factor, boundary correction factor or geometry factor) and depends on the geometrical and load differences of the real structure in respect to the infinite sheet under remote tension loading conditions.
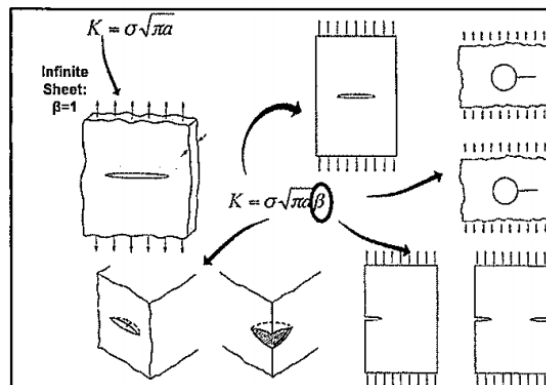
Fig. II-VII Beta Correction Factor – Infinite Sheet vs. Real Engineering Structure

As it has been already mentioned, for an infinite sheet β=1 and K can described as:

$$K = S\sqrt{\pi a}$$

Beta correction factors for various geometries and loading conditions can be found in the literature [4][5], for real engineering structures. To derive such beta correction factors various approaches have been applied by many researchers and engineers. Among these approaches some are of analytical nature, such as the weight functions methods [5][6][7], and others use numerical approaches via Finite Element Methods (FEM) [7][8].

Stress Intensity Factor's beta correction factors which are derived by experiments are very expensive and limited in application because of the limited number of tests and thus investigated parameters. Testing approaches are applied when simulation and analytical approaches demand extremely high efforts [9]. This is the case when the complexity in geometry or load systems applied to the structure is hardly representable by models which could be derived by approaches mentioned previously. However, since most of the standard engineering cases for daily operation are already covered in the specific literature, engineers and researches also superimpose SIF solutions when applicable [10].

2.4   Griffith Theory

Fracture mechanics was develop by Griffith, who suggested that the low fracture strength observed in experiments, as well as the size-dependence of strength, was due to the presence of microscopic flaws in the bulk material.

He considered an infinite size cracked plate of unit thickness with a central transverse crack of length 2a loaded with a stress of σ (see Fig. II-III Ideal Infinite Sheet Under Tension Load).

Griffith stated that the elastic energy contained in the due to the load applied must be sufficient to provide all the energy required for the crack propagation.

$$\frac{dU}{da} = \frac{dW}{da}$$

Where W is the energy required for crack growth and U is the elastic energy.

For a crack in an infinite elastic plate:

$$\frac{dU}{da} = G = \frac{\pi \sigma^2 a}{E}$$

Where E is the elastic modulus and G is the strain energy release rate.

It can be noticed that the energy condition for crack propagation is that G must be at least equal to the energy required for crack growth (dW/da), which lead to:

$$\sigma_{cr} = \sqrt{\frac{G_{IC}E}{\pi a}}$$

If $\sigma > \sigma_{cr}$ the crack will grow in an unstable manner.
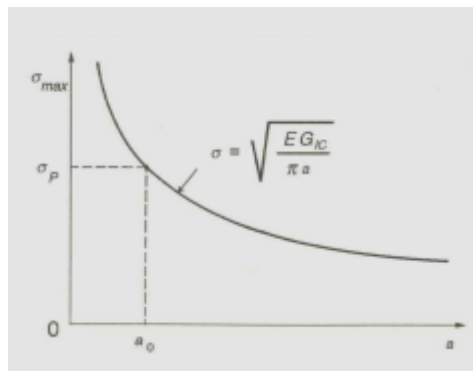
Fig. II-VIII Limit Curve for Critical Crack Length

It is also possible to determine the crack length a_0 below which the material yielding precede the unstable crack propagation.

2.5   J-integral

The J-integral is a widely used parameter to calculate SIFs in the field of LEFM and it is based on energy considerations. The J-integral represent the strain energy release rate, or work per unit fracture surface area for a cracked body under monotonic loading. For isotropic, perfectly brittle, linear elastic materials, the J-Integral can be directly related to the strain energy release rate:

$$J = G$$

This is generally true for linear elastic materials. For materials that experience small-scale yielding at the crack tip, J can be used to compute the energy release rate under special circumstances (e.g. monotonic loading in mode III).

Mathematically, it is a contour integral or line integral, as illustrated in figure, which completely enclosed the crack tip and is described by the following equation:

$$J = \int_{\Gamma} \left(W \cdot dy - T \cdot n \cdot \frac{\partial u}{\partial x} \cdot ds \right)$$

Where:

- J is the energy release rate
- W is the elastic strain energy density
- Γ is an arbitrary contour
- T is the stress tension vector
- n is the outward unit normal to Γ
- u is the displacement vector
- and ds is a differential element along the contour
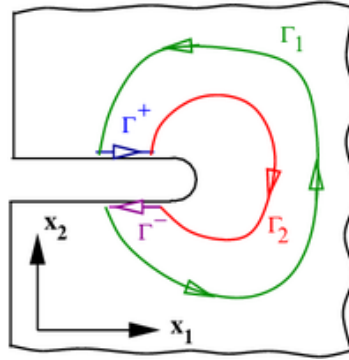
Fig. II-IX Contour Integral Path

The J-integral and the SIF are related to each other for a linear elastic material through:

$$J = \frac{1}{8\pi} K^T \cdot B^{-1} \cdot K$$

Where:

- $K = [\ K_I,\ K_{II},\ K_{III}]^T$
- B is the pre-logarithmic energy factor matrix

For homogeneous, isotropic material B is diagonal and the above equation for mode I loading condition simplifies to:

$$J = \frac{K_I^2}{E} \rightarrow Plane\ Stress$$

$$J = \frac{K_I^2}{E}(1 - v^2) \rightarrow Plane\ Strain$$

In most cases, the J-integral ad thus the SIF is determined by means of FEM in engineering application 109[1][3][11]. Finite Element Methods to determine SIFs are described in more detail in chapter V.

Ⅲ. Surface Enhancement Treatments

Fatigue failures of structural components are primarily caused by tensile stresses that are generated by service loads. These tensile stresses tend to initiate cracks on the surface, which could lead to catastrophic failure. Surface enhancement treatments inducing compressive residual stresses in the surface layers to counteract the tensile stresses, could prevent or delay the fatigue failure. Surface enhancement treatments of specimens are widespread to slow down problems related to the fatigue life phenomenon in aeronautical structures, or in wider terms in any metallic structure. One of the most effective methods is to introduce compressive residual stresses in some specific interested areas.

There are a lot of surface enhancement technologies that include many processed for strengthening metals and alloys to extend fatigue life in critical safety applications. Some of them are Laser Shock Peening, shot peening, low plasticity burnishing, waterjet peening, ultrasonic peening, cavitation peening, superfinishing.

3.1   Shot Peening

Shot Peening is a cold working process in which the surface of a part is bombarded with millions of small spherical media, called "shots", which are of steel, glass or ceramic. During the process, each shot striking the material acts as a tiny peening hammer creating a small dimple on the surface. In order for

the dimple to be created, the surface fibers of the material must be yielded in tension [12]. Below the surface, the fibers try to restore the surface to its original shape, thereby producing below the dimple, a hemisphere of cold-worked material highly stressed in compression.

In most of the case, cracks will not initiate or propagate in a compressively stressed zone. The overlapping dimples from shot peening create a uniform layer of compressive at metal surfaces, this is the reason why shot peening can provide considerable increases in part fatigue life. Compressive stresses are beneficial in increasing resistance to fatigue failures, corrosion fatigue, stress corrosion cracking, hydrogen assisted cracking, fretting, galling and erosion caused by cavitation. The maximum compressive residual stress produced just below the surface of a part by shot peening is at least as great as one-half the yield strength of the material being shot peened [13].

The advantages of Shot Peening (SP) relies in a relatively inexpensive technique, using robust process equipment and it can be used on large or small areas as required. Nevertheless, the shot peening technique has several downsides. Firstly, in producing the compressive residual stresses, the process is semi-quantitative and is dependent on a metal strip, or Almen type gauge, to define the SP intensity. This gauge cannot guarantee that the SP intensity is uniform across the component surface. Secondly, the compressive residual stresses are limited in depth and they usually do not exceed 0.25 mm in soft metals such aluminum alloys, and even less in harder metals [14]. Thirdly, the process provides a highly roughened surface, especially in soft metals as aluminum. This roughness may need to be removed for some applications, in particular for aeronautics applications, but typical removal processes often eliminate the majority of the peened layer.

3.2   Laser Shock Peening

Laser Shock Peening (LSP) is one of the surface enhancement technique that has been demonstrated to increase the fatigue life of a component subjected to fatigue loading.

The Laser Shock Peening process produces several beneficial effects in metals and alloys. One of the most important benefits is to increase the resistance of materials to surface related failures, such as fatigue, stress corrosion and fretting fatigue. This is possible thanks to compressive residual stresses introduced beneath the treated surface of the material. This technique is capable of introducing much deeper residual stresses than the shot peening process, which is the reason why it is successfully and increasingly used.

The Laser Shock Peening process might be used also to strengthen thin sections, work-harden surfaces, shape or straighten parts, break up hard materials, possibly to consolidate or compact powdered metals.

The Laser Shock Peening treatment produces mechanical shock waves due to the high pressure plasma created on the surface of the treated specimen, as a consequence of high-power density laser irradiation. Most of the times, the surface is covered with an ablative layer, which may be a black paint or an extra thin layer of pure aluminum, over which runs a thin layer of water acting as a tamping layer. The laser light pulse passes through the tamping layer and hits the ablative layer, which evaporates into the plasma state. The plasma expands rapidly, while the plasma-tamping layer reacting force causes a compression shock wave propagating into the metal.

Fig. III-I Laser Shock Peening Process

It is interesting to observe that, even if developed plasma reached temperatures up to 10000 °C, the process is often considered mechanical and not thermal, since plasma-specimen interaction time are of the order of nanoseconds [15].

The Laser Shock Peening process can also be implemented without ablative layer, it is then called Laser Peening without coating (LSPwC) [16]. In this case, the laser beam is fired directly to the treated specimen, reason why the size of the laser beam needs to be smaller than the one used with protective coating, so that the treated object is no damaged. This is the case of localized treatment around holes, and in and along notches, keyways, fillets, splines, welds and other highly stressed regions.
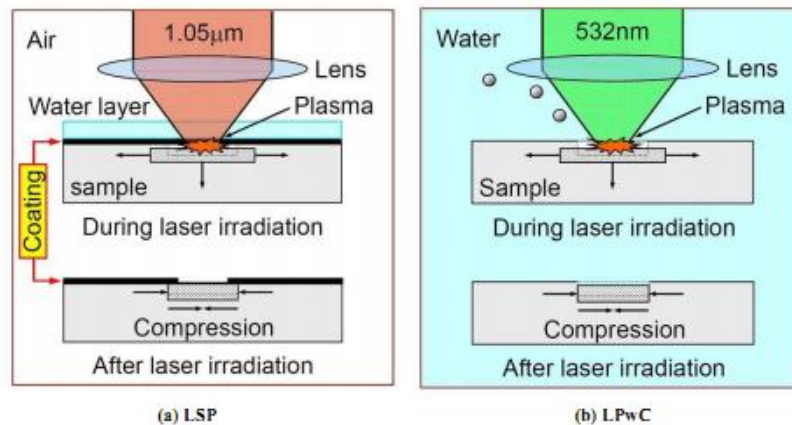
Fig. III-II Comparison Between LSP and LSPwC [43]

Laser Shock Peening can often be applied to the finished surface of a part, or just prior to the final finishing step. The effects of the mechanical forces on the surface itself are minimal. However, in softer alloys, a very shallow surface depression occurs, which decreases in depth in harder materials. For example, in aluminum alloys, the depression is about 6 µm deep, but on machined surfaces of harder alloys, it is difficult to see where the surface was laser shocked. The depth of the depression does increase with increasing intensity of LSP.

The intensity of Laser Shock Peening can be easily controlled and monitored, allowing the process to be tailored to the specific service and manufacturing requirements demanded by the part. The flexible nature of the process accommodates a wide range of part geometries and sizes. It can also be used

in combination with other treatments to achieve the most beneficial property and cost advantages for each part. It is important to notice that Laser Shock Peening can produce high magnitude compressive residual stresses of more than 1 mm in depth, 4 times deeper than traditional shot peening [17].

3.3   Laser Shock Peening vs. Shot Peening

For instance, the efficiency of LSP to extend the fatigue life of thick Al 7050-T751 structural coupon (up to 30mm thick) containing stress concentration factor of 2 has been proved as well as a deep compression residual stress up to the depth of more than 3mm [41].
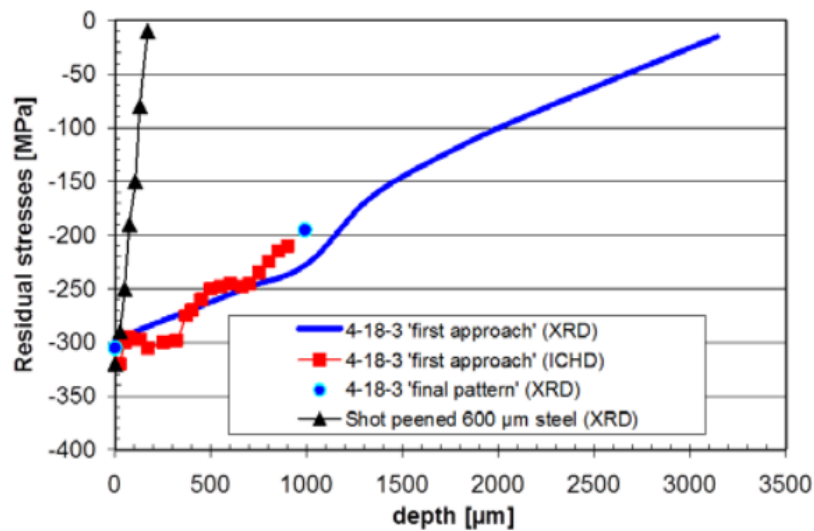
Fig. III-III Induced Residual Stress: LSP vs. SP

This effect is directly related with an advantage in terms of longer nucleation and initial propagation periods for cracks present in mechanical components. Moreover, Laser Shock Peening allows better accuracy and reproducibility, with smoother surface as a result, when confronted with shot peening. One of the main disadvantages is that this technique is usually connected with longer preparation times of the specimen and equipment costs.

Laser Shock Peening can often be applied to the finished surface of a part, or just prior to the final finishing step. In machine components, tooling or other parts, application to external surface and internal surfaces with line-of-sight access is straightforward. Application to internal surface without line-of-sight access is quite possible, but the method used needs to be studied for each application. LSP can also be used in manufacturing processes requiring a high, controllable, mechanical impact over a defined area, where mechanical punches are limited in how they can be adapted to the task. The impact area could have a variety of shapes depending on final goals that have to be reached.

The use of Laser Shock Peening in order to increase the strength and resistance to failure offers several advantages. In fact, it can be noticed that after applying Laser Shock Peening to failure-prone areas on troublesome parts, the service life of the parts and the maintenance intervals of machinery can be increased while the downtime is decreased, without changing the design. On second thought, a part can be redesigned to make it lighter, easier to manufacture or less expensive, using the Laser Shock Peening technique to upgrade the properties to meet the original design performance requirements.

In comparison with the Shot Peening treatment, the Laser Shock Peening process can produce a compressive residual stress minimum four times deeper than conventional shot peening (1 mm for hard metal such as titanium or steel and up to 4 mm in depth for aluminum alloys) [18]. Furthermore, in most modes of long-term failure, the common denominator is tensile stress. Tensile stresses attempt to stretch or pull the surface apart and may eventually lead to crack initiation. For this reason, increasing the depth of this layer increases crack resistance as the crack grow slowdown is significant in a compressive layer.

In addition, using Laser Shock Peening treatment, the treated surface of the component is essentially unaffected and the laser peened components do not lose any dimensional accuracy. Moreover, the process can become more efficient in application as the laser pulse can be adjusted and optimized in real time and the spot geometry of laser beam can be changed to suit the

problem. The main disadvantages of LSP is that it requires high equipment costs and long preparation times due to the necessity of having a specially protected environment for treatment and skilled operators needed before/during/after processing.

In the table below the main advantages and disadvantages of the two above mentioned technique are summarized:

Shot Peening	Laser Shock Peening
✓ Easy to apply and inexpensive ✓ Risk to introduce external material in the treated component ✓ Lead to a roughness surface	✓ Longer preparation times and equipment costs ✓ It does not lead to any macroscopic variation of the treated area ✓ It does not increase the surface roughness ✓ The laser beam can reach areas which are not accessible with conventional shot peening technique ✓ Treated area dimensions starts from few micrometer up to 100 mm^2 ✓ Easily verifiable and rapid process applications ✓ Deformation rate up to 10^6/s ✓ Ability to introduce compressive residual stresses in areas deeper up to 10 times than the conventional shot peening process

Table III-I LSP vs. SP: Advantages and Disadvantages

3.4   Generation of the Compressive Residual Stresses

One of the main advantages of the Laser Shock Peening technique is that the pressure pulse, generated by the blow-off of the plasma, creates almost a pure uniaxial compression in the direction of the shock wave propagation and tensile extension in the plane parallel to the surface.
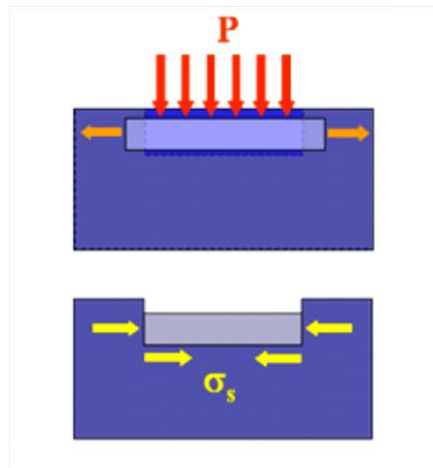
Fig. III-IV Compressive Residual Stresses Generation

After the reaction of the elastic material of the surrounding zones, a compressive stress field is generated within the affected volume, while the underlying layers are in a tensile state[19]. As the shock wave propagates into the material, plastic deformations occurs to a depth at which the peak stress no longer exceeds the Hugoniot Elastic Limit (HEL), which represents the maximum stress a material can withstand under uniaxial shock compression without any internal rearrangement. HEL is related to the dynamic yield strength according to [20]:

$$HEL = \frac{(1-v)\sigma_Y^{dyn}}{(1-2v)}$$

Where v is Poisson's ratio and σ_Y^{dyn} is the dynamic yield strength at high strain rates.

When the dynamic stresses of shock waves within a material are above the dynamic yield strength of the material, plastic deformations occurs and it

continues until the peak of dynamic stress falls below the dynamic yield strength. The plastic deformation induced by the shock waves results in strain hardening and compressive residual stresses at the material surface [21].

Ni-base alloy are widely used in high serving temperature fields such as space navigation, nuclear energy and petroleum industry due to excellent fatigue resistance, radiation resistance, corrosion resistance, good machinability and welding performance. Various mechanical surface treatment technologies, such as shot peening, low plastic polishing and Laser Shock Peening, have been used to restrain the propensity of fatigue initiation or growth by inducing compressive stresses on the surface and fellow-surface regions to improve the fatigue performance of metallic materials. Compared with other surface treatment technologies, LSP has unique advantages that it could be performed without the contact with the component and without heat-affected zone.

The temperature and exposure time are the primary parameters for the thermal relaxation of residual stress. Masmoudi et al. [22] have studied the thermal relaxation of residual stress in shot peened Ni-base alloy IN100 as exposed to different temperatures (500-750 °C). During the initial period of exposure, the surface residual stress decreased rapidly. Cao et al. [23] also observed similar phenomena. Khadhraoui et al. [24] performed an experiment to investigate thermal stress relaxation in IN718 with different exposure times at 600 °C and 650 °C. Prevey et al. [25] studied the thermal stress relaxation of the compressive layer produced by LSP. Cai et al. [26] studied the residual compressive stress field of IN718 induced by shot peening and the relaxation behavior during aging, and the relaxation process was described by the Zener-Wert-Avrami function [27][28].

In most cases [29], the residual stress relaxation of surface treated alloys is studied through experimental trials which are expensive, time-consuming and unreliable resulting from the factors arising from setting up the Laser Shock Peening process and residual stress measurements. Recently, the finite element (FE) method has been used to study LSP induced residual stress in the material, and the simulations results are well consistent with the experimental results.

IV. Design Of Crack Growth Slowdown

4.1 Introduction

The centered through crack specimen is used extensively for fatigue testing. The fatigue characteristics of the M(T) specimen are well understood and it therefore offers a good opportunity to fundamentally explore the effect on fatigue life of LSP induced residual stress fields.

The effect of Laser Shock Peening induced residual stress on fatigue performance in the aluminum specimen has been studied in the literature [30][33]. However, the relationship between the induced residual stress field and the resultant change to the fatigue life have receive little consideration.

In the first part of this work thesis, it was used the AFGROW Software to determine the fatigue crack growth behavior of the specimen under investigation. It was employed the version 4.0012.15, which is the last version owned by the Air Force Research Laboratory and it is free of charge.

The AFGROW software applies the damage tolerance philosophy to help eliminate the type of structural failures and cracking problems that had been encountered on various military aircraft. In the early 1970's, the United States Air Force review of structural failures had revealed that the safe life philosophy did not protect against designs that were intolerant to defects that could be introduced during manufacturing or during in-service-use. From the standpoint of flight safety, it was found prudent to assume that new airframe structures could contain initial damage and that not all crack would be found during inspections of older airframes. Accordingly, a damage tolerance

philosophy was formulated based on the demonstration of structural safety under the assumption that pre-existing damage would be present at critical locations of all structurally significant details.

4.2   Afgrow Software

AFGROW is a workstation-based, graphically interactive computer program for simulations of fatigue crack growth in common structures subject to spectral loading. It is a highly flexible code that utilizes standard user-interface objects to create a simple and intuitive environment for the fracture mechanics analysis.

The Stress Intensity Factor calculations in AFGROW are based on the concepts of Linear Elastic Fracture Mechanics. For most structural configurations these are determined based on closed-form solutions built into the code. The exceptions are the user-defined configurations, for which the SIF values for different crack lengths are obtained from an external source and specified by the user [34].

Moreover, one of the main advantages of the AFGROW software is the possibility to employ different user-defined specimen configurations through a graphical user interface with file management capability which allows the visualization and plotting of crack growth in real-time.

4.3   Objectives of the Work

The aim of this work is to determine the crack growth behavior in the M(T) specimen analyzed when residual stress fields are induced by Laser Shock Peening treatment. In order to that, it was first predict the crack growth rate

of the as machined specimen so that to compare it with the experimental results available to check the reliability of the adopted analysis method. Once the software is proved to be reliable, it was predicted the crack growth behavior of the specimen after the LSP treatment, therefore with residual stress fields applied.

The next step was to detect the improvement in the crack growth behavior achieved with the Laser Shock Peening treatment and then to determine the optimum residual stress field to reduce fatigue crack growth rate in centered through cracked specimens.

Finally, it is necessary to validate modeling predictions via sample manufacture, laser peening treatment and measurement of residual stress fields and fatigue lives.

4.4   Analysis Implementation

4.4.1   Geometry

It was chosen to studied the crack growth behavior in two different centered crack specimens of the following geometry:
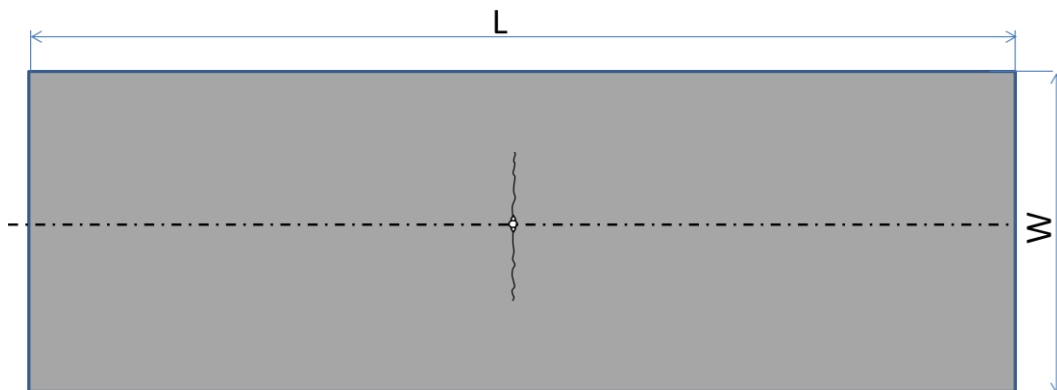
Fig. IV-I Specimen Geometry

	Specimen A	Specimen B
W	160 mm	400 mm
L	400 mm	800 mm
Thickness	2 mm	

Table IV-I Specimen Dimensions

The first step of the implementation is to define the model that should be introduced in the software. AFGROW has two different types of classic stress intensity factor solutions available:

❖ Standard Stress Intensity Solutions
❖ Weight Function Stress Intensity Solutions

For what it counts in this thesis work it has been used a classic model geometry with an internal through crack as reported in the figure below:
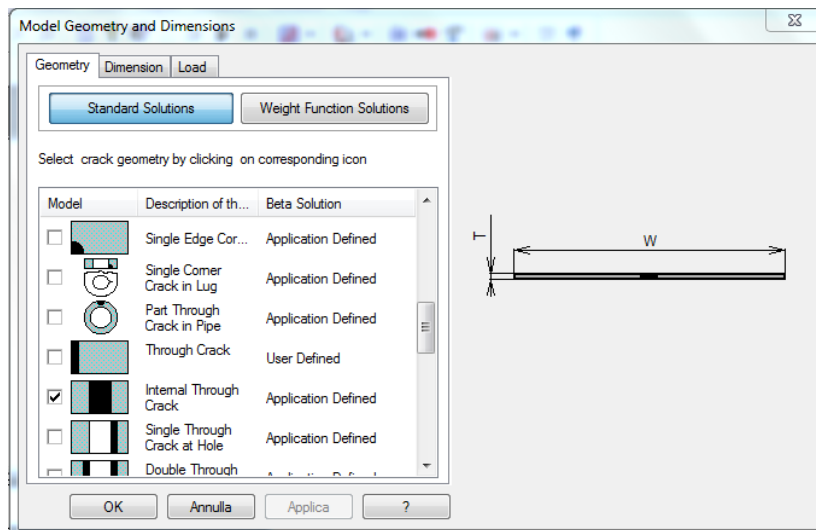
Fig. IV-II Standard Solutions – Internal Through Crack

The beta correction factor that the AFGROW software uses to determine the Stress Intensity Factor value for a tension load is the one used in [35].

$$K = \sigma\sqrt{\pi a}\left(1 - 0.025\left(\frac{2a}{W}\right)^2 + 0.06\left(\frac{2a}{W}\right)^4\right)\cdot\sqrt{\sec\left(\frac{\pi a}{W}\right)}$$

This solution is valid for 0 < a/W ≤ 0.5.

4.4.2   Load

AFGROW allows to introduce a cyclic load to the specimen in the form of spectrum which can be created by the user. Spectra are assumed to have been cycle counted so that each max-min pair describes a complete cycle. A cycle is defined as a stress (or load) excursion from a given starting level to a different level and return again to the same starting level.

Using the spectrum dialog box it is possible to introduce the Spectrum Multiplication Factor (SMF) which is multiplied by each maximum and minimum value in the user input stress spectrum. This allows a user to input spectra, which are normalized, and simply use one factor to predict the life for different stress levels.

In the case of interest it was used a constant amplitude loading with a SMF of 70 MPa and the R ratio of 0.1, so that it is not necessary to create a spectrum file as AFGROW will create it by itself.
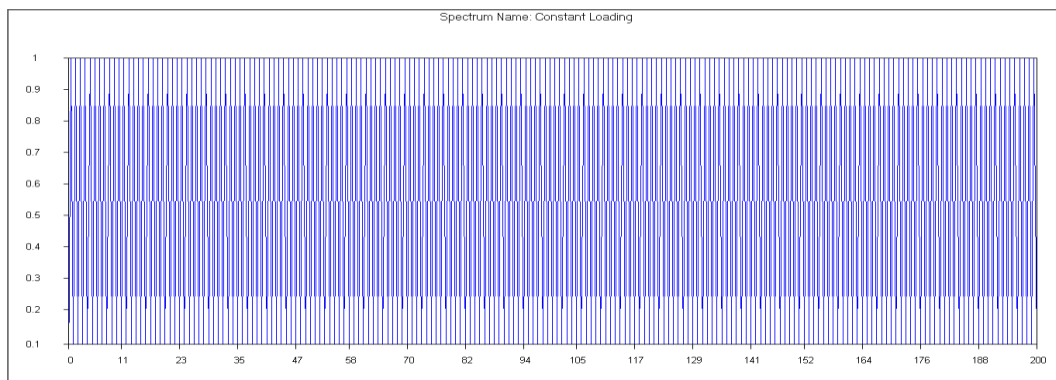
Fig. IV-III Constant Amplitude Loading

4.4.3   Material

The material used in this analysis is the Aluminum 2024-T351 which has been introduced in the AFGROW software using the tabular look-up crack growth rate.

A tabular look-up crack growth rate allows the user to input their own crack growth rate curves. The tabular data utilizes the Walker equation on a point-by-point basis to extrapolate/interpolate data for any two, adjacent R-values.

$$\frac{da}{dN} = C[\Delta K(1-R)^{m-1}]^n \qquad [Walker\ Equation]$$

The difference in the tabular lookup table is that the user doesn't have to calculate all of the m values because AFGROW does it internally between each two input R curves.

However, as it has been used a constant amplitude loading, it was necessary to introduce data only for a single R-value, which is the one of interest. In this case, the user-defined data will be used regardless of the stress ratio for a given analysis.

Beside the crack growth rate curves, the tabular look-up crack growth rate needs to be filled up also with other material parameters such as the ultimate strength, the Young's modulus, the Poisson's ratio and so on.
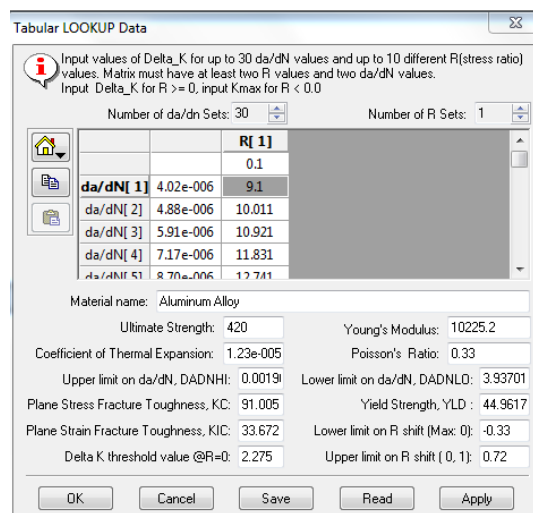
Fig. IV-IV Tabular Look-Up Data

The crack growth rate curves used in the analysis were derived by an average trend of the curve da/dN vs. ΔK values given by experimental results. In fact, in order to have a good agreement between the experimental results and the AFGROW ones, it is necessary to introduce da/dn and ΔK values manually. In the interest of finding average values which could represent in an acceptable way the Aluminum 2024-T351, different experimental values were taken into account [36].

The experimental values which were available are:
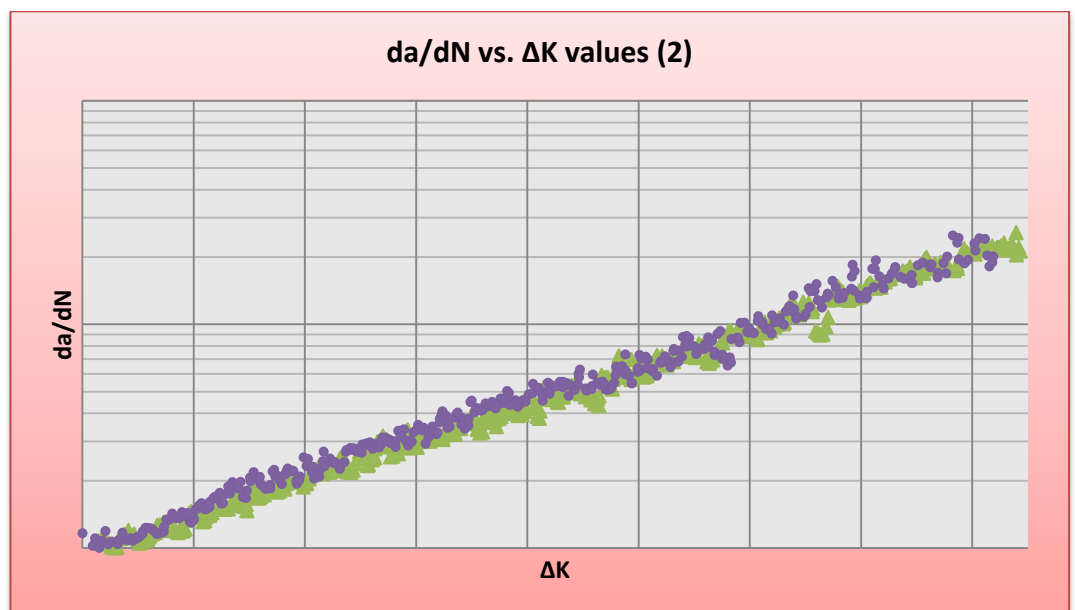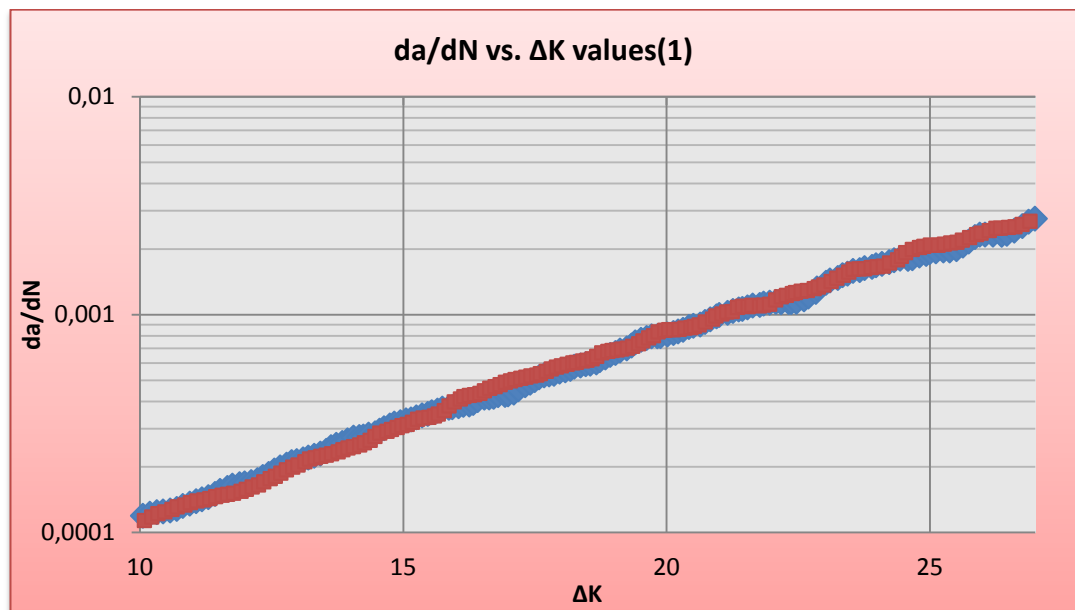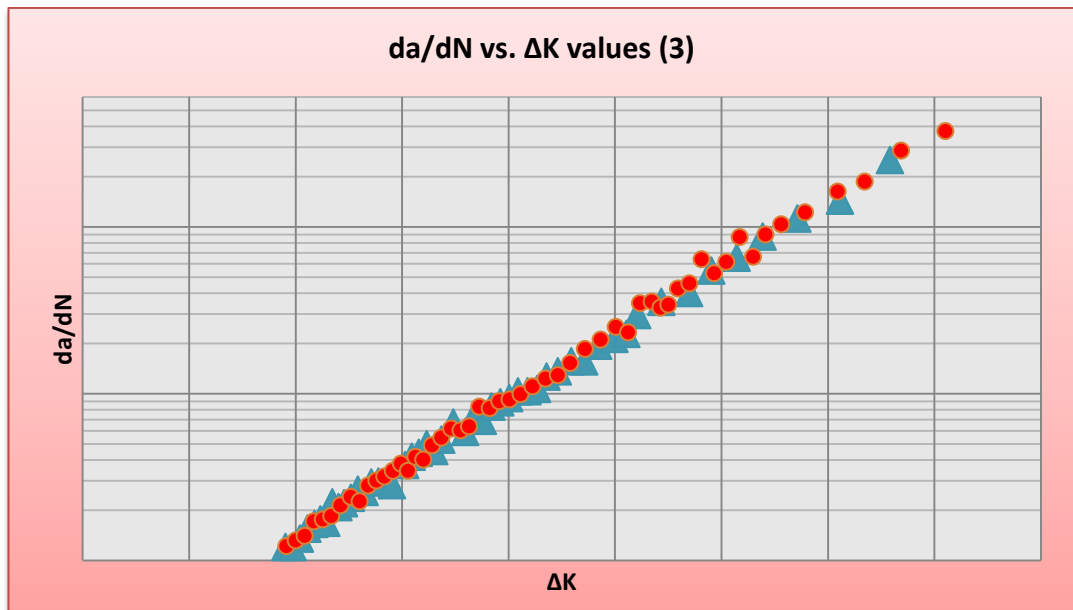
It needs to be noticed that the experimental values(1) are taken into account until a ΔK value at about 30 MPa√m, in fact the experimental specimens had a LSP stripe far 50mm from the centre line. For this reason it has been considered only the crack growth property of the specimen before the crack entered the LSP stripe which happens when ΔK is at about 35 MPa√m.

Putting all together, it can be sketched an average trend which will be used as a reference material in simulations from now on:
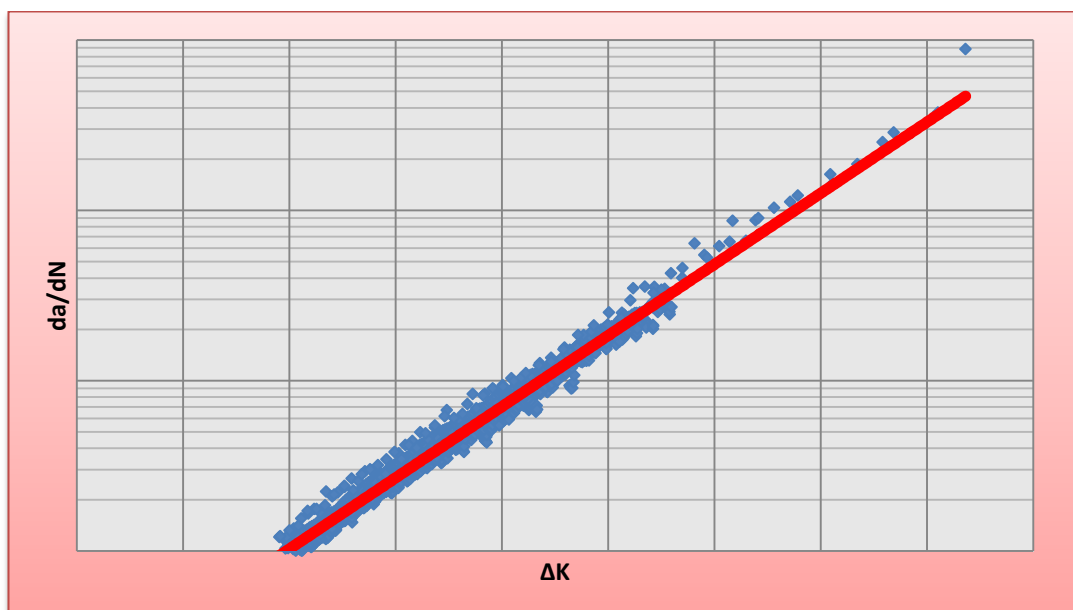
As it can be seen, it has been chosen to use the exponential trend as it seems to better represent the da/dN vs. ΔK experimental values.

Finally, using the trend line equation:

$$y = 1.5 \cdot 10^{-5} e^{0.192x}$$

It can be calculated 30 values of da/dN and ΔK to introduce in AFGROW in the tabular look-up crack growth rate in order to represent the material Aluminum 2024-T351 used in simulations.

da/dN	ΔK
1,02E-04	10
1,24E-04	11
1,50E-04	12
1,82E-04	13
2,21E-04	14
2,67E-04	15
3,24E-04	16
3,92E-04	17
4,75E-04	18
5,76E-04	19
6,98E-04	20
8,46E-04	21
1,02E-03	22
1,24E-03	23
1,50E-3	24
1,82E-03	25
2,21E-03	26
2,68E-03	27
3,24E-03	28
3,93E-03	29
4,76E-03	30

5,77E-03	**31**
6,99E-03	**32**
8,47E-03	**33**
1,03E-02	**34**
1,24E-02	**35**
1,51E-02	**36**
1,83E-02	**37**
2,21E-02	**38**
2,68E-02	**39**

Table IV-II da/dn and ΔK Values Used in Simulations

4.5   Baseline Results

Once all properties of the specimen are determinate, it is possible to run the simulation and to compare the results with the experimental ones [36] for the specimen 160x400 mm wide as there are no experimental results available for the specimen 400x800 mm wide.
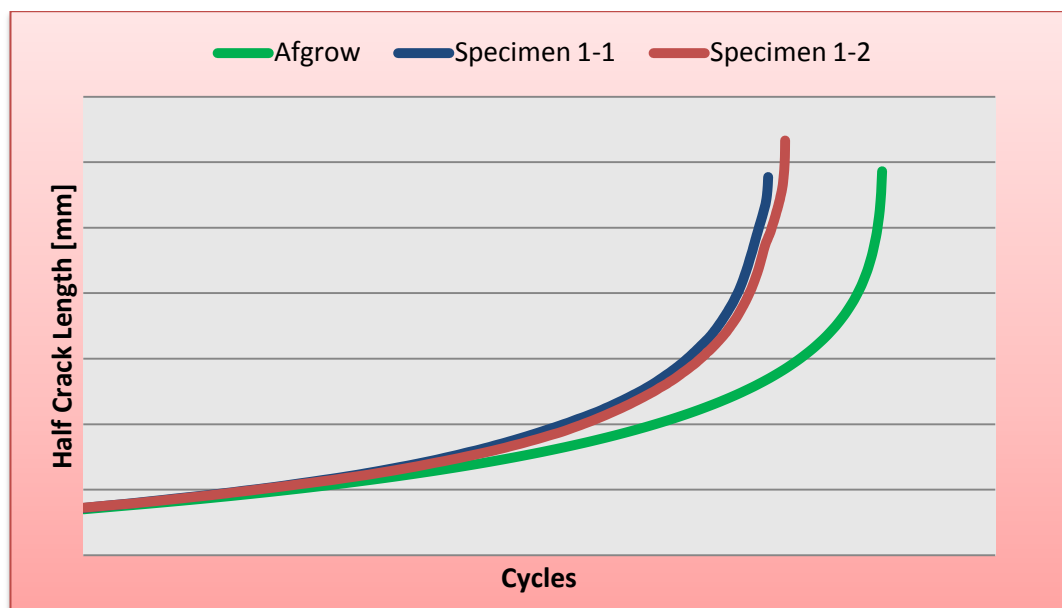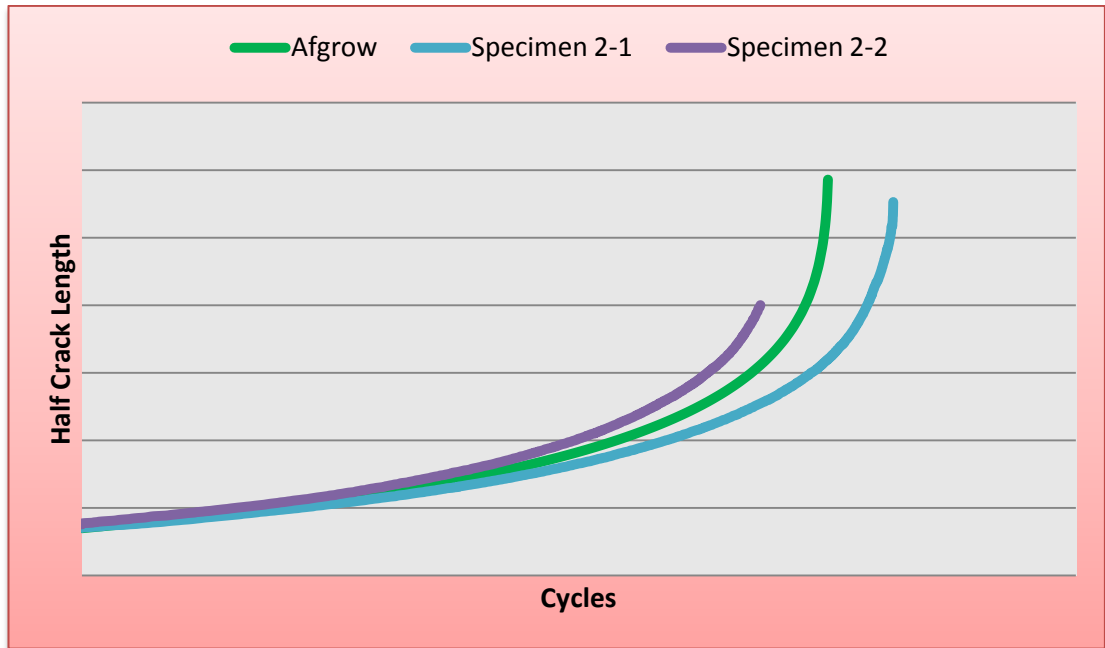
The results achieved represent the behavior of the baseline specimen using an average da/dN vs. ΔK curve. All things considered, results achieved seem to be similar with the experimental ones, therefore the described procedure can be used to represent the behavior of an Aluminum 2024-T351 specimen without any treatment on it.

4.6   Residual Stress Engineering

Once Afgrow is proved to better depict the trend of non treated specimens, it can be used to introduce residual stress and to predict the enhancement in the crack growth behavior achieved after the Laser Shock Peening treatment.

Afgrow can account for the existence of residual stresses by calculating additive residual stress intensities at user defined crack length increments.
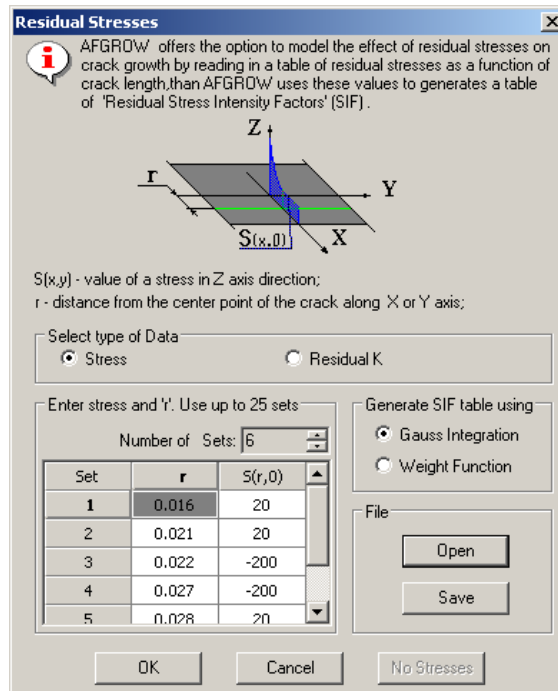
Fig. IV-V Residual Stress Simulation

It is possible to introduce normalized stress values in the crack plane and allow the Software to calculate residual stress intensity factors or enter pre-determined residual K values. In this application, negative stress can be used since the residual K is merely added to the stress intensities caused by applied load. This will not change ΔK, but will change the stress ratio, which will result in a change in the crack growth rate.

There are two methods available in Afgrow to calculate the residual stress intensities:

- ➢ Gaussian Integration Method
- ➢ Weight Function Solution

The Gaussian Integration Method uses the point load stress intensity solution from the Tada, Paris and Irwin Stress intensity handbook to integrate a given 2-D unflawed stress field to estimate K at user defined crack lengths increments.
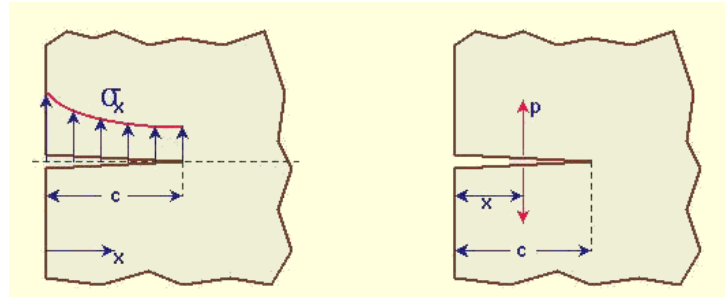
Fig. IV-VI Cracked Model For SIF Evaluation

$$K_I = \sum_{x=0}^{c} \sigma_x^* \cdot F(c,x) dx$$

$$F(c,x) = \frac{2}{\sqrt{\pi c}} \cdot \frac{1.3 - 0.05\left(\frac{x}{c}\right) - 0.2\left(\frac{x}{c}\right)^2 - 0.3\left(\frac{x}{c}\right)^3 + 0.25\left(\frac{x}{c}\right)^4}{\sqrt{1 - \left(\frac{x}{c}\right)^2}}$$

The weight function solutions provided through the effort of Prof. Glinka (University of Waterloo, CA) will only be possible if a weight function solution is available for the geometry being analyzed. The currently available weight function solutions are given below:

Model	Description of Configuration	Beta Solution
	Center Semi-Elliptical Surface Crack	Prof. Glinka
	Center Single Corner Crack at Hole	Prof. Glinka
	Internal Axial Crack in Thick Pipe	Prof. Glinka
	External Axial Crack in Thick Pipe	Prof. Glinka
	Center Through Crack	Prof. Glinka
	Single Edge Through Crack	Prof. Glinka
	Double Edge Through Crack	Prof. Glinka
	Radial Edge Crack in Disc	Prof. Glinka
	Axial Through Crack in Thick Pipe	Prof. Glinka

Fig. IV-VII Models For Which The Weight Function Solution is Available

The work plan is divided in three parts:

I   In the first one it is studied the crack growth improvement achieved with a LSP stripe wide 5 mm for specimens 160 and 400 mm wide

II In the second part it is implemented the analysis for the two geometries when a 10 mm wide LSP stripe is used.

III In the third part is studied how to balance the tensile and compressive residual stress which are introduced by the Laser Shock Peening treatment for different configurations.

The aim of the work is to find the best achievement in the crack growth behavior reached with the lowest number of LSP stripes in order to reduce the manufacturing costs of specimens.

It has to be noticed that in any case it was chosen to use an average value of residual stresses. It was decided to use the highest compressive residual stresses which allow the crack to propagate through the stripe.

4.6.1   Specimen 160 mm Wide

The first specimen studied is the one shown in figure:
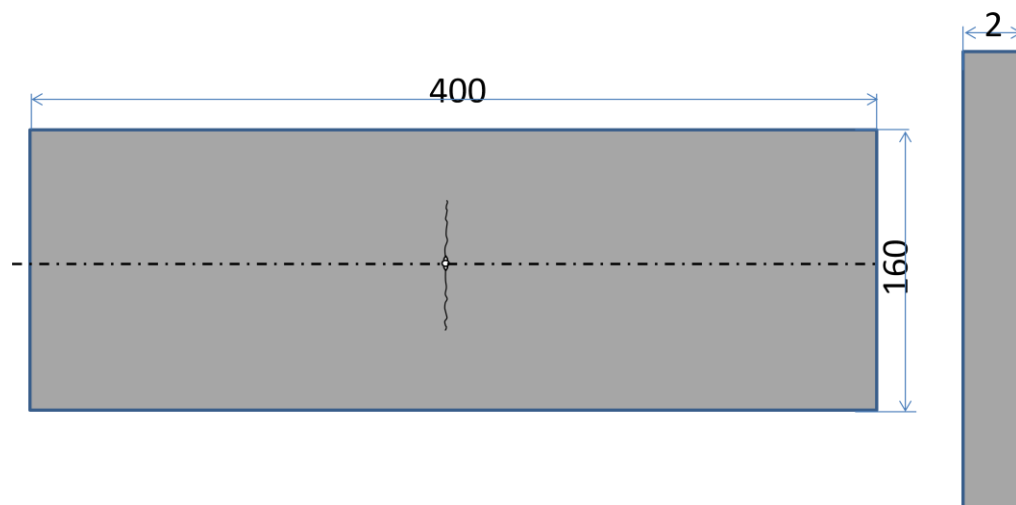
Fig. IV-VIII Specimen A

In the first step of the analysis it has been studied the crack growth behavior enhancement obtained with a LSP stripe 5 mm wide. For a very first approach, it has been considered a constant through thickness residual stress field. Several simulations were carried out, finally the best improvement in the crack growth behavior is reached when two LSP stripes 5 mm wide are placed as shown in the figure.
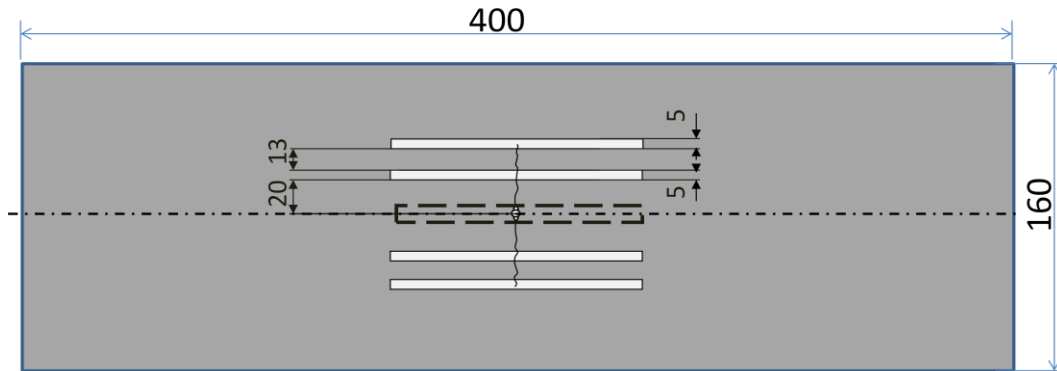
Fig. IV-IX Specimen A: Residual Stress Configuration – 5 mm Stripes
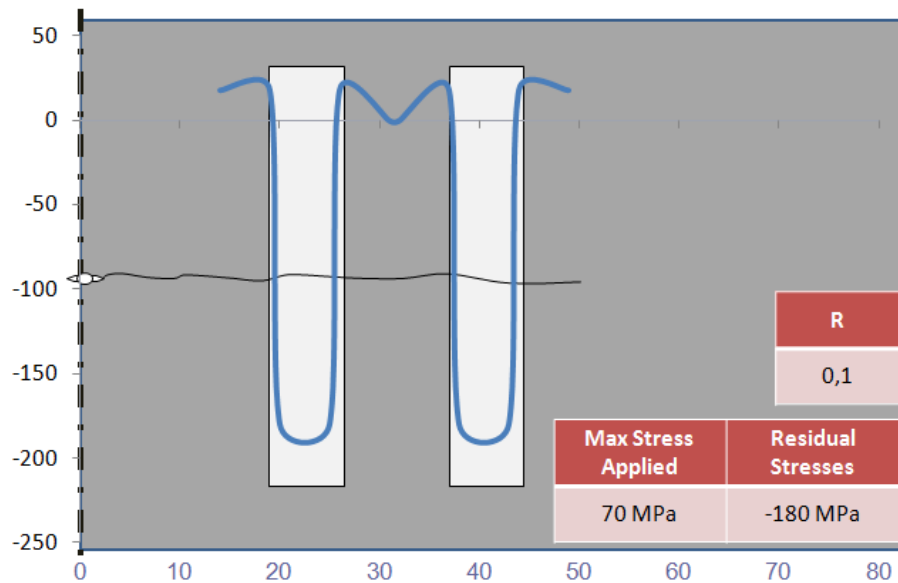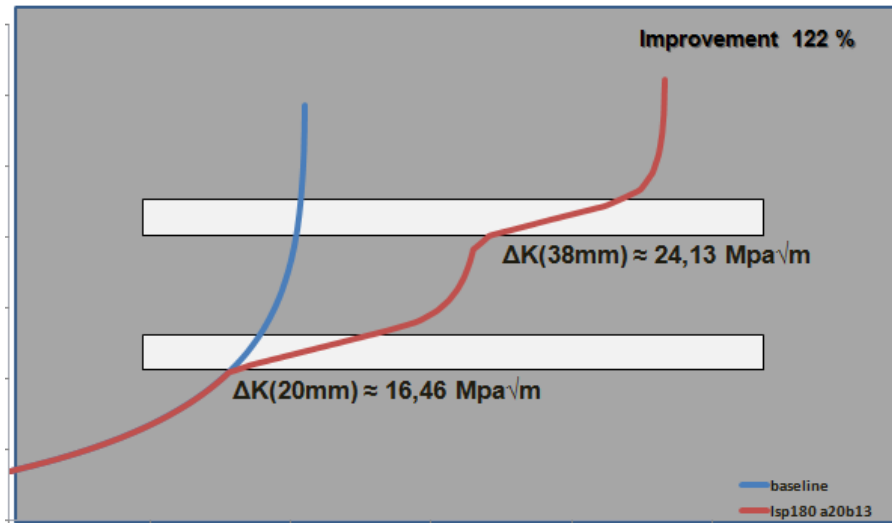
The best improvement in the crack growth behavior is reached when the two stripes are placed really close from each other but further from the centre line. It has been tried to add a third stripes but the crack growth improvement was at about 10% more than the previous simulation. The improvement gained is not worth the cost of the stripe, so the best configuration at the lowest cost is the one with two LSP stripes as shown.

In the second part of the simulation, LSP stripes 10 mm wide have been simulated, leading to a better crack growth behavior. The configuration reported in the next figure is the one which gained the best improvement.
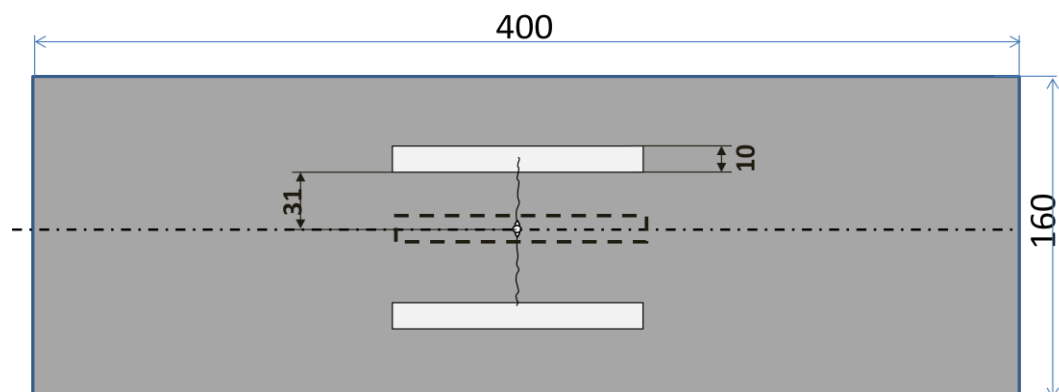
Fig. IV-X Specimen A: Residual Stress Configuration – 10 mm Stripe
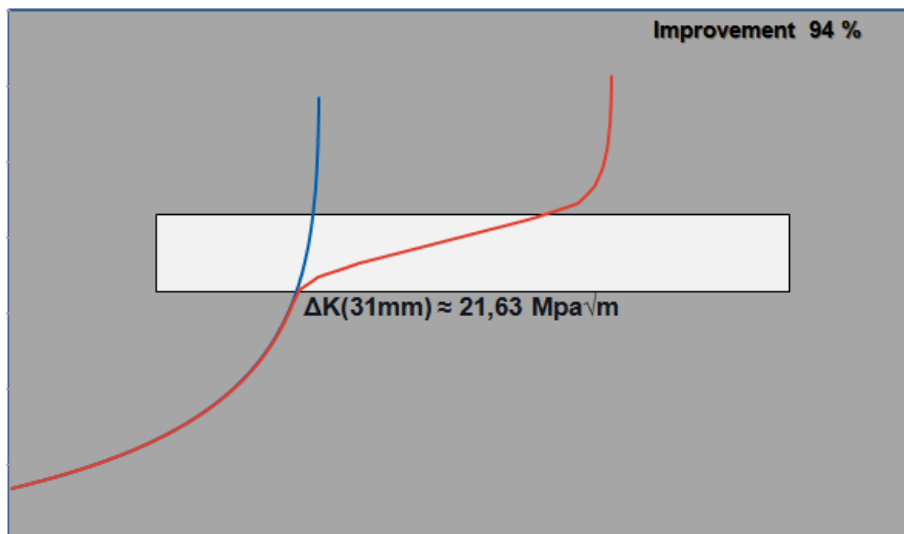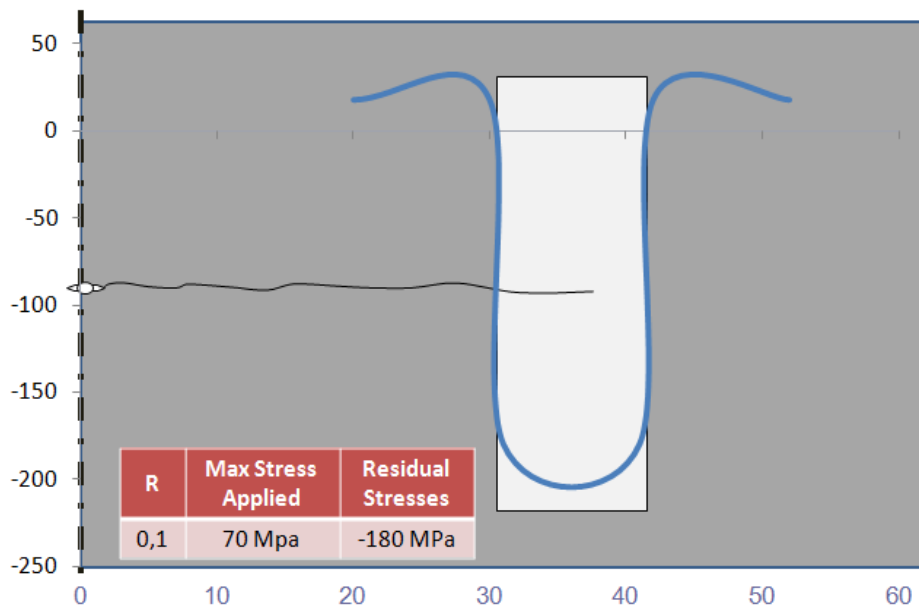
In the specimen 160 mm wide it not possible to introduce more than one LSP stripe 10 mm wide due to the net section yield reached when the half crack length is about 60 mm. In any case, it can be notice that using wider stripes lead to a better crack growth behavior, in fact with only one LSP stripe the fatigue life of the specimen is almost doubled.

Finally, the more the LSP stripe is placed near the centre line the better the crack growth behavior is. However, it is not possible to place the LSP stripe too close to the centre line. In fact, thinking about a real aircraft structure it is not known a priori where the crack would initiate and therefore the LSP

stripes should be equally spaced one from each other, and if the distance is too short the number of the LSP stripes would increase together with the manufacturing costs.

In the second step of the work it has been studied how to balance the tensile forces and the compressive forces which are introduced by the LSP process in order to have a stress-free surface which will not be lead to any deformations.

In the interest of doing that it was introduced a simplified residual stress profile with a linear piecewise trend and it was calculated the average force per unit of area in the tensile and compressive regions. The geometry used is shown in the figure.
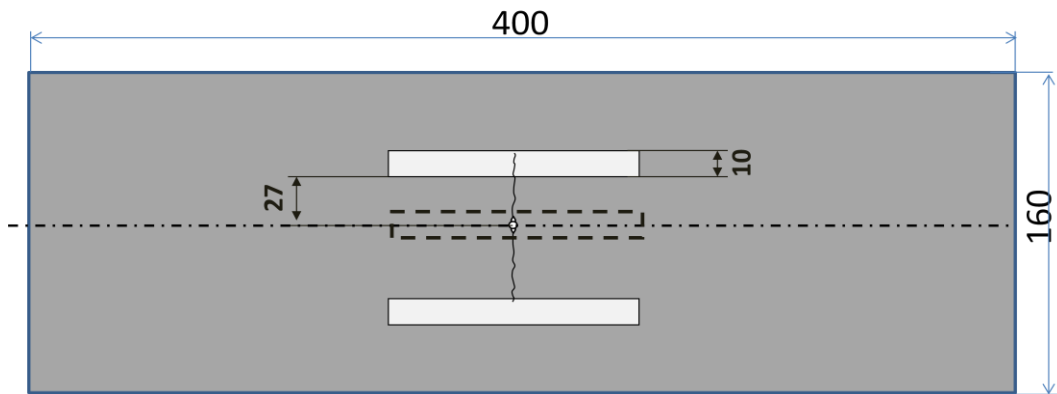
Fig. IV-XI Specimen A: Residual Stress Balanced Configuration – 10 mm Stripes

R	Max Stress Applied	Residual Stresses
0,1	70 Mpa	-150 MPa
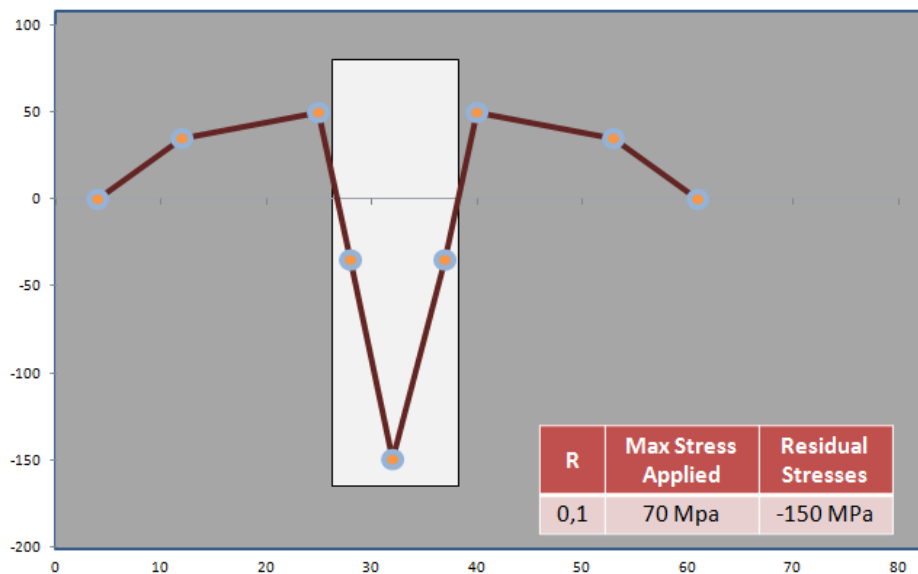
Using the residual stress profile shown in the picture it is possible to calculate the average force per unit area:

	Tensile	Compressive
Average Stress	42 MPa	-73 MPa
Total Area	1473 mm^2	858 mm^2
Average Force	62613 N	-62937 N

Table IV-III Specimen A: Tensile and Compressive Average Force

Results achieved using this residual stress field profile seem to present some issues. In fact, for the residual stress profile described previously there were not substantial differences when using the Gaussian Integration Method or the Weight Function Solutions, on the contrary, using this configuration lead to a totally different crack growth behavior, which is still not well understood.

It seems that the fatigue life prediction follows two different path, although it was demonstrate that the Weight Function Solutions were compared to existing closed form solutions to prove the accuracy of the Weight Function Solutions method.

4.6.2   Specimen 400 mm Wide

The second specimen studied is the one shown in figure:
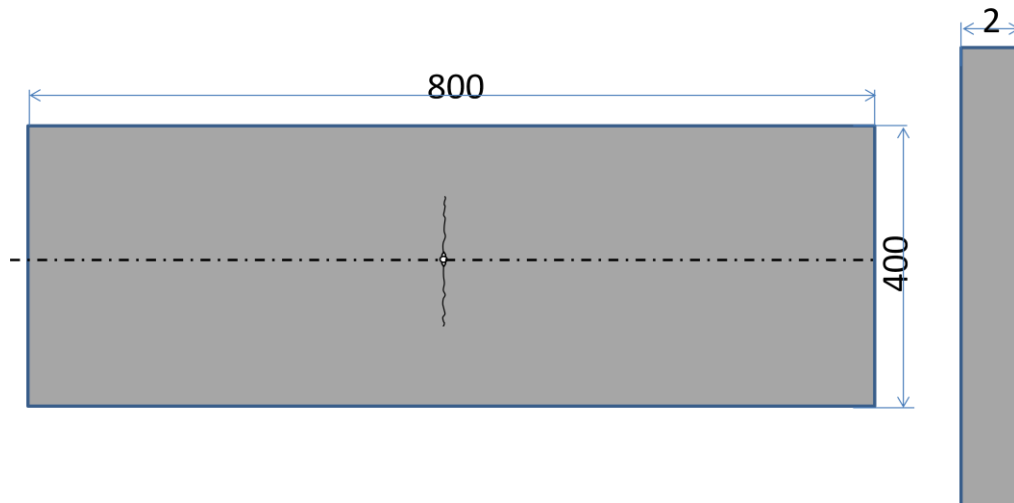
Fig. IV-XII Specimen B

As it has been explained in the previous paragraph, in the first step of the analysis there were studied different configurations of LSP stripes 5 mm wide. Considering a constant through thickness residual stress field, the best improvement in the crack growth behavior is obtained with three stripes placed as shown.
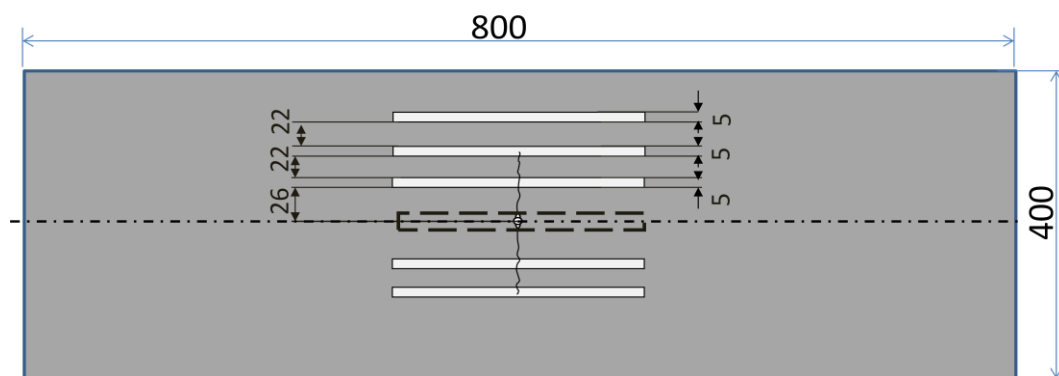
Fig. IV-XIII Specimen B: Residual Stress Configuration – 5 mm Stripes
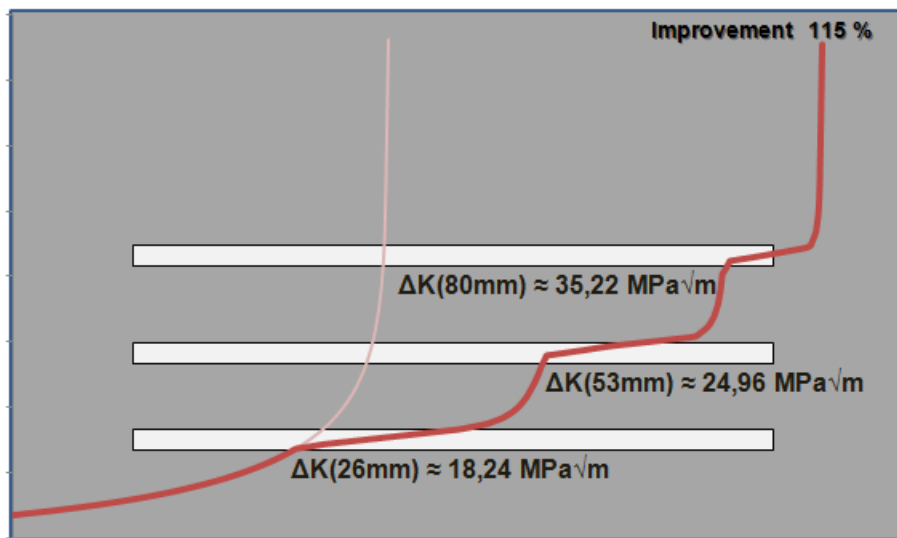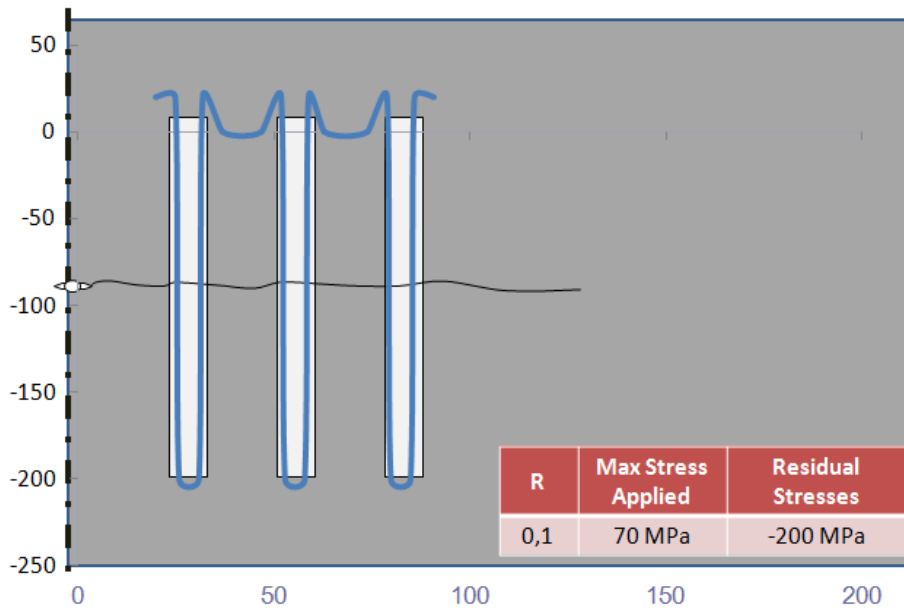
The best crack growth behavior is reached when three stripes are placed as close as possible to each other. Moreover, if a fourth LSP stripe is added, there is an enhancement in the crack growth behavior compared to the 3-stripes configuration. Nevertheless, at higher value of ΔK (i.e. circa 37 MPa√m) the crack growth behavior doesn't change substantially and it is not worth to add more stripes as the cost of the stripe will not justify the slightly improvement in the crack growth behavior.

In the second part of the simulation, it was studied the crack growth behavior when one or more LSP stripes 10mm wide are used. The configuration shown is the one which lead to the best enhancement in the fatigue life.
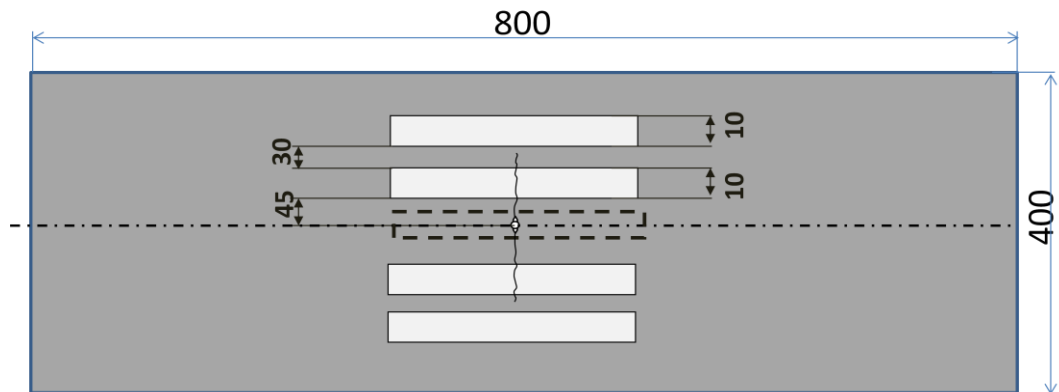
Fig. IV-XIV Specimen B: Residual Stress Configuration – 10 mm Stripes
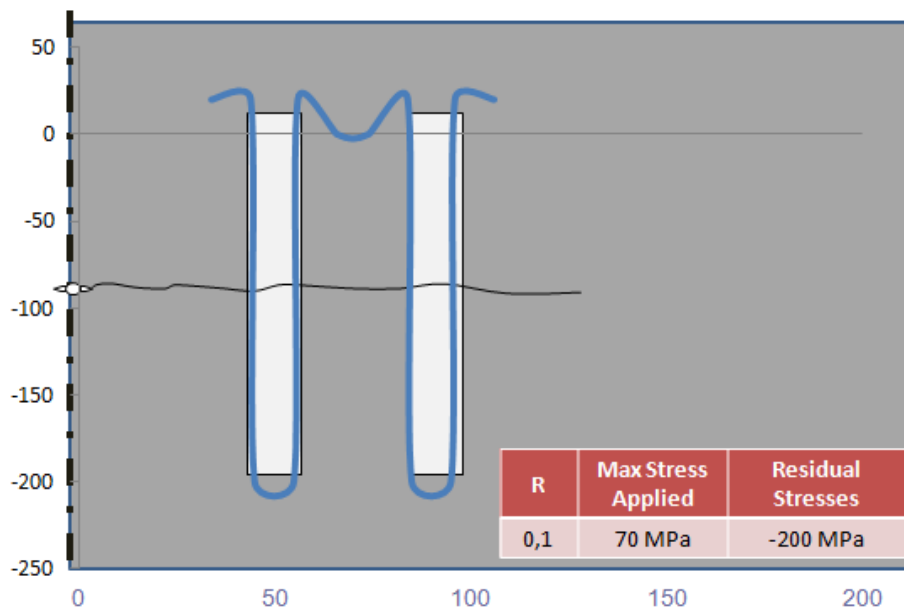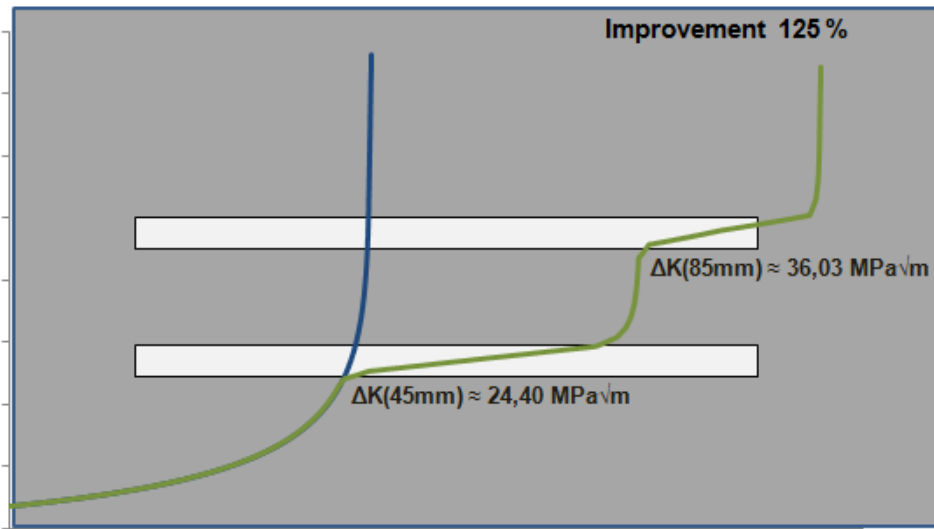
In this case, it was possible to introduce two LSP stripe 10 mm wide because the net section yielding occurred far away from the last stripe, that is when the crack length is about 140 mm.

It can be observed that using LSP stripes 10 mm wide, a better crack growth behavior can be achieved. However, it is recommended to reduce the number of LSP stripes in order to reduce the manufacturing costs.

In this example it has been also studied the enhancement in the fatigue life achieved when a LSP stripe 20mm wide is used. In fact, it is clear that the more the residual stress area increases the better the crack growth behavior is. It is not possible to study this configuration in the previous geometry due to the limited space that the crack has to propagate. Considering a LSP stripe 20mm wide, results achieved are shown.
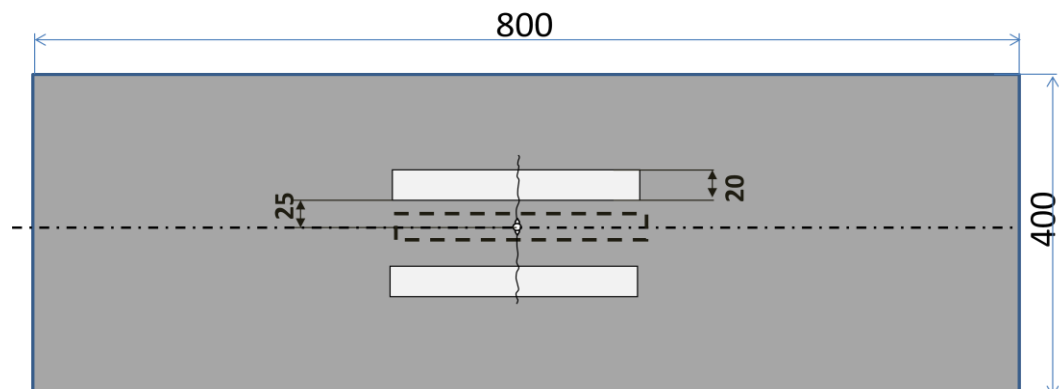
Fig. IV-XV Specimen B: Residual Stress Configuration – 20 mm Stripe

R	Max Stress Applied	Residual Stresses
0,1	70 Mpa	-120 MPa

Improvement 315 %

ΔK(25mm) ≈ 13,71 MPa√m
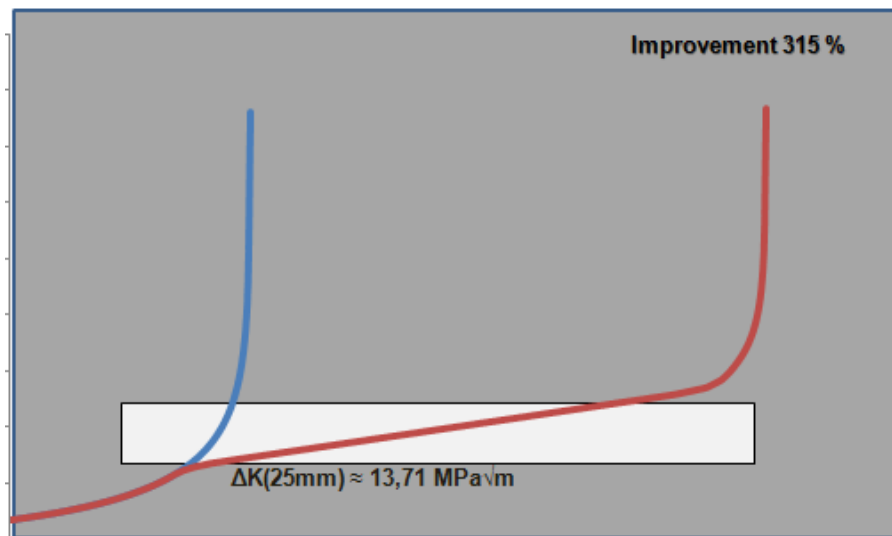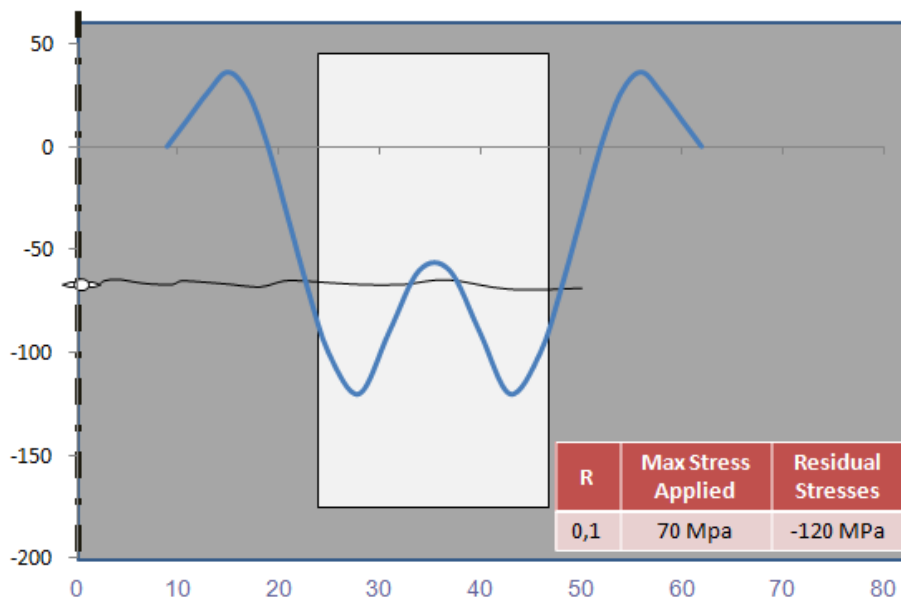
In this case, due to the width of the LSP stripe it is necessary to take into account that it might be a small drop in the stress intensity at the centre of the stripe.

Nevertheless, it is perfectly clear that the widest is the LSP stripe the better is the improvement in the crack growth behavior, in fact, using a stripe 20mm wide it is possible to triple the baseline fatigue life.

In the second step of the work, as it has been explained in the previous paragraph, it has been studied how to balance the tensile forces and the

compressive forces in order to have a stress-free surface which will not be lead to any deformations.

It was introduced a simplified residual stress profile with a linear piecewise trend and it was calculated the average force per unit of area in the tensile and compressive regions. The analysis were put in practice for the LSP stripe 10 and 20 mm wide.

The first geometry studied is reported in the figure:
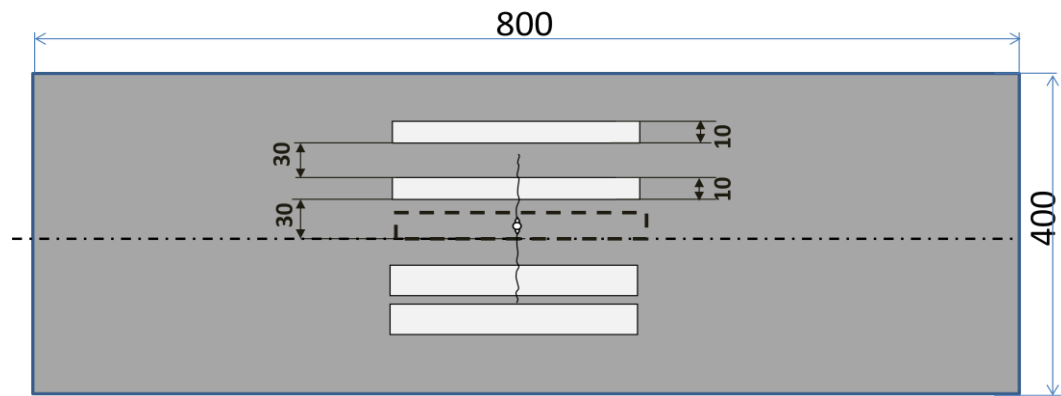
Fig. IV-XVI Specimen B: Residual Stress Balanced Configuration – 10 mm Stripes
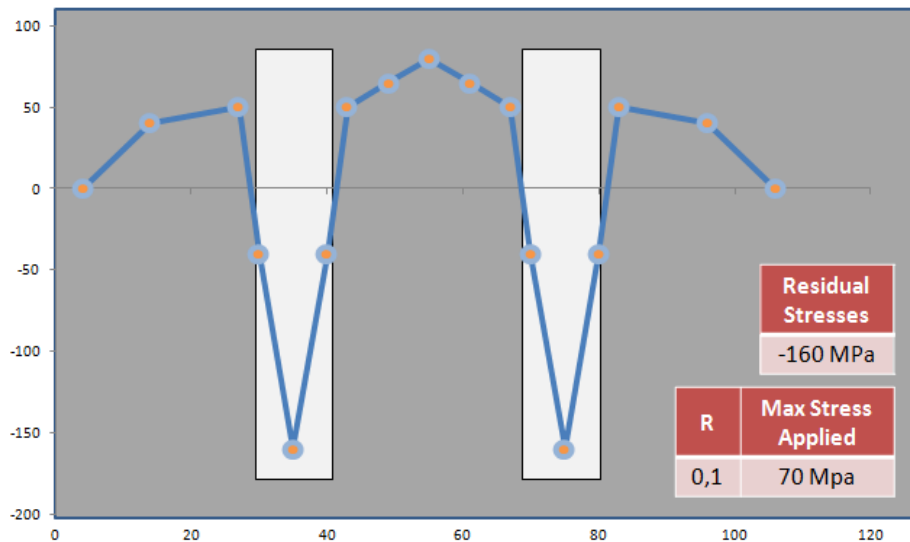
With the residual stress profile shown in the picture it is possible to calculate the average force per unit area:

	Tensile	Compressive
Average Stress	51 MPa	-80 MPa
Total Area	3296 mm^2	2107 mm^2
Average Force	168954 N	-168533 N

Table IV-IV Specimen B: Tensile and Compressive Average Force – 10 mm Stripes

Results obtained using the balanced forces seems to present some issues as it was explained in the previous paragraph. In particular, when the simulation is running using the Gaussian Integration Method or the Weight Function Solutions two totally different crack growth rates are surprisingly achieved.
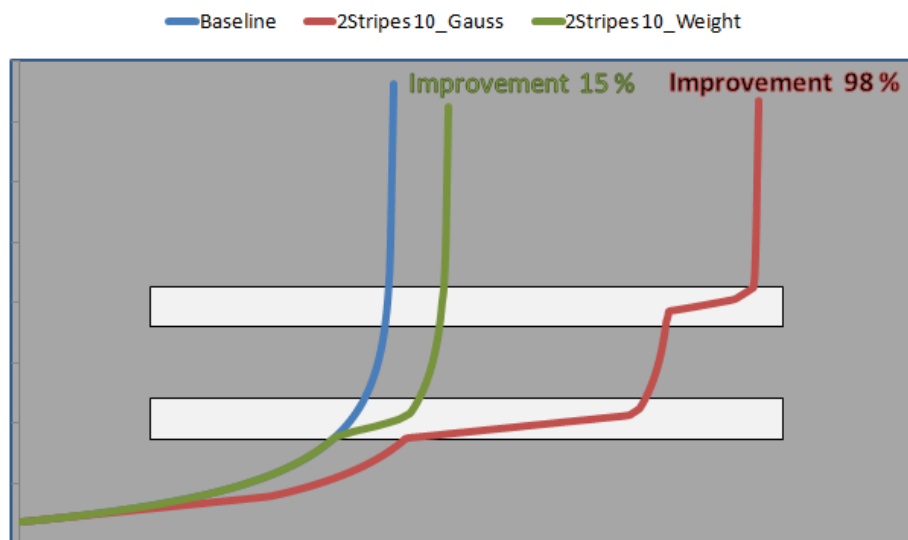
The same analysis was expanded for the LSP stripe 20 mm wide as reported in the next figures.
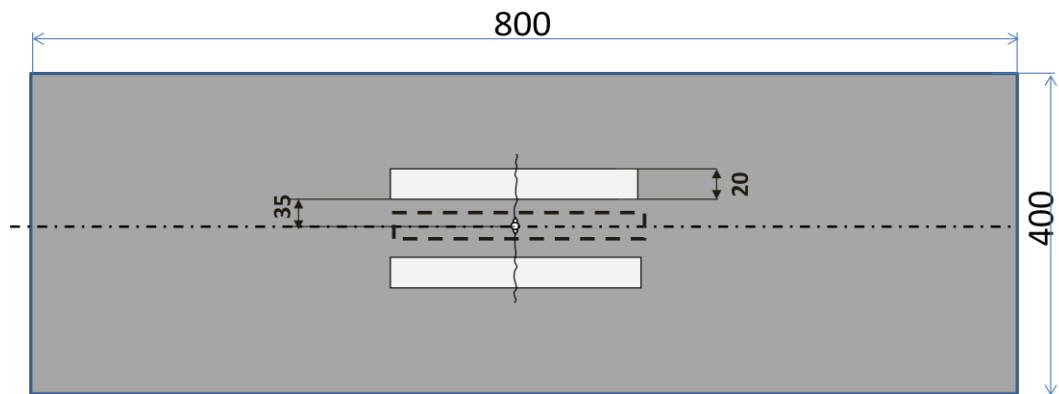
Fig. IV-XVII Specimen B: Residual Stress Balanced Configuration – 20 mm Stripe
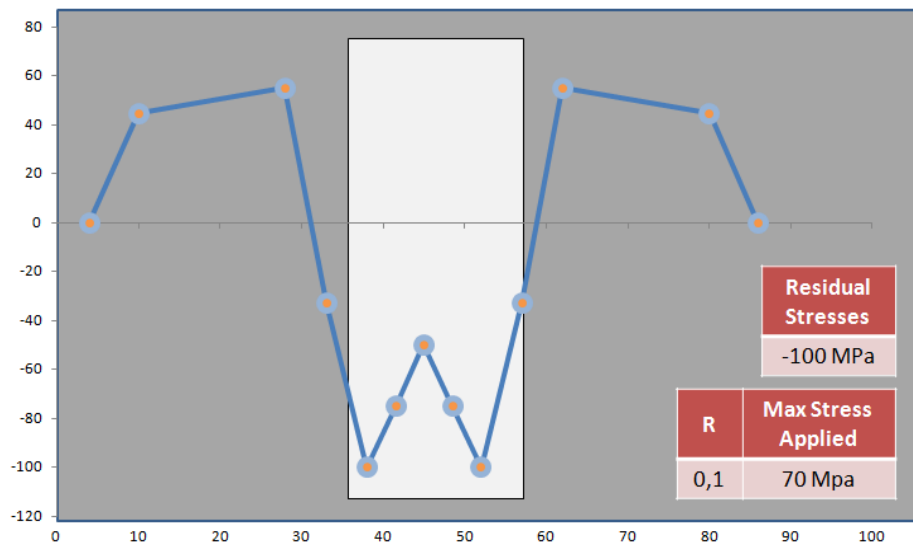
	Tensile	Compressive
Average Stress	50 MPa	-66 MPa
Total Area	2265 mm^2	1695 mm^2
Average Force	113258 N	-112607 N

Table IV-V Specimen B: Tensile and Compressive Average Force – 20 mm Stripe
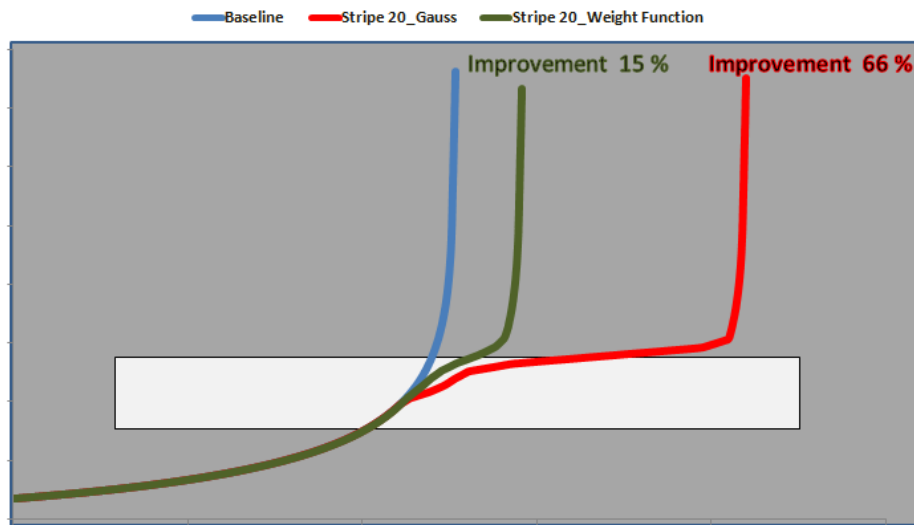
4.7   Treated Specimen Results

Results achieved in the first simulations seem to better represent the crack growth behavior of the treated specimen and seem to obtain an enhancement of the fatigue life property which is really promising. In particular, for both geometries studied, the improvement in the crack growth behavior enhances when the width of the stripe increases and the distance from the centre line and between two different stripes decreases.

In any case, as it has already been above mentioned, the distance between two stripes or from the centre line cannot be too short, as this would lead the number of the LSP stripes on a real aircraft structure to increase whereas the aim of the analysis is to find the best achievement in the crack growth life with the lowest number of stripes.

Finally, the best improvement in the crack growth behavior with the smallest number of LSP stripes for the specimen 160mm wide is the one with a LSP stripe 10 mm wide:
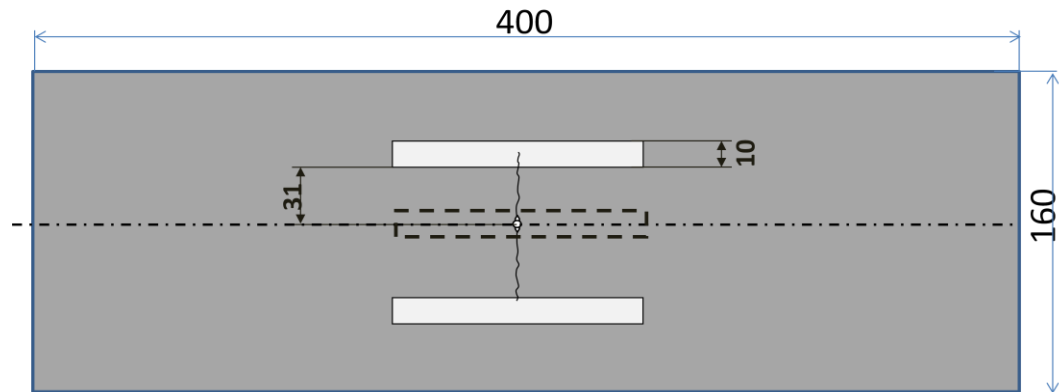
Fig. IV-XVIII Specimen A: Best Residual Stress Configuration

This configuration causes an improvement of about 94%, that is almost doubled the life of the specimen.

Concerning the specimen 400 mm wide the best configuration is:
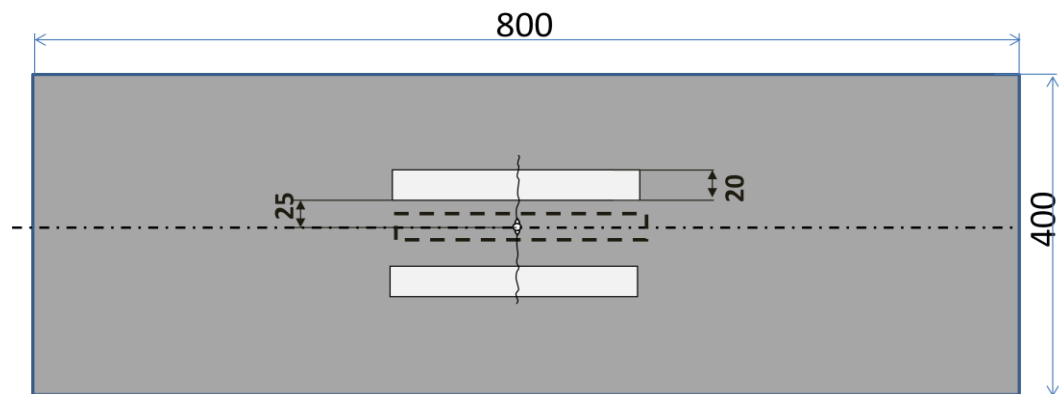
Fig. IV-XIX Specimen B: Best Residual Stress Configuration

The LSP stripe 20 mm wide achieves an improvement in the crack growth behavior rate which triplicate the fatigue life of the specimen comparing to the non treated one.

Nevertheless, even though these results seem to be really promising in improving the crack growth property of the specimen, it is necessary to remark that the compressive residual stress field need to be balanced with a tensile residual stress field, that it is exactly what happens in the reality as it can be seen from experimental measurement of the residual stress fields inside and outside the LSP stripe carried out by Open University, UK [36]. For

this reason, there were conducted further simulations where the balance of the tensile and compressive forces is taken into account.

However, the difference noted in the crack growth rate when using the Gaussian Integration Method or the Weight Function solutions is not realistic, or at least it should not be so evident.

4.8   Conclusion

It is not clear the reason why the AFGROW software gives two different Stress Intensity Factor table when the two methods are used with the same stress intensity value used, but these results for sure don't match the experimental results and cannot be reliable for further investigations.

Moreover, it is still not comprehensible the AFGROW procedure to evaluate the crack growth prediction starting from a residual stress field manually introduced. It is not well understood which are the steps used by the software and how it converts the residual stress introduced manually into a slowdown of the crack propagation in the model. In fact, it seems that AFGROW is using some algorithms that generate an error in the crack growth prediction when two different methods are used.

For this reason it has been decided to split the analysis in different steps, knowing exactly the theory which is beyond each step calculation. In particular, it has been chosen to restart simulations using the Finite Element analysis with the Abaqus software, which is a complete and reliable software already used successfully for different purposes, to evaluate the Stress Intensity Factor for different crack lengths. The second step would be to re-use the AFGROW software to predict the crack growth behavior of the model, using as input a dimensionless parameter evaluated after the Finite Element Analysis which hopefully would avoid the unexpected behavior detected in the AFGROW software when a balanced compressive/tensile residual stress field is introduced in the model.

Ⅴ. Introduction to the FEM Analysis

With an increasing computing power, the finite element method has become one of the most important methods for the numerical solution of partial differential equations. Originally invented by engineering disciplines, the method has been given a thorough mathematical foundation over the past decades.

Finite Element Analysis (FEA) was first develop in 1943 by R. Courant, who utilized the Ritz method of numerical analysis and minimization of variational calculus to obtain an approximate solutions to vibration systems.

By the early 70's, FEA was limited to expensive mainframe computers generally owned by the aeronautics, automotive, defense and nuclear industries. Since the rapid decline in the cost of computers and the phenomenal increase in computing power, FEA has been developed to an incredible precision.

At present days, FEA modeling is possible to be used by any industries thanks to the supercomputers which are now available to produce accurate results for all kind of parameters.

FEA can provide solutions to problems that would otherwise be difficult to obtain. In terms of fracture, FEA most often involves the determination of stress intensity factors, but it has applications in a much broader range of areas, as fluid flow and heat transfer.

5.1   Fundamentals of the FEM

There are generally two types of analysis that are used in industries: 2-D modeling and 3-D modeling. While the 2-D modeling conserves simplicity and allows the analysis to be run on a relatively normal computer, it tends to yield less accurate results. On the other hand, 3-D modeling produces more accurate results while sacrificing the ability to run on all but the fastest computers effectively. Within each of these modeling schemes, the programmer can insert numerous algorithm which may take into account plastic deformation. Non-linear systems do account for plastic deformation, and many also are capable of testing a material all the way to fracture.

In this work thesis, it has been used the FE software Abaqus/CAE which provides a complete modeling and visualization environment for Abaqus/Explicit and Abaqus/Implicit analysis products.

FEA uses a complex system of points called nodes which make a grid called a mesh. The mesh is programmed to contain the material and structural properties which define how the structure will react to certain loading conditions. Nodes are assigned at a certain density throughout the material depending on the anticipated stress levels of a particular area. Regions which will receive large amounts of stress usually have a higher node density (i.e. a finer mesh) than those which experience little or no stress.

FEA has become a solution to the task of predicting failure due to unknown stresses by showing problem area in a material and allowing designers to see all of the theoretical stress within it. This method of product design and testing is far superior to the manufacturing costs which would accrue if each sample was actually built and tested.

5.2   Practical Application of FEM

Every FE analysis consists of model identification by node coordinate definition, element property definition, material definition, load definition and boundary conditions definition. Once all these information are given, the FE software tool derives the elements of the stiffness matrix and further defines the global stiffness matrix, the load vector and integrates the constraints to formulate a set of equation which represents the structure under analysis. Finally, the solver outputs the results (i.e. the deformations) of the set of equations. All other outputs, such as stresses or strains are calculated afterwards.

For a complete FE analysis three basic steps which are independent from each other are necessary:
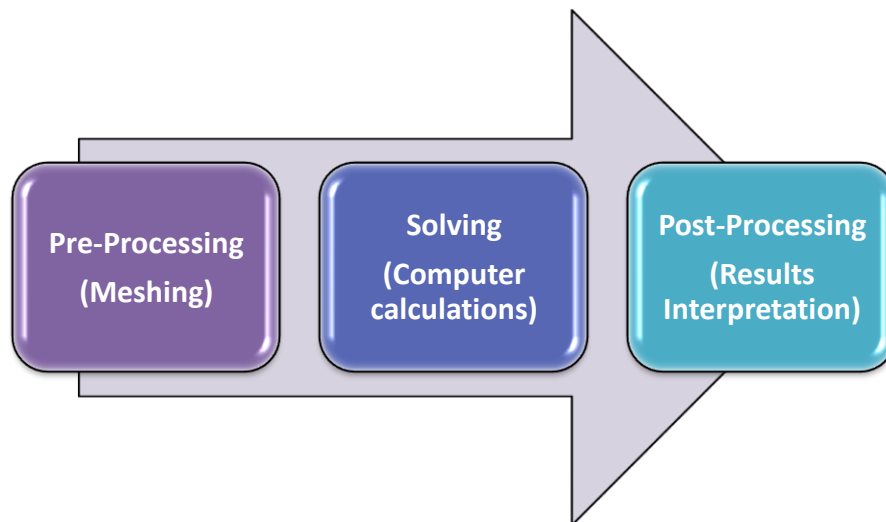
Fig. V-I FE Analysis Steps

5.2.1   Pre-Processing

The pre-processing step involves building a mathematical model of the part which is analyzed and breaking it down into thousands of tiny pieces that are regularly shaped through a process called meshing. In this way, stresses and

strains can be calculated for all the regular elements and then adding all those results together, it is possible to figure out the overall stress and strain within the part and the way it deform due to the applied loads.

Element type, size, shape and quality does have a big effect on the accuracy of results though. In fact, the more elements are present, the more accurate results will be, but the analysis will take longer to run. So it is a matter of finding a balance between the accuracy of the model and the run time.

Once the model is meshed, material properties need to be defined and applied to the meshed part. These properties include the Young's modulus, its density, its elastic and plastic properties and more, depending on the complexity of the analysis. The next step in the pre-processing stage is to apply loads and boundary conditions to the model.

5.2.2   Solving

The solving stage's purpose is to send the model off and let the computer do all the calculation work. The software goes through the meshed model and solves a set of mathematical equations for each of the nodes to figure out the overall stress and deformation of the part.

These equations are based on the F=k·x elastic equation for a spring. In FEA most structures can be considered as a big, complex spring, where the displacement needs to be calculated for each node of the model.
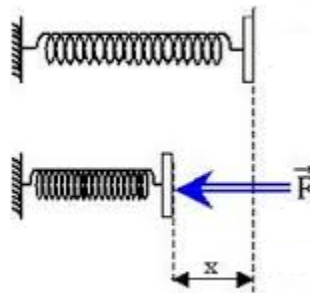
Fig. V-II Spring Subjected to an Elastic Force

Once it knows the nodal displacements and how each element is deforming, it can also calculate stress within the element, determining if the part is going to break or not.

5.2.3   Post-Processing

Post-Processing is the part of the analysis process that involves reviewing and interpreting the results from the solver. The output is usually a deformed shape of the part with a stress intensity distribution based on colored contours where it is possible to easily understand if any 'hot spots' are present.

The Post-Processing stage allows to understand how the stresses are developing and what changes can be made to improve the design in order to reduce areas of high stress and even to determine how much material can be removed from area of low stress, resulting in a stronger, lighter part.

The final step is to determine whether a part will break by comparing the stress values from the analysis results to the strength of the material and to evaluate if any plasticity effect is present. Ideally, the whole aim of the analysis is to make sure the stresses within the part remain below the yield strength of the material.

5.3   FEM Simulation Strategy

In the fracture mechanics field, the study of defects propagation in materials covers a predominant role. In fact, starting from the design phase, it is fundamental to know by means of theoretical and numerical model, how flaws propagate, in a stable or unstable manner, and in which direction.

In the last decades, different theories were formulated, and starting from them it was possible to introduce several numerical techniques to reproduce a specific phenomenon in order to deeply understand its effects and its causes on a real structure.

5.4   Objectives of the Work

To investigate the mechanical behavior and predict the crack growth property of the material subjected to a residual stress field, Finite Element Method is first introduce by Braisted and Brockman with software Abaqus in 1999 [37]. In the past decade, several researchers have used Abaqus to analyze the laser generated shock waves propagating into different materials and some of these simulations have a close match with experimentally measured residual stresses. A lot of work has already been done on simulation of the Laser Shock Peening process via FEM analysis, simulating the geometrical constraints impact on Residual Stress distribution after LSP [38], or simulating the LSP process on curved surfaces [39], and so on.

The effect of LSP induced residual stress on fatigue performance in different materials has been studied in the literature. However, the relationship between the induced residual stress field and the resultant change to the fatigue life has received little consideration.

The aim of this thesis is indeed to study the enhancement of the crack growth behavior due to the introduction of compressive residual stress field after the

Laser Shock Peening treatment. It will not be studied the simulation of the process as it has already been done by several researches in the past decades. Therefore, the inputs of the work are the residual stress field intensity which are represented as a LSP stripe that is supposed to slow down the crack growth rate when passing through it, and the output of the FE analysis is the SIF table of the specimen at different crack lengths when a LSP stripe is present.

5.5 Finite Element Analysis of Stress Intensity Factors

Finite Element Analysis (FEA) is a useful and verified method to obtain SIFs for widespread geometries and loading conditions which cannot be found or composed by standard cases in the literature. Currently, there are two FEA approaches existing to create a crack:

- ✓ The "classic" FEM approach
- ✓ The XFEM approach

The XFEM approach (Enriched Finite Element Analysis) is the most innovative function which allows to study the crack growth along an arbitrary, solution-dependent path without needing to remesh the model, so to reduce a lot the work effort. In reality, investigations have shown that the XFEM is still a research area and that it is not practical for certain geometrical boundary conditions to obtain accurate SIF solutions. For instance, any geometry with stress raisers (e.g. holes) could not contribute to accurate results for SIFs by using XFEM [40].

On the other hand, the "classical" FEM approach is capable to produce accurate results, but it is coupled with much bigger efforts, since a relatively fine and focused mesh must follow the crack front.

Basically, there are three approaches for SIF evaluation via FEM:

I.   Direct Method: SIFs are obtained by numerical results of   stress, displacements or crack-opening displacements

II.   Indirect Method: The stress intensity is obtained from its relation to other quantities such as elastic energy, work energy for crack-closure

III. Cracked Element: A cracked element capable to represent stress intensities in the finite-element grid can be used to determine SIFs from nodal displacements along the periphery of the cracked element

In this work thesis, the method which has been used is the indirect method. The indirect method uses the relationship existing between the elastic-energy present in a cracked structure, represented by the J-integral, and the stress intensity. In Abaqus the relation between the J-Integral and the SIF is the following:

$$J = \frac{1}{E}(K_I^2 + K_{II}^2) + \frac{1}{2G}\ K_{III}^2$$

For plane stress, axisymmetric and three dimensional conditions.

The FE mesh must be structured around the crack tip and the crack front to account for the contour integral calculations. Abaqus uses the crack front to compute the first contour integral using all of the elements inside the crack front and one layer of elements outside the crack front. It is possible to request more than one contour integral, in which case Abaqus adds a single layer of elements to the group of elements that were used to calculate the previous contour integral.
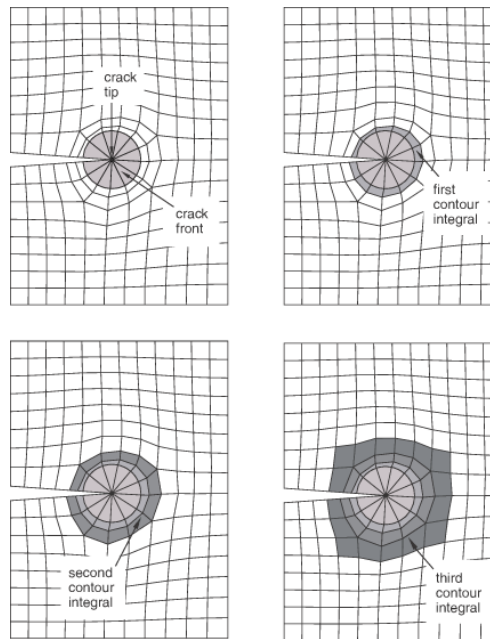
Fig. V-III Structured FE Mesh for Contour Integral Evaluation

Moreover, if the geometry of the crack region defines a sharp crack, the strain field becomes singular at the crack tip, so it is necessary to include the singularity in the model for a small-strain analysis improving the accuracy of the contour integral and the stress and strain calculations.

Finally, the mesh must allow the crack to open or close along the crack flanks. This needs to be implemented by generating double overlapping nodes along the crack flanks.

Solutions for SIFs or J-integrals, respectively, can either be determined stationary for different crack sizes or by unzipping nodes as the crack is propagating through the FE grid.

5.6   Analytical Solutions for Through Centered Crack in a Finite Plate

Current stress intensity factor solutions for part-through crack in narrow finite width plates are really accurate. In this work thesis, it has been studied a M(T) specimen with a centered through crack which propagate through the width of the panel.
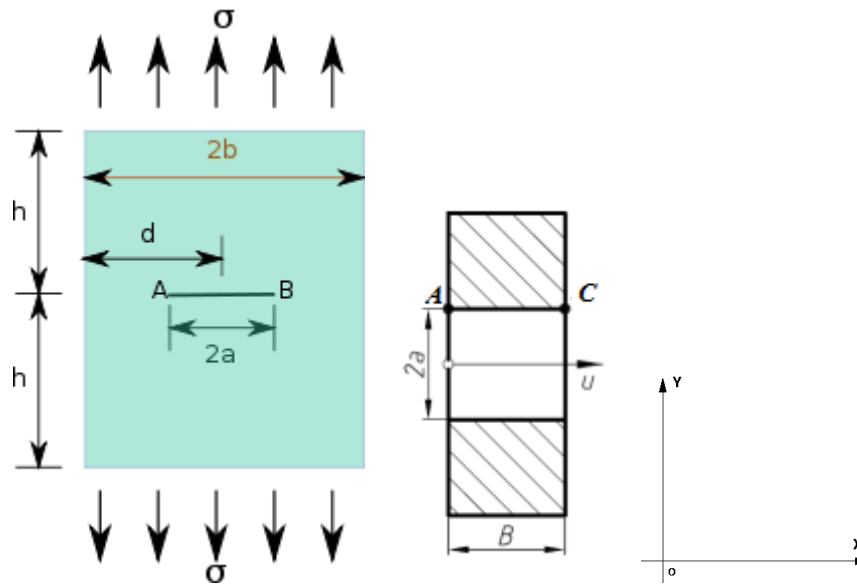
Fig. V-IV Centered Through Crack Finite Plate

The crack is characterized by the surface crack length 2a and it is a through-thickness crack. The SIF along the crack front for this configuration under a remote uniform stress P normal to the crack pane is described by:

$$K_I = \sigma\sqrt{\pi a}\sqrt{\sec\left(\frac{\pi a}{2b}\right)} \qquad with\ P = \frac{\sigma}{2b}$$

For a linearly varying stress distribution through the thickness, which does not vary with the in-plane coordinate x, the stress intensity factor K_I is given by:

$$K_I = \sqrt{\pi a}\ (P_m + P_b f_b)$$

Where P_m and P_b are the membrane and bending stress components respectively, which define the stress distribution P according to:

$$P = P(u) = P_m + P_b \left(1 - \frac{2u}{B}\right) \qquad for\ 0 \le u \le B$$

P is to be taken normal to the prospective crack plane in an uncracked plate. The co-ordinate u is defined in the sketch above.

The geometry function f_b is equal to 1.0 at the free surface at u=0 (point A) and f_b=-1.0 at u=B (point C), see sketch above.

For a stress which is constant through the thickness but varies with the in-plane dimension as P(x),

$$K_I = \frac{1}{\sqrt{\pi a}} \int_{-a}^{a} P(x) \left[\frac{a + x}{a - x}\right]^{1/2} dx$$

5.7   Crack Growth Predictions

Crack growth predictions are very complex in nature because of the vast amount of influences on the crack life by many different factors. However, any prediction model must be based on the assumption that flaws or small cracks are already present in the structure.

Therefore, crack growth predictions represent only the crack propagation period, which is only a small step in the fatigue life of the components.
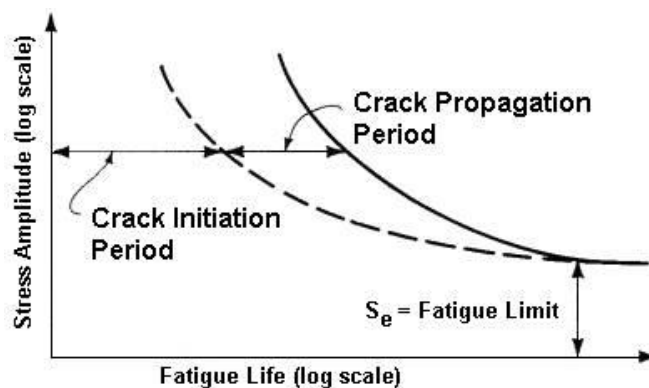
Fig. V-V Fatigue Life of a Component

The main factor for the crack propagation period is the SIF and further the SIF range, completive. The use of the SIF range is mainly based on the similitude concept which will be described in the next paragraph.

In addition, crack growth prediction models take into account other mechanism, e.g. crack closure behavior. There are several crack growth prediction models established by researches and engineers to accurately model crack growth for a specific configuration.

VI. FEM Modeling Strategy

6.1   Work Purpose

The aim of this work is to simulate the crack growth prediction of Aluminum specimen with a residual stress area defined by one or more LSP stripe.

In order to simulate the crack growth behavior it has been used the AFGROW software which was already described in chapter IV. Unfortunately, it was proved that introducing compressive residual stress directly in AFGROW, a dissimilar crack growth prediction was obtained when two different methods were used, therefore it was decided to calculate the beta correction factor first using the Abaqus software and then introducing it in AFGROW, trying to avoid the different crack growth behavior.
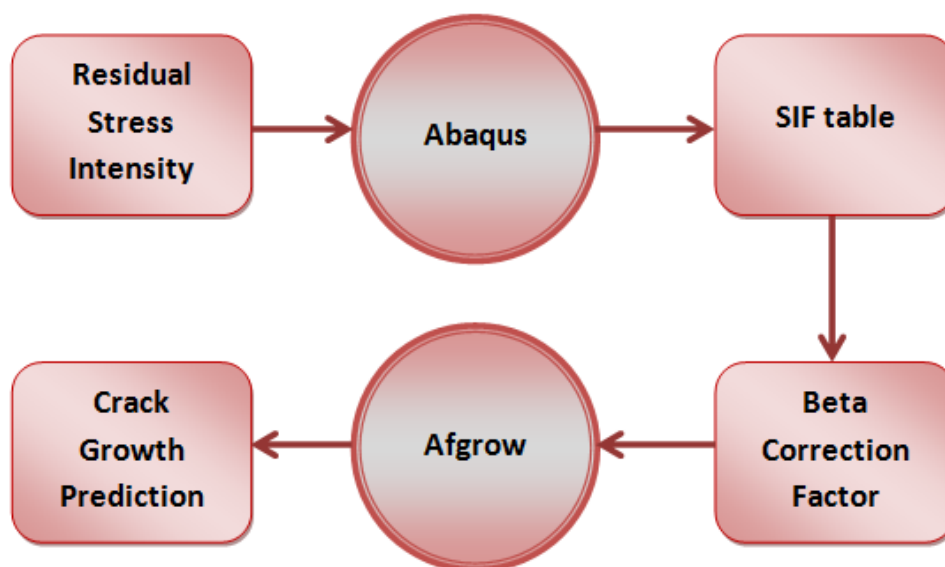
Fig. VI-I Work Flow Chart

In order to obtain reliable results using the Abaqus software, it has been decided to predict the crack growth behavior of the baseline specimen and to compare it with the analytical results so that the reliability of the adopted analysis method will be proved.

The second step of the work is to model the specimen with one or more LSP stripe and to evaluate the SIF values, and finally the beta correction factor, at different crack lengths.

It has been carried out a linear elastic analysis with two different steps representing:

1. The step where the residual stress field is introduced
2. The step where the compressive and tensile stresses are redistributed in the model in order to achieve the equilibrium

6.2 Modeling of the Baseline Specimen

6.2.1 Geometry and Material

For thin products the crack initiation is not important, mainly the crack propagation within the range of long cracks is a major design criterion. In this thesis, it has been studied the crack growth behavior in center-cracked tension M(T) Specimen with a width of 160 mm as it is a typical specimen for the investigation of the crack propagation behavior of fuselage materials [36].
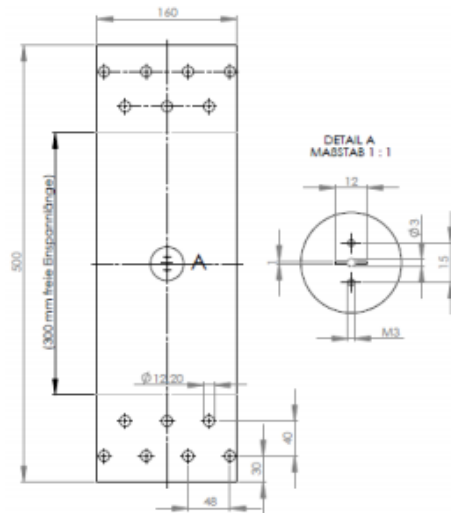
Fig. VI-II M(T) Specimen

Due to symmetry reason it was possible to model in Abaqus only half of the specimen as shown in the picture:
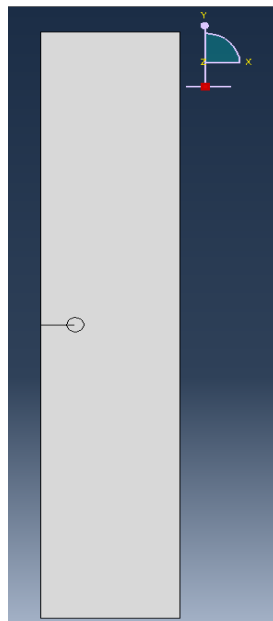
Fig. VI-III Baseline Geometry

The material used for the simulation is the typical skin alloy Al 2024-T351 clad which shows a good machinability and surface finish capabilities, and it is a high strength material of adequate workability, successfully used for structural applications. Composition and mechanical properties are reported in the next charts and they are provided by the Aluminum Association, Inc.

Component	Wt. %
Al	90.7 – 94.7
Cr	Max 0.1
Cu	3.8 – 4.9
Fe	Max 0.5
Mg	1.2 – 1.8
Mn	0.3 – 0.9
Other, each	Max 0.5
Other, total	Max 0.15
Si	Max 0.5
Ti	Max 0.15
Zn	Max 0.25

Table VI-I Aluminum 2024-T351 Composition

Mechanical Properties

Hardness, Brinell	120	AA; Typical; 500 g load; 10 mm ball
Hardness, Knoop	150	Converted from Brinell Hardness Value
Hardness, Rockwell A	46.8	Converted from Brinell Hardness Value
Hardness, Rockwell B	75	Converted from Brinell Hardness Value
Hardness, Vickers	137	Converted from Brinell Hardness Value
Ultimate Tensile Strength	469 MPa	AA; Typical
Tensile Yield Strength	324 MPa	AA; Typical
Elongation at Break	19 %	AA; Typical; 12.7 mm diameter
Elongation at Break	20 %	AA; Typical; 1.6 mm Thickness
Modulus of Elasticity	73.1 GPa	AA; Typical; Average of tension and compression
Ultimate Bearing Strength	814 MPa	Edge distance/pin diameter=2.0
Bearing Yield Strength	441 MPa	Edge distance/pin diameter=2.0

Poisson's Ratio	0.33	
Fatigue Strength	138 MPa	AA; 500'000'000 cycles completely reversed stress
Fracture Toughness	26 MPa·√m	K(IC) in S-L Direction
Fracture Toughness	32 MPa·√m	K(IC) in T-L Direction
Fracture Toughness	37 MPa·√m	K(IC) in L-T Direction
Machinability	70 %	0-100 Scale of Aluminum Alloys
Shear Modulus	28 GPa	
Shear Strength	283 MPa	AA; Typical

Table VI-II Aluminum 2024-T351 Mechanical Properties

In Abaqus, the material was simulated as a linear elastic material with the following characteristics:

- Density: 2780 kg/m^3
- Young's Modulus: 70500·10^6 Pa
- Poisson's Ratio: 0.33

6.2.2   Boundary and Loading Conditions

In order to simulate the crack growth behavior of the specimen as close as possible to the real one, three different boundary conditions are introduced. In the picture it is possible to see the real machine used for the experimental test and the three boundary condition introduced in Abaqus to simulate the same conditions as the real machine.

Fig. VI-IV Fatigue Test Machine
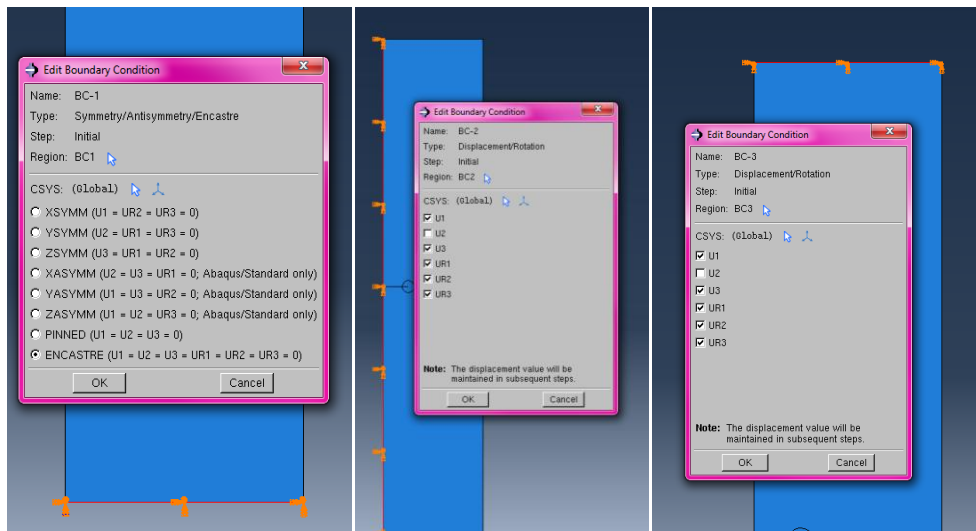
Fig. VI-V Model Boundary Conditions

The three boundary conditions needs to take into account that one edge is totally clamped and every displacements and rotations are not allowed. Indeed, the opposite edge is allowed to move only in the load direction as it is the edge on which the load is applied. The last boundary conditions is introduced to take into account that only half of the specimen is simulated, therefore symmetry conditions of the panel needs to be considered.

Moreover, it has been introduced a rigid body constraint on the edge where the load is applied. In fact, a rigid body constraint allows to constrain the motion of the edge to the motion of a reference point. Doing so, the relative

positions of the edge and the reference point remain constant throughout the analysis and it avoids any deformations of the free edge outside the loading plane.

The model is loaded with a constant tensile stress of 70 MPa and it is simulated as a concentrated force in the reference point of 11200 N, taking into account that it is applied only to half of the specimen.
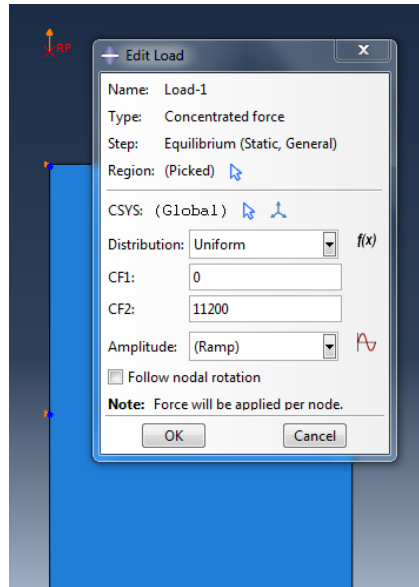
Fig. VI-VI Model Loading Condition

6.2.3   Crack

Once the geometry and the loading conditions are defined , it is necessary to introduce the half crack in the model. The crack is introduced using the contour method integral and it is basically defined by the crack tip which corresponds to the first contour integral value and by the crack propagation direction . Moreover, as the geometry of the crack region defines a sharp crack and the stain becomes singular at the crack tip, it is indispensable to take into account the singularity at the crack tip in order to improve the accuracy of the contour integral evaluation, the stress intensity factors, and the stress and strain calculations.

If r is the distance from the crack tip, the strain singularity in small-strain analysis is:

- $\varepsilon \propto r^{-\frac{1}{2}}$ for linear elasticity
- $\varepsilon \propto r^{-1}$ for perfect plasticity
- $\varepsilon \propto r^{-\left(\frac{n}{n+1}\right)}$ for power-law hardening

The model used in this thesis simulates an elastic fracture mechanics application so it has been create a 1/√r strain singularity:

✓ The midside node parameter is set to 0.25 to move the midside nodes on the sides connected to the crack tip to the ¼ point nearest the crack tip

✓ The degenerate element control at the crack tip is set to collapsed element side, single node

The crack tip is modeled with a ring of collapsed quadrilateral elements as shown in the figure:
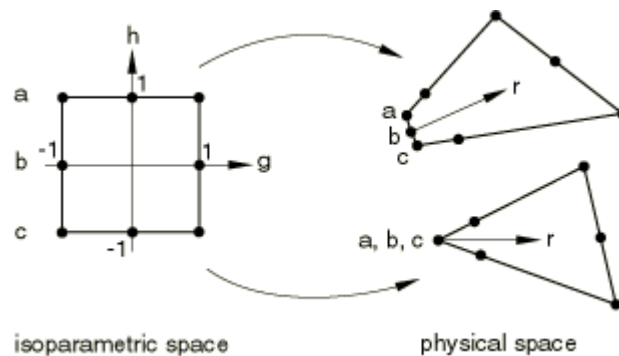
Fig. VI-VII Mesh Collapsed Elements

6.2.4   Mesh

For the mesh module there were used two-dimensional elements. Abaqus provides several different types of two-dimensional elements, for instance for structural applications these include plane stress elements and plane strain elements:

➢ Plane stress elements: they can be used when the thickness of a body or domain is small relative to its lateral (in-plane) dimensions. The stresses are functions of planar coordinates alone, and the out-of-plane normal and shear stresses are equal to zero.

Plane stress elements must be defined in the X-Y plane, and all loading and deformation are also restricted to this plane. This modeling method generally applies to thin, flat bodies.

➢ Plane strain elements: they can be used when it can be assumed that the strains in a loaded body or domain are functions of planar coordinates alone and the out-of-plane normal and shear strains are equal to zero.

Plane strain elements must be defined in the X-Y plane and all loading and deformation are also restricted to this plane. This modeling method is generally used for bodies that are very thick relative to their lateral dimensions.

Due to the thickness of the specimen simulated, plane stress two-dimensional quadrilateral elements are used in the whole model. In particular, the Abaqus elements type is CPS4R, a 4-node bilinear plane stress quadrilateral elements, reduced integration with hourglass control.

Regarding the mesh control parameter, it has been chosen to divide the model in two different zones and mesh them separately. In particular, the pink zone (see picture) is mesh with quadrilateral element shape with the free technique control; while the yellow zone, which represent the area near the crack
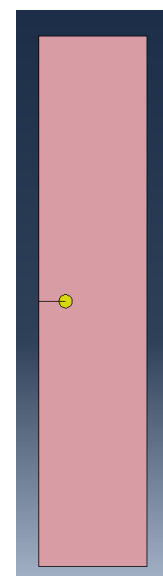
Fig. VI-VIII Meshing Areas

tip, is meshed with quadrilateral-dominated element shape with the sweep technique control. Moreover, also the element size is kept different in the two zones as it is not needed to have a finer mesh in the whole model, but only at the crack tip, where the singularity is present as it is the zone where higher stresses and deformations are present. For this reason, the element in pink zone are 2x2 mm wide, while the circle around the crack tip is meshed with 36 elements in the circumference direction and 18 elements in the radius direction, which lead to an approximate size of 0.7x0.2 mm.
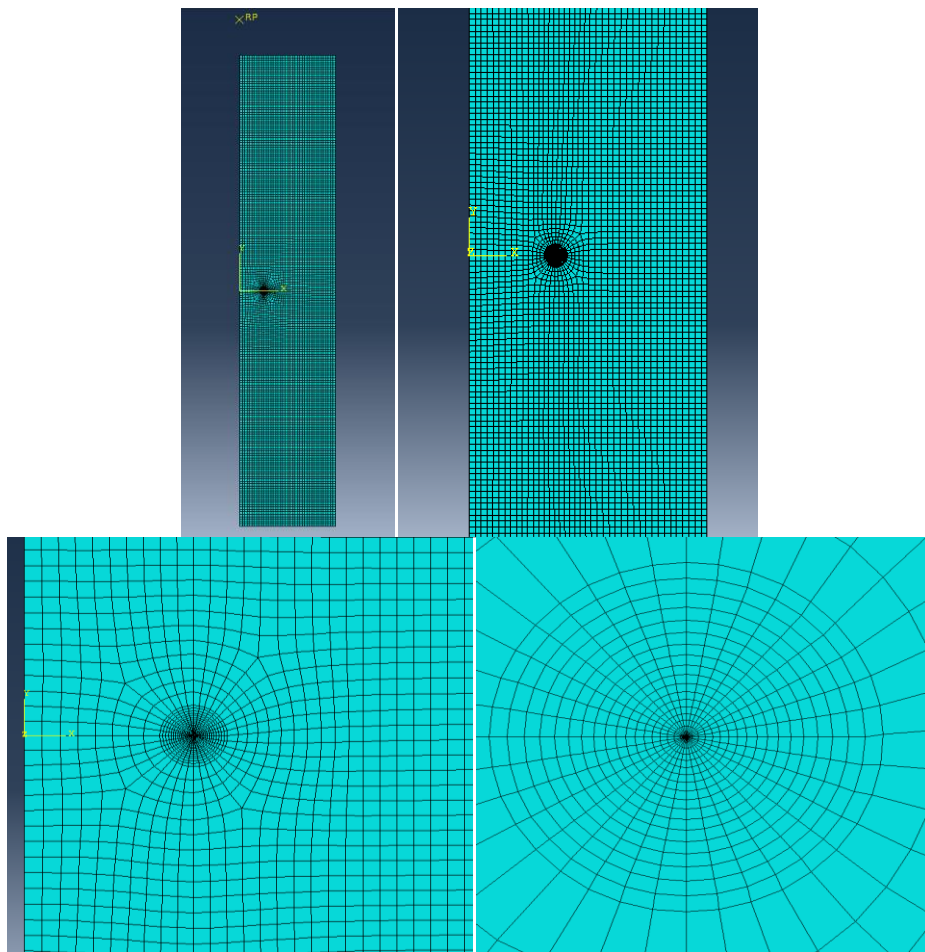
Fig. VI-IX Model Mesh

6.3   Baseline Simulations Results

The output of the simulation gives the value of the Stress Intensity Factor (SIF) for different crack length. In particular, for the analysis without any residual stress applied there were been carried out 15 simulations starting from a crack length of 5 mm until 50 mm.
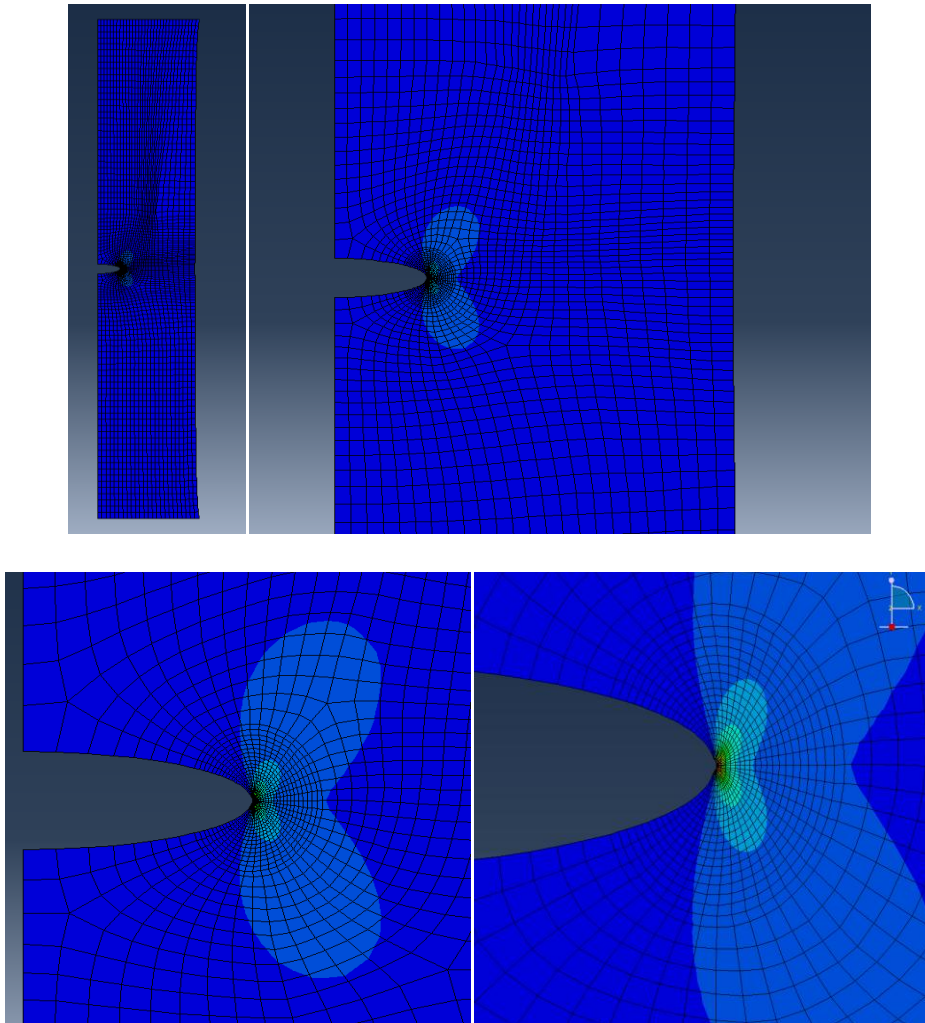
Fig. VI-X Baseline Simulation

Abaqus calculates the SIF through the integration of the J-Integral, if the material response is linear. The J-Integral is related to the energy release associated with crack growth and is a measure of the intensity of deformation at a notch or crack tip. In the context of quasi-static analysis the J-Integral is defined in two dimensions as:

$$J = \lim_{\Gamma \to 0} \int_{\Gamma} n \cdot H \cdot q \, d\Gamma$$

Where:

- Γ is a contour beginning on the bottom crack surface and ending on the top surface, as shown in figure
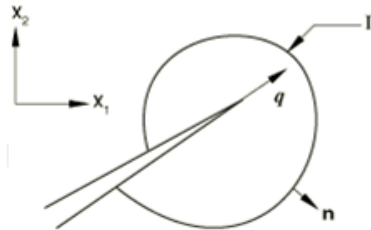
Fig. VI-XI Contour Integral

- The limit $\Gamma \to 0$ indicates that Γ shrinks into the crack tip
- q is a unit vector in the virtual crack extension direction
- n is the outward normal to Γ
- H is given by

$$H = WI - \sigma \frac{\partial u}{\partial x}$$

And W is the elastic strain energy for an elastic material behavior.

The Stress Intensity Factors K_I, K_{II} and K_{III} play an important role in the linear elastic fracture mechanics. They characterize the influence of load or deformation on the magnitude of the crack tip stress and strain fields, and measure the propensity for crack propagation or crack driving forces.

Furthermore, the SIF can be related to the energy release rate for a linear elastic material through:

$$J = \frac{1}{8\pi} K^T \cdot B^{-1} \cdot K$$

Where:

- $K = [K_I, K_{II}, K_{III}]^T$
- B is the pre-logarithmic energy factor matrix

For homogeneous, isotropic material B is diagonal and the above equation simplifies to:

$$J = \frac{1}{\tilde{E}}(K_I^2 + K_{II}^2) + \frac{1}{2G}K_{III}^2$$

- $\tilde{E} = E$ for plane stress
- $\tilde{E} = \frac{E}{1-\nu^2}$ for plane strain

Using the contour integral evaluation it is possible to calculate SIF values as an output of Abaqus simulations. SIF values achieved with the Abaqus software are shown in figure for different crack length.
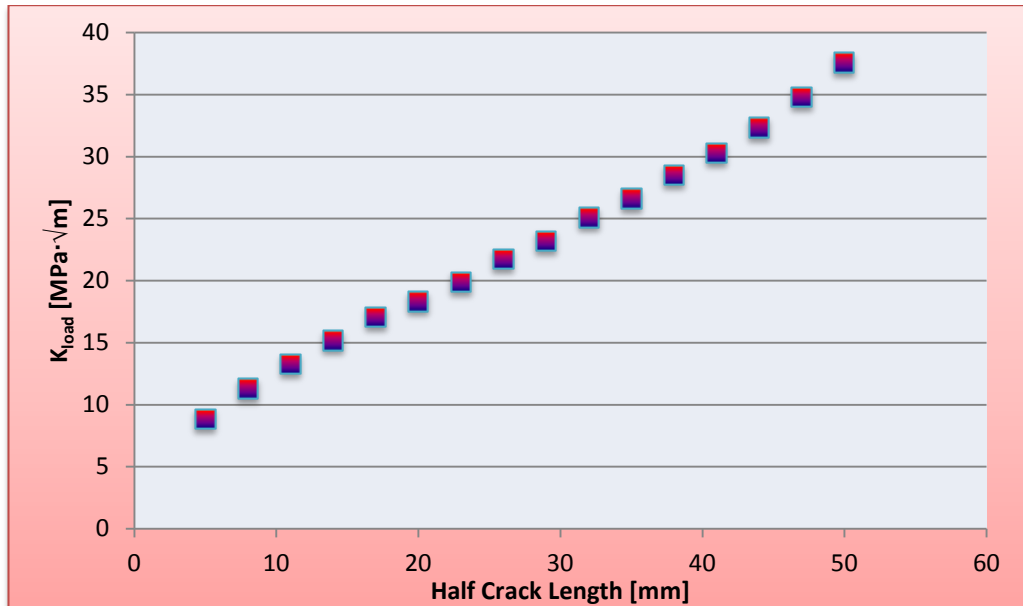
In order to check the reliability of the adopted analysis method, the FEM results needs to be compared to the analytical ones. The analytical results for a specimen with a centered through crack are present in the literature and they can be evaluated using the following formula:
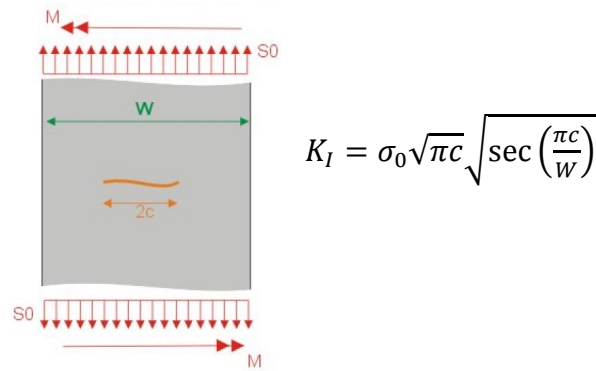
*Fig. VI-XII Centered
Through Crack
Specimen*

$$K_I = \sigma_0 \sqrt{\pi c} \sqrt{\sec\left(\frac{\pi c}{w}\right)}$$

Finally, it is possible to compare the analytical results with the FEM ones:
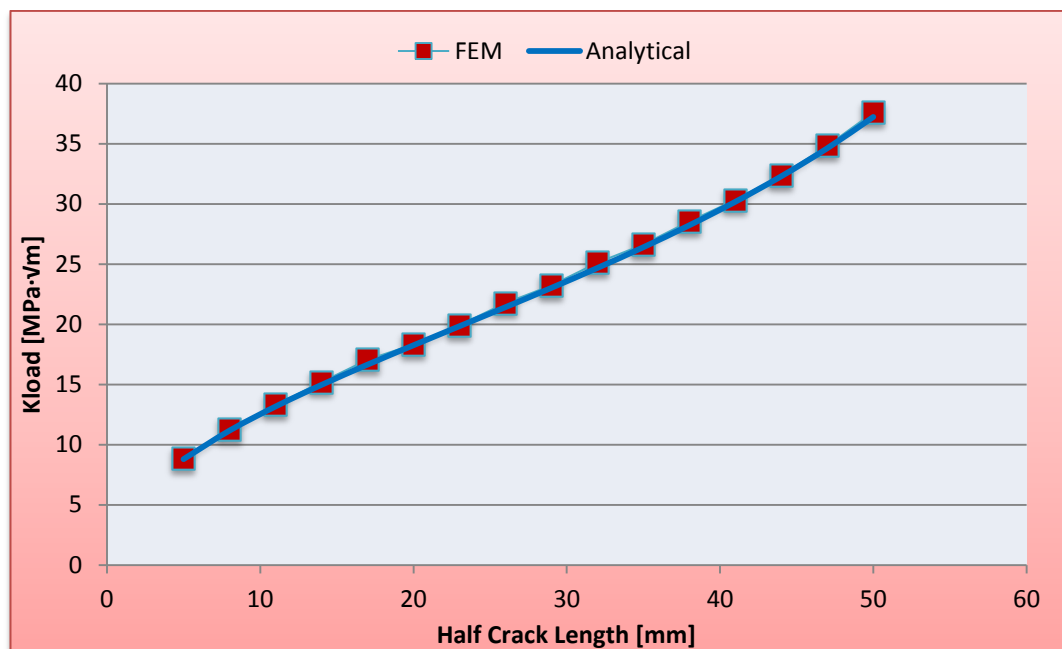
It can be noticed that FEM results are in good agreement with the analytical ones, proving that the adopted analysis method is reliable.

6.4   Modeling of the Treated Specimen

Once the adopted analysis method is proved to be reliable, the work has been focused on the simulation of the specimen after the Laser Shock Peening process in order to predict the Stress Intensity Factor due to the compressive residual stress introduced by the treatment plus the external load applied.

As it was shown in the previous paragraphs, due to symmetry reasons only half of the specimen was sketched and the geometry, as well as the boundary conditions and the meshing section, was modeled in the same way as it was shown for the baseline specimen. In addition, it was necessary to reproduce the residual stress field induced by the Laser Shock Peening, presuming that the residual stresses value was already known by experimental measurements.

It has been decided to simulate the crack growth behavior of a specimen with two symmetric LSP stripe 20 mm wide, placed at a distance of 20 mm from the centre line.
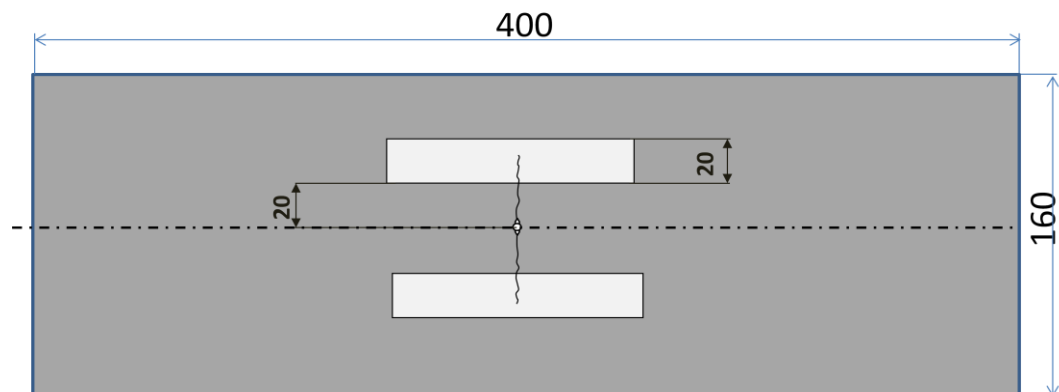
Fig. VI-XIII Treated Specimen Geometry

For a very first approach, the residual stress field is modeled as a constant stress field. It has to be noticed that this approach does not decrease the accuracy of the simulation, in fact it has been simulated a through crack model which doesn't strictly depends on what it is happening on the surface, but it is influenced mainly by the stresses at the core of the material. For this reason, it was decided not to model the residual stress through the thickness, which would have lead to a very complicate and time-consuming simulation,

but to consider the average stress to which the specimen is subjected in order to achieve some very first results for the crack propagation behavior of the model.

The compressive residual stress field is manually introduced and it is automatically balanced with a tensile residual stress by Abaqus analysis which calculates them in order to find the equilibrium for the whole model.
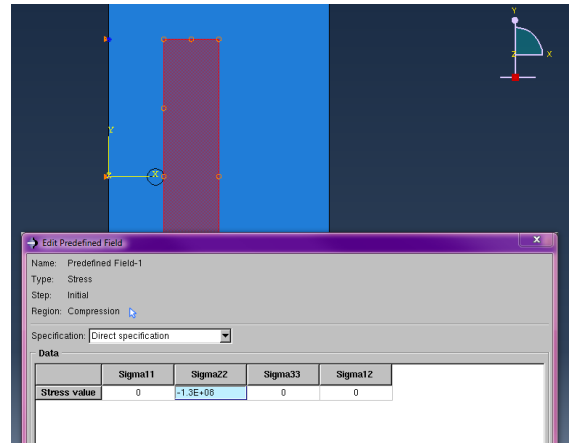
Fig. VI-XIV Residual Stress Modeling

As it can be seen in the picture above, the compressive residual stress field is introduced only in the y-direction (i.e. the loading direction) as constant predefined field with an average stress of -130 MPa, coming from experimental measurements of residual stress after the Laser Shock Peening treatment from Open University.

In particular the model under investigation was peened by Politecnica de Madrid on both sides of the specimen with a laser power setting as shown in the chart:

Overlapping distance [mm]	Pulse/cm^2	Spot diameter [mm]	Laser energy [J]
0.75	178	2.5	2.2

Table VI-III Laser Settings

Using these power settings, the compressive residual stress was measured with the hole drilling method at the centre of the stripe as it is reported in the next figure.
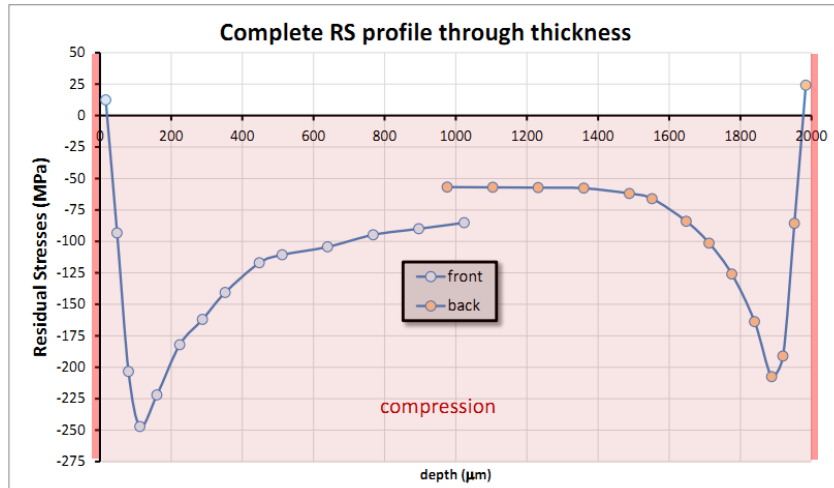
Fig. VI-XV Residual Stresses Experimental Measurements

It is still not clear why tensile stresses are measured on the surface, but in any case what is happening in the first 100 μm can be neglected because:

- ✓ The material is clad with pure aluminum. Therefore the clad material has mechanical properties much lower than the substrate material;

- ✓ The hole drilling technique is not suitable near surfaces stresses;

- ✓ Crack growth behavior for through crack is influenced mainly by stresses at the material core and slightly at near surfaces.

The average residual stress coming from the trend reported in the figure is about -130 MPa, reason why this value is used in the simulations.

6.4.1   Crack Modeling

The crack geometry is modeled in the same way as it was shown for the baseline specimen. However, during the simulation with the only compressive residual stress field applied, a deformation not compatible with the crack geometrical surface of the specimen occurred. In fact, if the crack is introduced without any contact definition, the two faces of the crack penetrate one into each other, as shown.
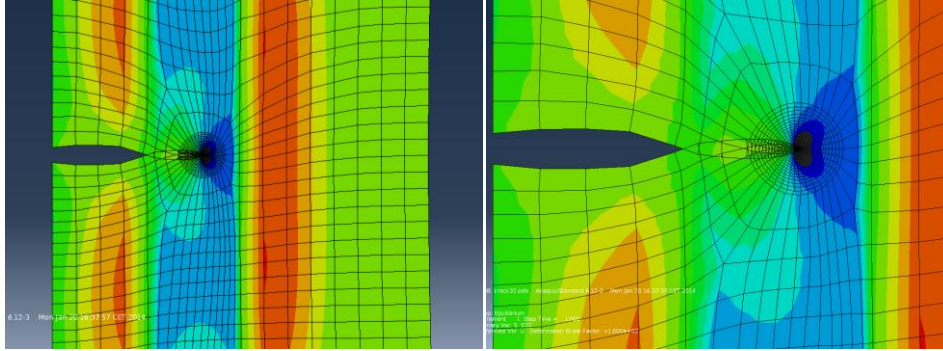
Fig. VI-XVI Crack Surfaces Penetration

This unrealistic behavior needs to be avoid. In order to elude the penetration of the surfaces, two different approaches might be used:

- ✓ Gap Elements Approach

- ✓ Surface-to-Surface Interaction Approach

6.4.2   Gap Elements Approach

Gap contact elements can be used to define the contact interactions in the model. These elements require that matching nodes should be present on the opposite sides of the contact surfaces and allow only for small relative sliding between the surfaces. This latter assumption is usually consistent with the assumption of linear behavior that is built into a substructure [42]. Gap elements are defined by specifying the two nodes forming the gap and providing geometric data defining the initial state and the direction of the gap.

In the case of interest, it is necessary to introduce as many gap elements as element nodes are in the compressive area so that the penetration of the surfaces is avoided.
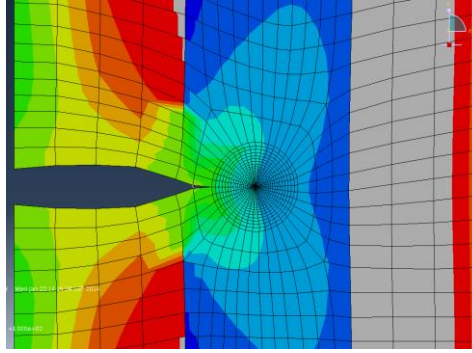
Fig. VI-XVII Gap Elements Approach

6.4.3   Surface-to-Surface Interaction Approach

Abaqus does not recognize mechanical contact between part instances or regions of an assembly unless that contact is specified in the Interaction module; the mere physical proximity of two surfaces in an assembly is not enough to indicate any type of interaction between the surfaces.

The surface-to-surface contact interaction describes contact between two deformable surfaces; in the analysis these two surfaces represent the upper and lower surface of the crack. It is necessary to define the master and slave surfaces and then it is assigned to them an interaction property which defines the tangential and normal behavior of the two surfaces avoiding penetration.
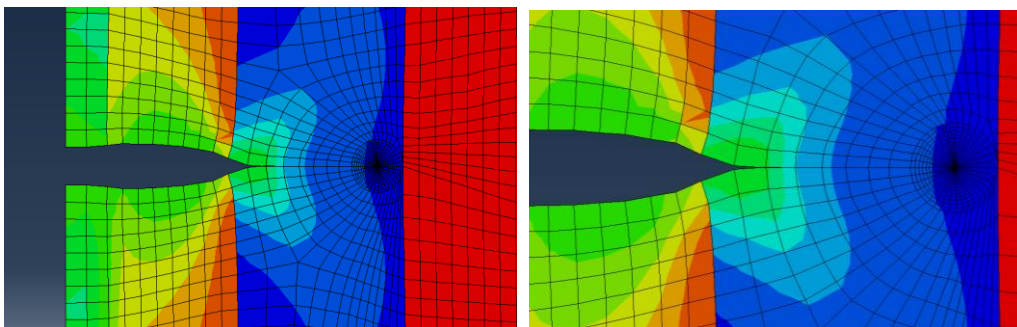
Fig. VI-XVIII Surface-To-Surface Interaction Approach

It can be noticed that the two approaches are equivalent and they have the same SIF output values. For the sake of simplicity from now on it has been decided to use the surface-to-surface interaction module as it is a more intuitive and faster way to avoid the penetration of the two surfaces.

6.5   Results With Only Residual Stress Applied

In the next figure are reported the results obtained with the Abaqus software when only a compressive residual stress field is applied (without any external load) and when surface-to-surface interaction properties are used.
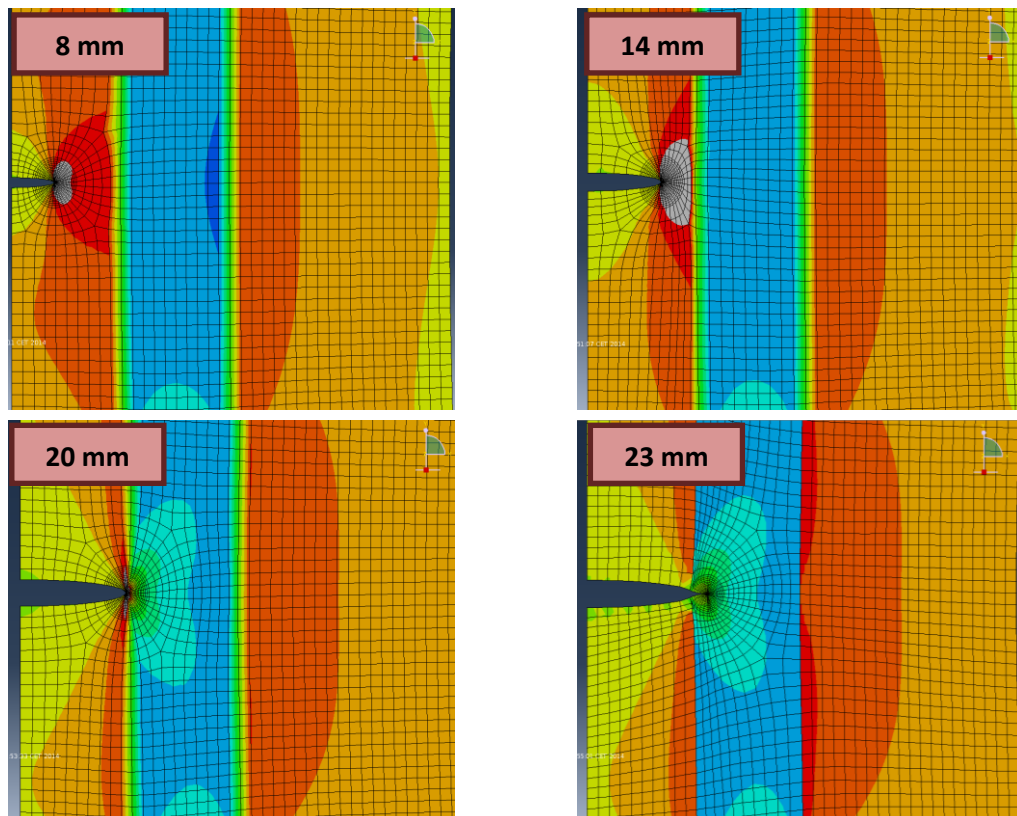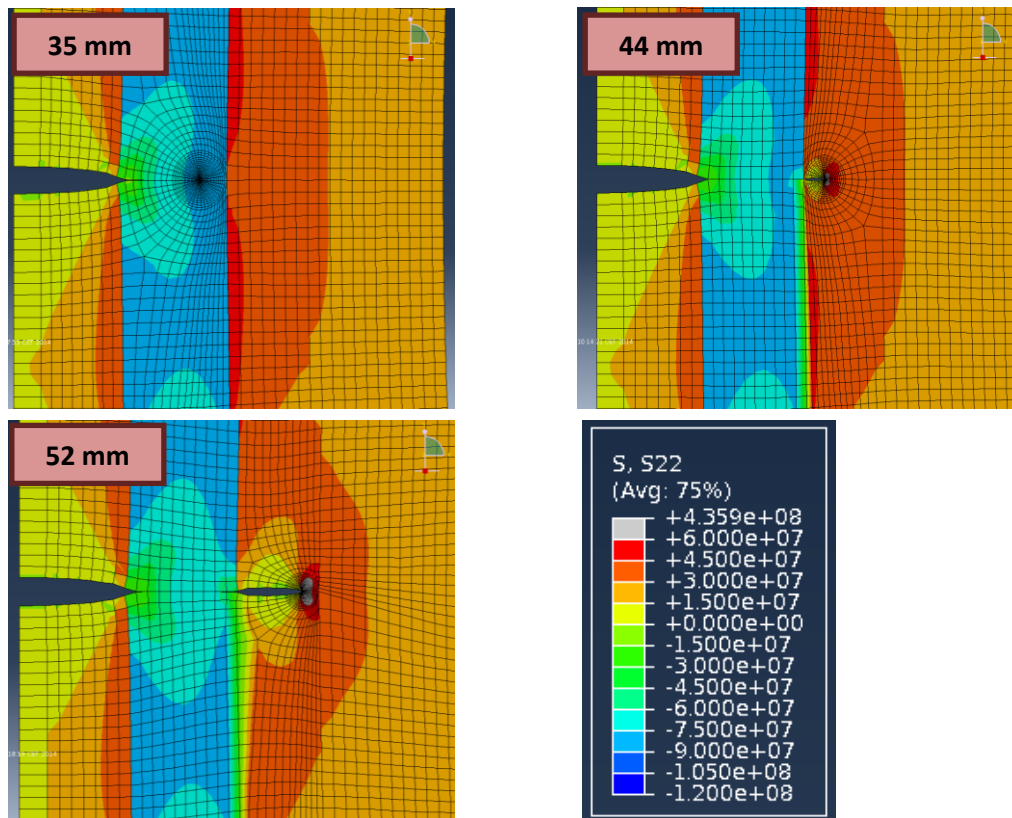
Fig. VI-XIX Simulations With Only Residual Stress Field Applied

Finally, it can be evaluated the Stress Intensity Factor due to the only compressive residual stress field applied (K_{RS}) at different crack lengths. Here is shown an example of K_{RS} at -130 MPa residual stress.
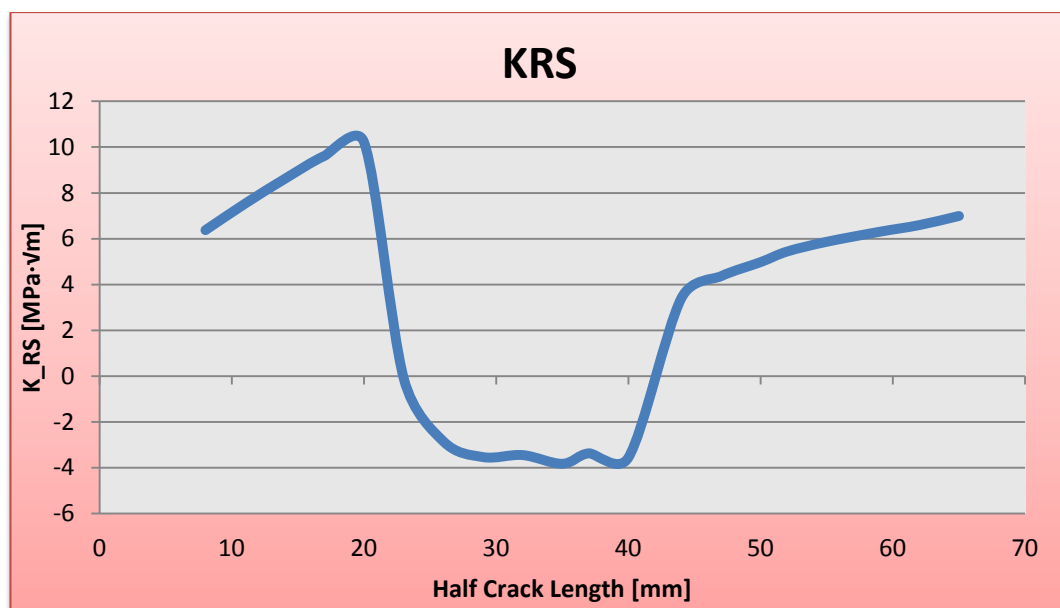
6.6   Results With External Load Applied

Theoretically, since the stresses are linearly proportional to the stress intensity factor, it follows that the superposition principle also applies to crack problems. Therefore, it should be possible to calculate the SIF value of the model spitting the analysis into two steps.
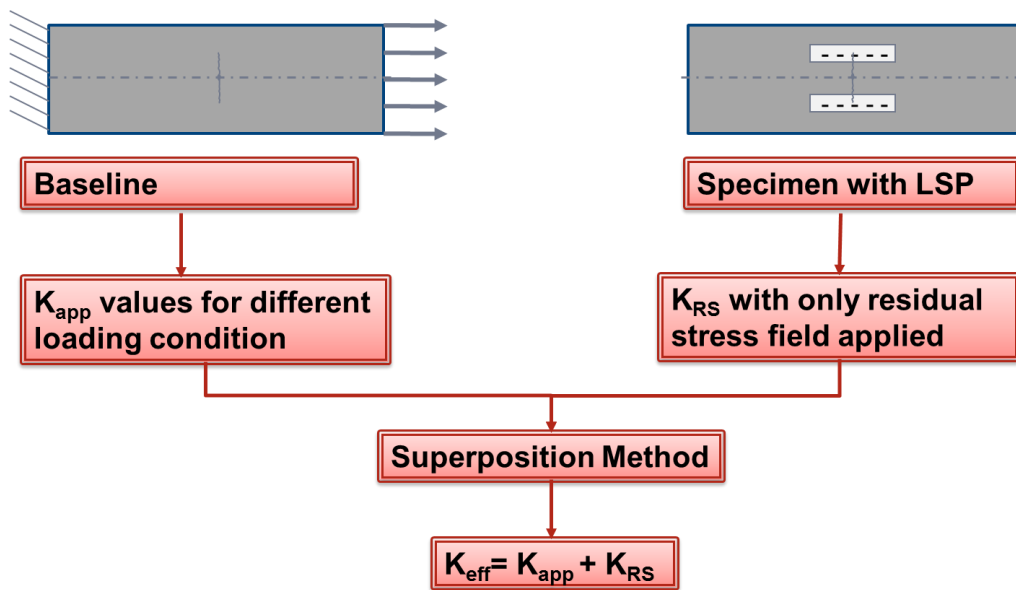
Fig. VI-XX Superposition Method

However, it is not possible to use the superposition method in the range of crack lengths in which the contact elements interaction is defined because contact is a nonlinear phenomenon and the concept of linear superposition of results is not valid anymore.

$$K(Load) + K(RS) \neq K(Load + RS)$$

This is the reason why further simulations were run including both the compressive residual stress field and the external load applied together.

Moreover, it has to be noticed that the Abaqus software run the simulations with a static external load applied as it is considering a static crack which is not growing during the analysis, but in AFGROW a cyclic loading is considered since it is studied the crack growth behavior of the model and the crack needs

to grow at every cycle. In particular it is used a constant amplitude loading with an upper stress of 130 MPa and R=0.1.
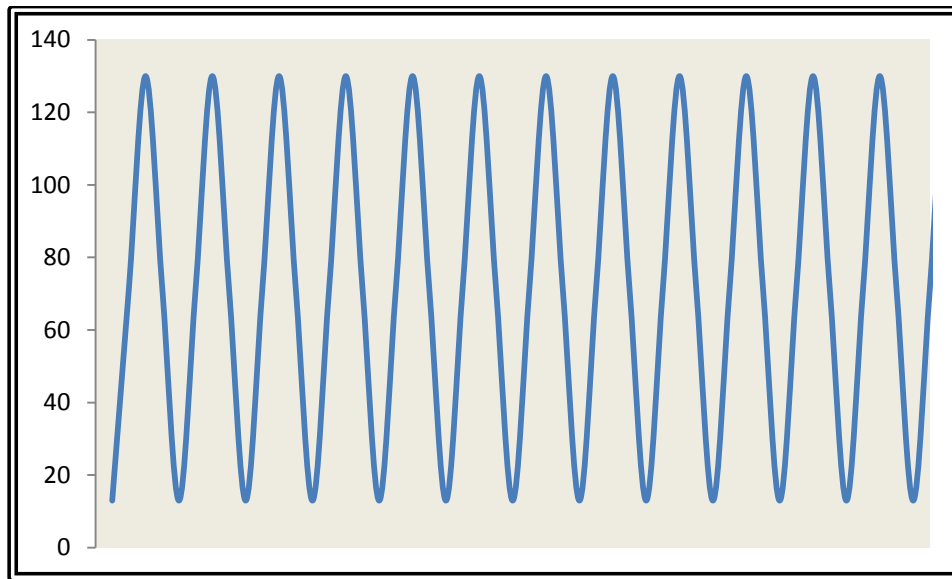
Fig. VI-XXI Constant Amplitude Loading Used in Simulations

For this reason, the K_{eff}, and at a later stage the beta factor, in Abaqus is estimated for a medium load in order not to overestimate or underestimate its effect in the cyclic loading analysis.

All the results are too much conservative

K_{eff} and beta correction factor at average stress are assumed as a first approach

All the results are underestimated
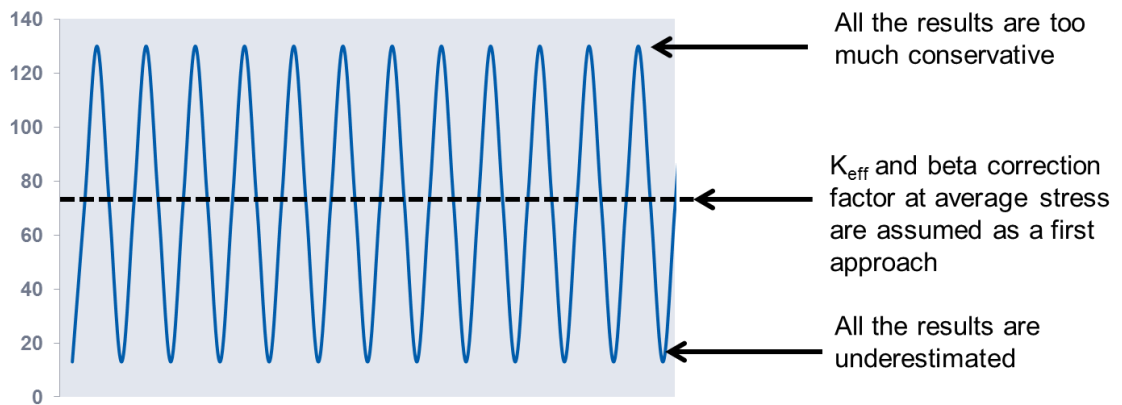
Finally, all simulations were carried out with an external load applied of 70 MPa and a constant residual stress field of -130 MPa for different crack lengths.
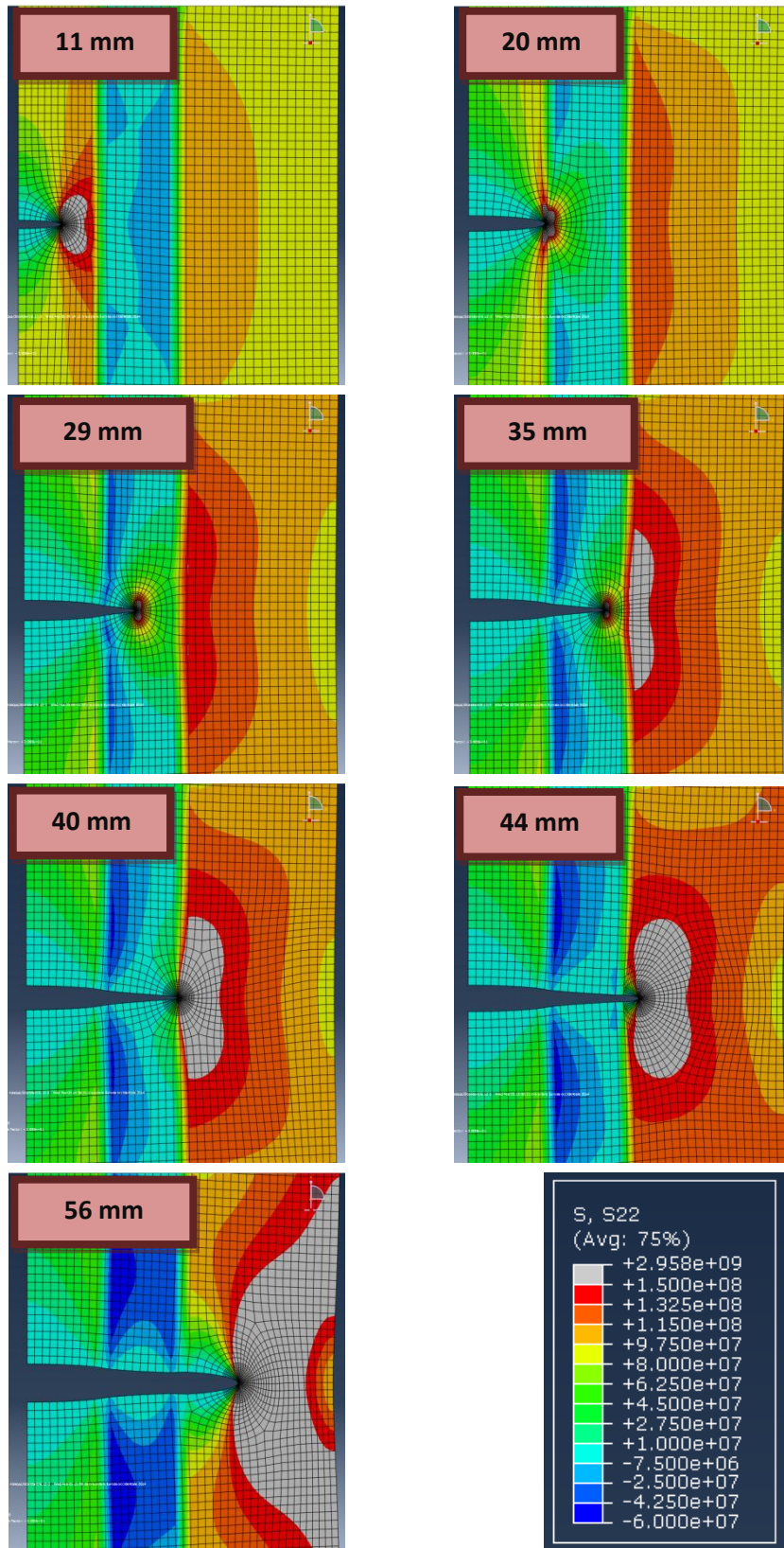
Fig. VI-XXII Simulations With Residual Stress Field And External Load Applied

The output of the Abaqus software gives the stress field at the crack tip for different crack length. In particular, it is possible to determine the Stress Intensity Factor by means of the J-Integral, providing that the material response is linear, which is related to the energy release associated with crack growth and it is a measure of the intensity of the deformation at the crack tip.

The K_{eff} was evaluated for different loading condition at different crack lengths, supposing that the same residual stress field is applied.
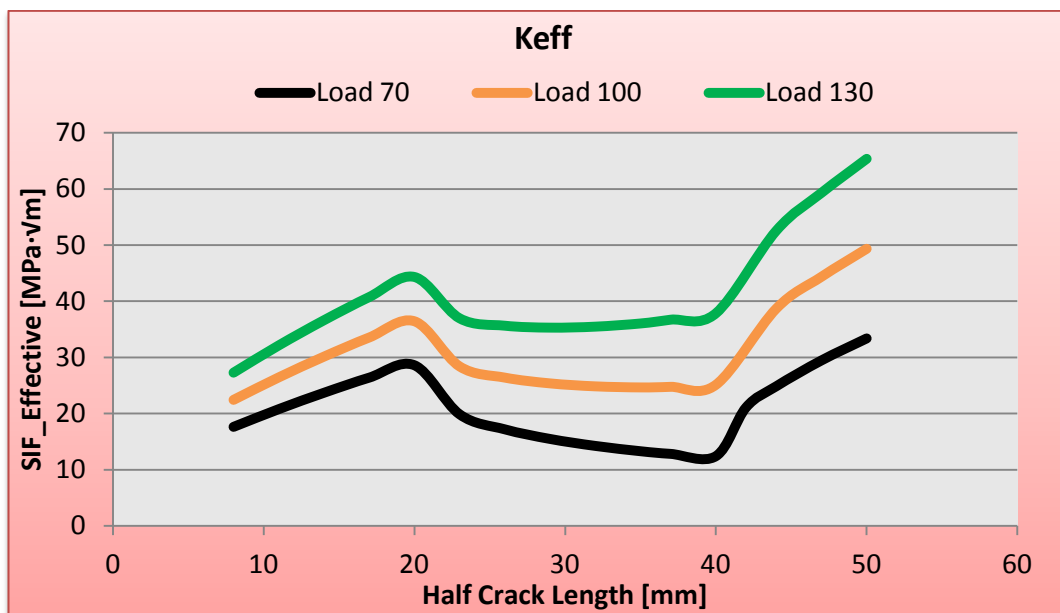
6.7   Beta Correction Factor Evaluation

The dimensionless factor β is called beta correction factor (also geometry correction factor, boundary correction factor or geometry factor) and depends on the geometrical and load differences of the real structure in respect to the infinite sheet under remote tension loading conditions.

For an infinite sheet β=1 and K can be described as:

$$K = S\sqrt{\pi a}$$

However, the $\tilde{\beta}$ correction factor which is used in this work must not be confused with the geometrical β correction factor used in the LEFM and above-mentioned. In fact, the $\tilde{\beta}$ correction factor is a dimensionless parameter which takes into account the residual stress distribution due to the LSP treatment and it is theoretically calculated as:

$$\tilde{\beta} = \frac{K_{load+RS}}{K_{load}}$$

It is introduced on purpose in this work to describe how the residual stress field gives benefit to the crack growth behavior of the model. It is clear that when $\tilde{\beta} > 1$, the crack speeds up leading to a decrease in the fatigue life of the component, while when $\tilde{\beta} < 1$, it is the case when the crack is inside the compressive residual stress area, the crack slows down leading to an improvement in the fatigue life of the component. The $\tilde{\beta}$ correction factor was evaluated for different loading condition and crack lengths and it is reported below:
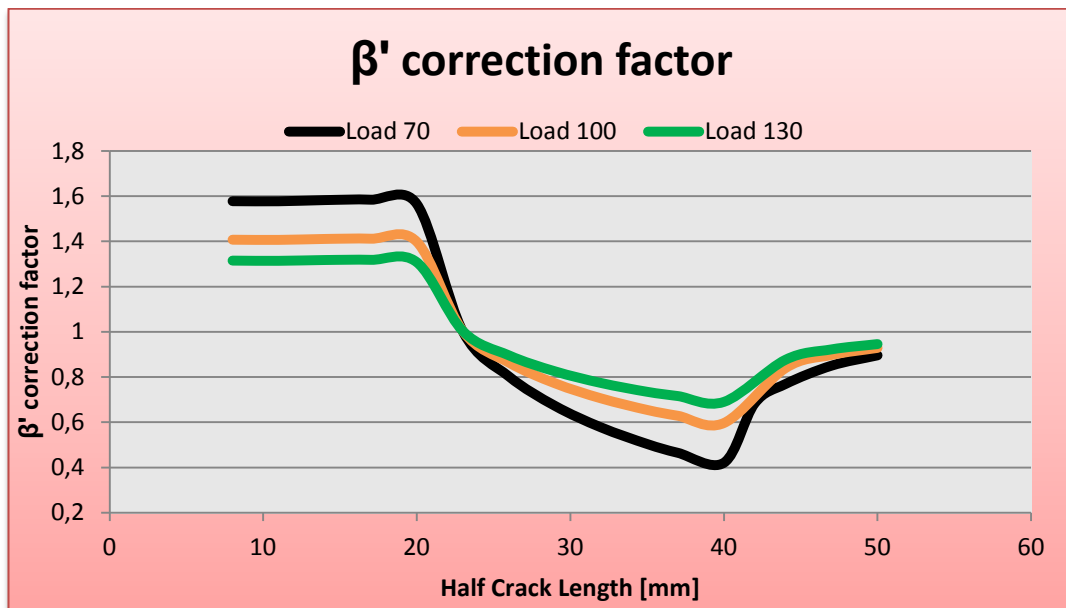
It is still not well understood the reason why for lower external load applied the $\tilde{\beta}$ correction factor is higher before the crack enters the stripe, i.e. the acceleration phase is more pronounced. In fact, it seems to be realistic that when a lower external load is applied the crack growth should be slower before it enters the stripe even though a slight acceleration should always be present.

VII.   Crack Growth Prediction

This chapter provides a meaning of calculating the fatigue damage evaluation of M(T) specimens after the Laser Shock Peening treatment is applied.

In order to evaluate the crack growth behavior of the model under investigation, it has been decided to use the AFGROW software introducing manually the $\tilde{\beta}$ correction factor evaluated as it was explained in the previous chapter.

7.1   Crack Growth Prediction Using the Afgrow Software

AFGROW includes an ability to estimate SIFs for cases that may not be an exact match for one of the K solutions in the AFGROW library; for example, if it is creating to model a case with a higher/lower stress gradient. This is the case under examination, where a residual stress field induces a lower Stress Intensity Factor which may be translated into a $\tilde{\beta}$ correction factor minor than one.

In AFGROW it is possible to enter normalized stress values in the crack plane and allow the software to calculate beta correction factors or enter pre-determined beta correction values.
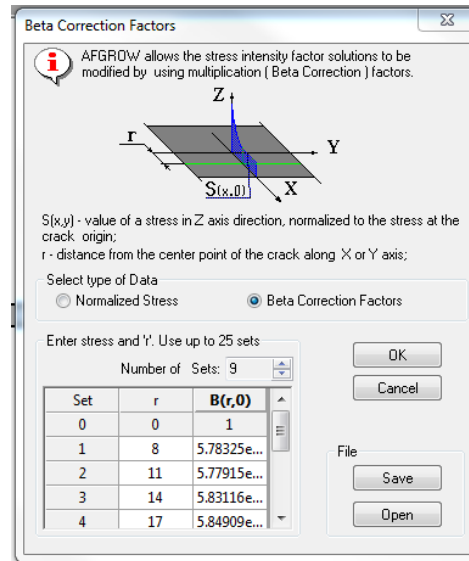
Fig. VII-I Beta Correction Factor Introduction

In this thesis, it has been decided to enter the beta correction factors manually, using the ones evaluated with the FEM analysis.

The beta correction at the crack origin is set equal to 1.0 by default because the values are required to be normalized at the crack origin when stress values are input. The beta correction value at the crack origin can only be used as an interpolation limit since all cracks must have a finite length.

The length dimension r is the radial distance from the crack origin. The input stress ratio values are shown for (r,0) along the y=0 axis which is the width direction

Introducing the $\tilde{\beta}$ correction factor into the AFGROW software it is possible to calculate the crack propagation rate due to the residual stress field induced by the LSP treatment.

Before using AFGROW to predict the crack growth behavior for the specimen treated by LSP, it is necessary to set up the process to verify the reliability of the material parameters used. For this reason it has been firstly simulated the crack growth behavior of the baseline specimen.

Nevertheless, if the material present in the AFGROW software library is used, the crack growth prediction shows a significant difference from the experimental results:
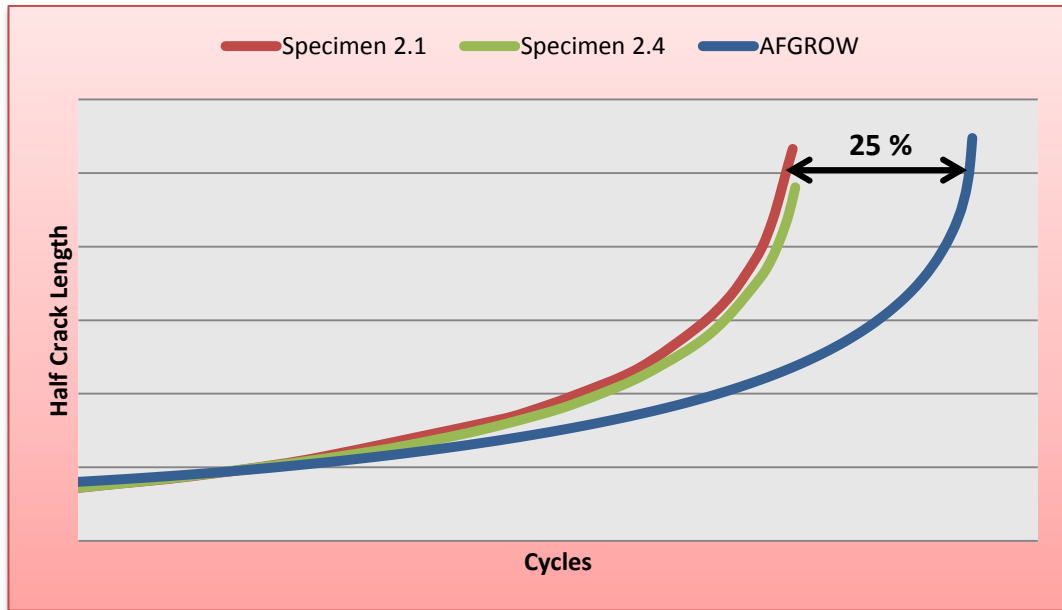
For this reason, it has been necessary to modify the material crack growth data so that the simulations results match as good as possible to the experimental ones. The material used for the simulation is the same one described in chapter IV which shows a good agreement compared to the experimental results.
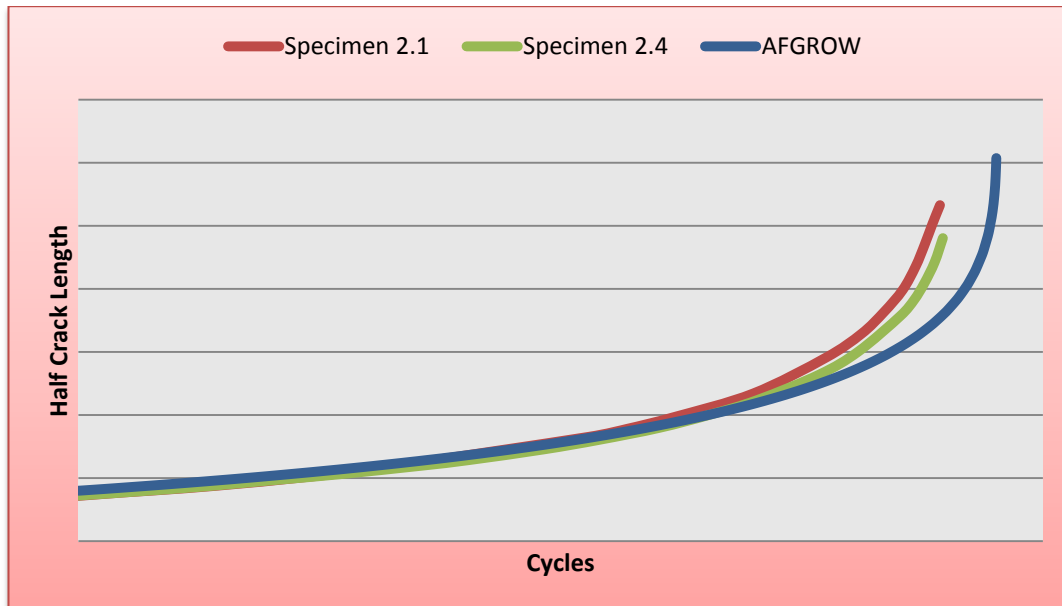
The tabular look up crack growth rate is used to introduce the material in the software and it allows the user to input their own crack growth rate curves. The tabular data utilizes the Walker equation on a point-by-point basis to extrapolate/interpolate data for any two, adjacent R-values.

In this work thesis, there were introduced data for a single R-value. In this case, data will be used regardless of the stress ratio for a given analysis. This may be useful in cases where rate data is scarce and the user is only interested in predicting constant amplitude loading, which is the analysis under investigation.

7.2   Results

Using as input the material data reported in the paragraph 4.4.3 and the $\tilde{\beta}$ correction factor evaluated via FEM analysis, it is possible to run simulations with the AFGROW software and to predict the crack growth behavior of the specimen after the Laser Shock Peening treatment.
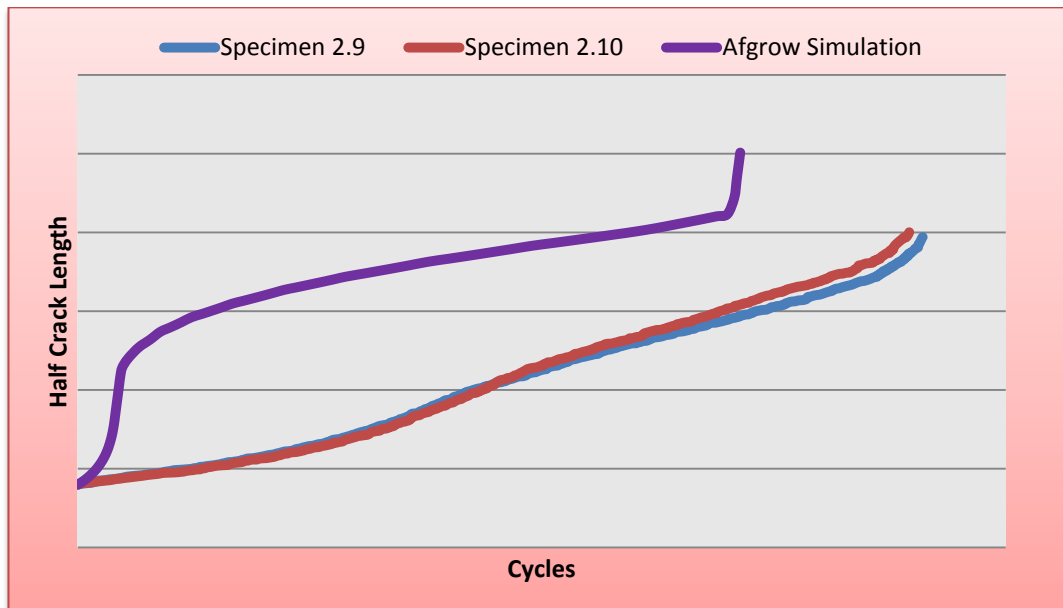
Loading Condition	Residual Stresses	$\tilde{\beta}$ evaluated at
130 MPa	-130 MPa	70 MPa

Table VII-I Simulation Parameters

However, it can be noticed that the acceleration at short crack lengths is way too high compared to the experimental results, as it is possible to observe from the da/dN vs. ΔK curve.
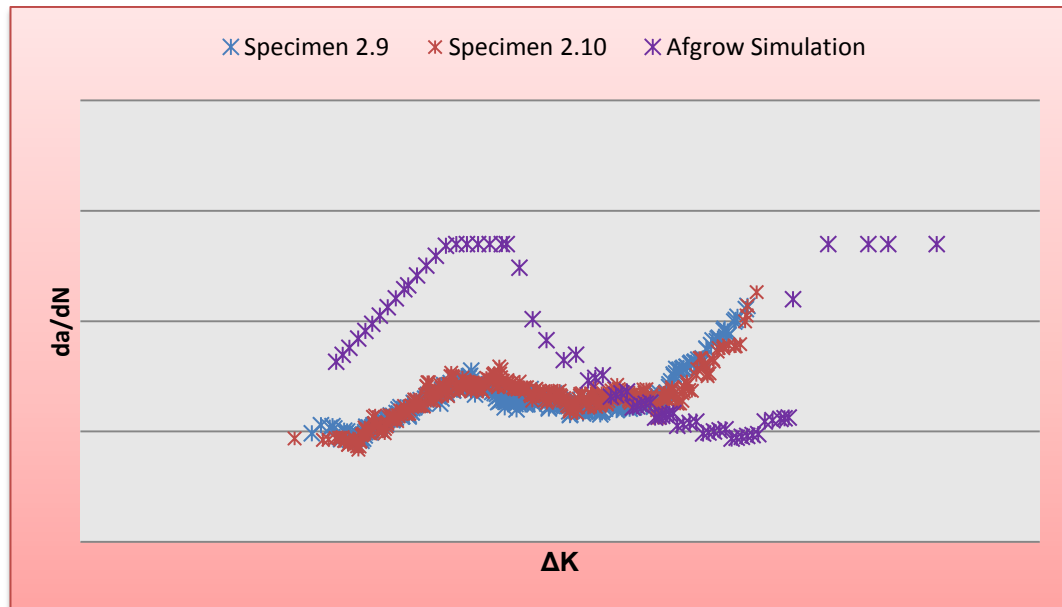
This unexpected behavior is due to the fact that at short crack lengths the $\tilde{\beta}$ correction factor evaluated has quite high values which leads to a pronounced acceleration before the crack enters the compressive residual stress area.

Nevertheless, it is possible to notice that this behavior is not present in the real model. In fact, when the baseline specimen is compared to the treated specimen, no relevant acceleration is detected before the crack enter the LSP area:
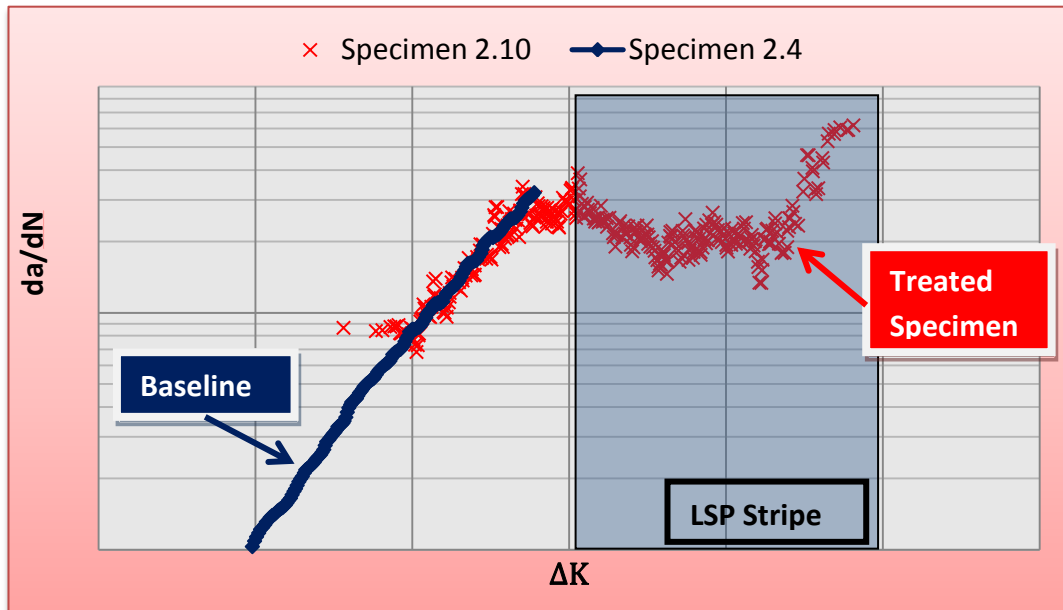
It is evident from the above chart that no acceleration is present before the crack enters the stripe as the da/dN values are really close to the baseline ones. Moreover, when ΔK≈40 MPa√m the crack propagation rate starts to grow again; this effect is due to the fact that the remaining net section is totally yielded and the experimental tests are no valid anymore.

Taking into account these considerations, further simulations were run with a modified $\tilde{\beta}$ correction factor which considers that no acceleration is present before the crack enters the compressive residual stress field and that the test is not valid when ΔK reaches 40 MPa√m values.
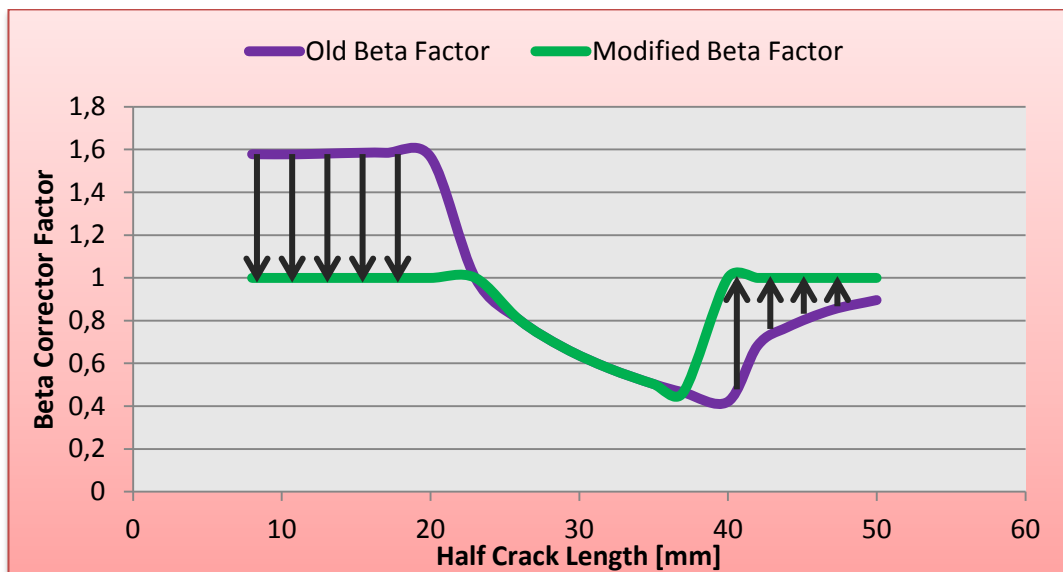
Simulation run with the modified $\tilde{\beta}$ correction factor is shown in the next figures, including the crack propagation rate and the da/dN vs. ΔK curve.
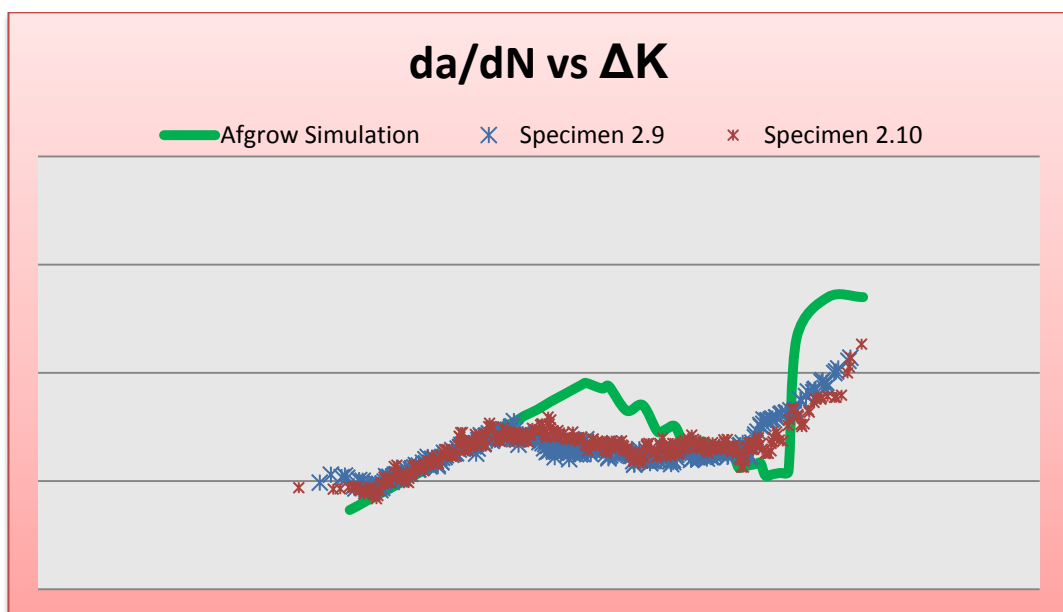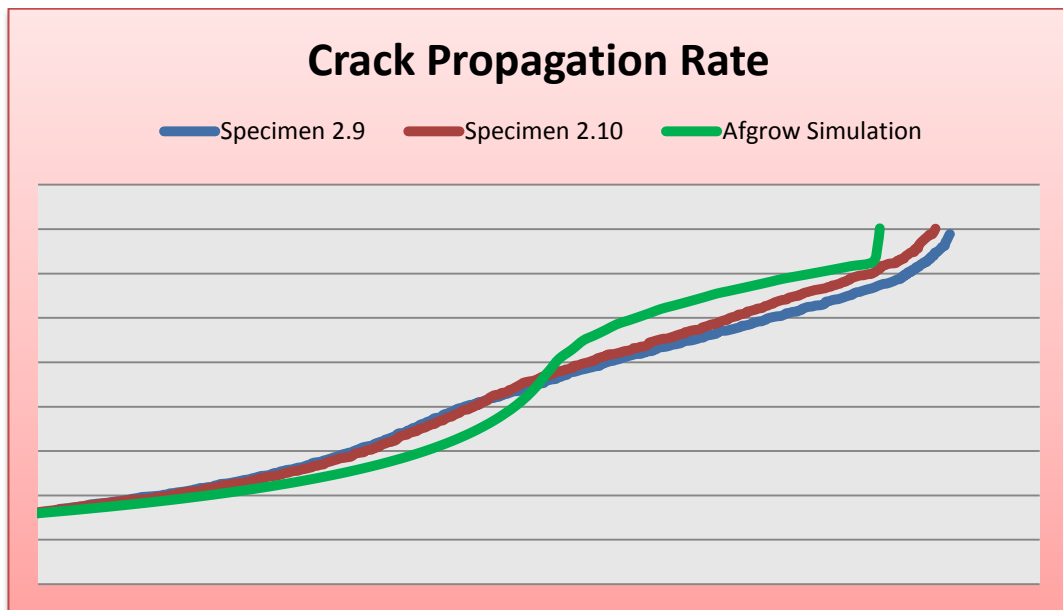
The good correlation of the crack growth behavior of numerical and experimental results induced by LSP has been verified for the adopted analysis method and the configuration used. These results labels the finite element model as a reliable model to simulate the residual stress field after the Laser Shock Peening process.

The results of the analysis, conducted by means of the FE simulations procedure described and confirmed by experimental measurements, proofs that the LSP treatment results in a significant improvement in fatigue behavior in metallic specimens, even for high external loads applied.
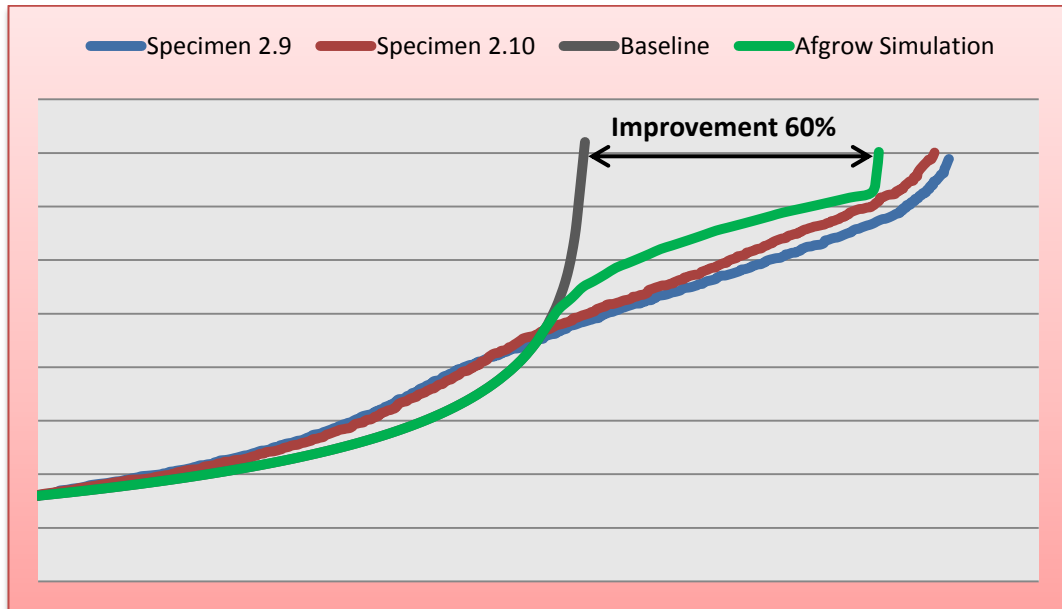
VIII. Conclusion And Future Work

8.1 Conclusion

Laser Shock Peening is a novel alternative surface processing technology to conventional stress field induction techniques which promises considerable improvement in the development of residual stress fields in aircraft construction.

From the results of the present work, LSP is confirmed as an effective surface treatment capable of introducing significant compressive residual stress in fatigue sensitive areas of metallic structures, improving their fatigue life.

The application of the numerical FE simulation to evaluate the Stress Intensity Factor value for different crack lengths and the prediction of the crack growth behavior showed to achieve reasonably results for the specimen under investigation. In fact, the slope of the crack growth rate predicted at the residual stress field is really similar to the one achieved by the experimental tests.

Nevertheless, it seems that the AFGROW software predicts an acceleration before the LSP stripe which is way too high compared to the tests one. This phenomenon might be caused by the interaction between the plastic zone at the crack tip and the tensile residual stresses area which is present before the LSP stripe as a consequence for the equilibrium of the whole model, which is not considered in this work as all simulations were carried out as linear elastic analysis that don't take into account the plasticity effects.

Moreover, it is not well understood the reason why the acceleration is more pronounced for lower external load applied when the crack front is approaching the compressive residual stress field which causes a higher $\tilde{\beta}$ correction factor at short crack lengths. This behavior would mean that the displacement of crack surfaces would be higher when a lower external load is applied and that the stresses distribution around the crack is greater.

However, this is a non realistic behavior which is not detected during the experimental tests and it is needed to be avoided in order to simulate the crack growth behavior as close as possible to the real one.

Simulations globally show a good fitting of the experimental results proving the adopted strategy to be reliable for the specimen under investigation.

8.2   Future Work

Further work might be focused to understand the reason why the accelerations phase is so pronounced comparing to the experimental results. The key point to explain this effect seems to rely in the study of how the plastic zone at the crack tip interacts when a tensile or compressive residual stress field is applied around it. Further simulations using plastic analysis could clarify better why the crack doesn't accelerate before it enters the Laser Shock Peening stripe.

Moreover, a study of the crack growth behavior for different geometry of the specimen (e.g. 3D cases) and for different position of the LSP stripe would be helpful to recognize if the adopted analysis method is still valid for different geometry conditions.

Finally, it should be proved that the same strategy can be used also in complex structure (e.g. curved stiffened panel) in order to move the aim of the work from a coupon level to a real aeronautical structure level.

Bibliography

[1]   Nadri B., Edwards L., Fitzpatrick M., Lodini A., "Analysis of residual stresses following overloading of cold expanded holes using the X-ray diffraction and finite element method"

[2]   Glinka G., "Development of weight function and computer integration procedures for calculating stress intensity factors around cracks subjected to complex stress fields" USA,1996.

[3]   Dai D. N., "Analysis of crack growth life from cold expanded holes. Part One", 2000.

[4]   Schijve J., "Fatigue of structures and materials", Kluwer Academic Publishers, 2004

[5]   Broek D., "The practical use of fracture mechanics", Galena, OH, USA, Kluwer Academic Publisher, 1988

[6]   Tan J.M., Pratihar S., Fitzpatrick M. E., Edwards L., "Residual stress redistribution at fatigue-aged stress wave cold-worked holes", in the 3rd conference on stress evaluation with neutrons and synchrotron radiation (Meca Sens 3), Santa Fe, New Mexico, USA, 2005

[7]   Perez N., "Fracture Mechanics", Kluwer Academic Publishers, 2004

[8]   Lacarac V., Garcia-Granada A., Smith D., Pavier M., "Prediction of the growth rate for fatigue crack emanating from cold expanded holes", International Journal of Fatigue, 2003

[9]   Carlson S. S., "Experimentally derived beta corrections to accurately model the fatigue crack behavior at cold expanded holes in 2024-T351 aluminum alloys", University of Utah, Utah, USA, 2008

[10]   Newman J. C., Raju I. S., "Stress-Intensity factor equations for cracks in three dimensional finite bodies subjected to tension and bending loads", Elsevier Science Publisher, USA, 1986

[11]   U.S. Air Force "www.AFGROW.net", 2011

[12]   A. Tolga Bozdana: "On the mechanical surface enhancement techniques in aerospace industry" – A research by University of Nottingham

[13]   Metal Improvement Company, "A business unit of Curtiss-Wright Surface Technologies", An overview of the SP Technique

[14]   Clauer, A.H.: "Laser shock peening for fatigue resistance, Surface Performance of Titanium"; J.K.Gregory, H.J.Rack, and D.Eylon (eds.), The Minerals, Metals & Materials Society, pp.217-230, 1996.

[15]   Troiani E., Crudo C., Molinari G., Taddia S., "Investigation on Laser Shock Peening capability by finite element simulation", 27th ICAF Symposium, Jerusalem, 2013

[16]   Sano, Y., Akita, K., Masaki, K., Ochi, Y., Altenberger, I. and Scholtes, B. (2006), "Journal of Laser Micro/Nanoengineering", vol. 1, n. 3, p. 161

[17]   Heckenberger U., Hobergsmeier E., Holzinger V., Von Bestenbostel W., "Advances in Laser Shock Peening theory and practice around the world: present solutions and future challenges" Proceeding of the 2nd International Conference on Laser Peening, Ivetic G., Emerald Group Publishing Ltd., Bradford

[18]   H. Luong, M. R. Hill: "The effects of laser peening on high-cycle fatigue in 7085-T7651 aluminum alloy", 2007

[19]   Peyre, P. and Fabbro, R.: "Laser shock processing: a review of the physics and applications"; Optical and Quantum Electronics, Vol.27, pp.1213-1229,

[20]   Johnson, J. N. and Rohde, R. W.:"Dynamic deformation twinning in shock-loaded iron"; J. Appl. Phys., Vol.42, pp.4171-4182, 1971.

[21]   Ballard, P., Fournier, J., Fabbro, R. and Frelat, J.: "Residual Stresses Induced by Laser-Shocks"; J.de Physique IV, C3, pp.487-494, 1991.

[22]   Masmoudi N., Castex L., Bertoli. "Influence of temperature and time on the stress relaxation process f shot peened IN 100 superalloys." Mater Tech (Paris) 1989.

[23] Cao W., Khadhraoui M., Brenier B., "Thermomechanical relaxations of residual stress in shot peened nickel base superalloy" Mater Sci Technol, 1994.

[24] Khadhraoui M., Cao W., Castex L., "Experimental investigation and modeling of relaxation behavior of shot peening residual stresses at high temperature for nickel base superalloys" Mater Schi Technol, 1997.

[25] Prevey P., Ilornbach D., Mason P., "Thermal residual stress relaxation and distortion in surface enhanced gas turbine engine components" In: Proceedings of the 17th heat treating society conference and exposition and the 1st international induction heat treating symposium. Park, OII: ASM Materials. 1998.

[26] Cai DY, Nie PL, Shan JP, "Precipitation and residual stress relaxation kinetics in shot-peened Inconel 718" J Mater Eng Perform, 2006.

[27] Zhong Z., Sagar B., Gokul R., "Thermal relaxation of residual stress in laser shock peened Ti-6Al-1V alloy" Surf Coating Technol, 2012.

[28] Zhong Z., Amrinder SG, Dong Q., "A finite element study of thermal relaxation of residual stress in laser shock peened IN718 superalloy" Int J Impact Eng, 2011.

[29] Dennis JB, Reji J., Robert AB, "A coupled creep plasticity model for residual stress relaxation of a shot peened Nickel-base superalloy" Mater Technol, 2009.

[30] Adekola, T.R., Diep, H.T., Ramulu, M. & Kobayashi, "Effects of peening on fatigue crack propagation" *SEM Annual Conference and Exposition on Experimental and Applied Mechanics*, Springfield, MA, Proceedings of the SEM Annual Conference and Exposition on Experimental and Applied Mechanics 2007

[31] Wang, C.D., Zhou, J.Z., Huang, S., Yang, X.D., Xu, Z.C. & Ruan, H.Y. 2011, "Study on the improvement of fatigue crack growth performance of 6061-T6 aluminum alloy subject to laser shot peening" *Key Engineering Materials*, 2011

[32]   Tsay, L.W., Young, M.C. & Chen, "Fatigue crack growth behavior of laser-processed 304 stainless steel in air and gaseous hydrogen", *Corrosion Science*, 2003

[33]   Ren, X.D., Zhang, T., Zhang, Y.K., Jiang, D.W. & Chen, "Analysis of 7050 aluminum alloy crack growth by laser shock processing" *Advanced Materials Research*, 2010

[34]   Harter J. A., "AFGROW users guide and technical manual", 1999

[35]   Tada, Paris and Irwin "The Stress Analysis of Cracks Handbook" Second Edition, Paris Productions Inc., St. Louis, MO, 1985

[36]   Hombergsmeier E., Holzinger V., Heckenberger U. C., "Fatigue crack retardation in LSP and SP treated aluminum specimens", 11th International Fatigue Congress, Melbourne, Australia, 2014

[37]   Braisted, W. and Brockman, R.: "Finite element simulation of laser shock peening"; Inter. J. Fatigue, 1999.

[38]   Sticchi M., "Finite element modeling of laser shock peening − Geometrical constraints impact on residual stress distribution after laser shock peening", Master Science Thesis, 2011

[39]   Taddia S., "Applicazione della tecnologia laser shock peening per l'aumento della vita a fatica di componenti aeronautici ", Master Thesis, 2011

[40]   Zhang X., Wang Z., "Fatigue life improvement in fatigue-aged fastener holes using cold expansion technique", International Journal of Fatigue, 2003

[41]   Furfari D., Hombergsmeier E., Heckenberger U., Bestenbbostel W. V., Holzinger V., "LSP to improve the fatigue resistance of highly stressed AA7050 components", 2nd International Conference on Laser Peening, San Francisco,2010

[42]   Dassault Systèmes Simulia Corp., "Abaqus 6.13 Documentation"

[43]   Ivetic G., "Residual Stress Effects on Fatigue Phenomena in Aerospace Structures", PhD Thesis in Aerospace Engineering, University of Pisa, 2010